



Lehrstuhl für Technische Mechanik

Comparative Numerical
Analysis of Free Field
Acoustics using Finite and
Boundary Element
Methods

Masterarbeit

Prashanth Setty

23016649

03.02.2025

Prof. Dr.-Ing. Julia Mergheim, LTM, FAU
Oliver Eichelhard, Dipl.-Ing, Wölfel
Oezge Akar, M. Sc., LTM, FAU

I confirm that I have written this thesis unaided and without using sources other than those listed and that this thesis has never been submitted to another examination authority and accepted as part of an examination achievement, neither in this form nor in a similar form. All content that was taken from a third party either verbatim or in substance has been acknowledged as such.

.....
Date

.....
Signature

Abstract

Excessive noise in industrial and environmental settings poses significant risks to human health, safety, and comfort. This thesis investigates two prominent numerical techniques—Finite Element Method (FEM) and Boundary Element Method (BEM)—for calculating sound pressure level under free-field boundary conditions. The commercial software Abaqus is used for the FEM-based analyses, while the open-source Boundary Element Method Python Package (BEMPP) is used for the BEM-based simulations.

A comparative study between fully coupled and sequentially coupled acoustic simulations methodologies of Abaqus is conducted using a prototype cube model to evaluate computational efficiency and accuracy. The results illustrate the extent to which sequentially coupled analyses can serve as reliable alternatives to fully coupled approaches. Building on these insights, a streamlined workflow for wind turbine gearbox acoustic analysis is developed by integrating time-domain multibody simulation data from commercial software Simpack with Abaqus. This integration addresses crucial challenges such as data compatibility and conversion between the two platforms.

To broaden the investigation, complementary simulations are performed in BEMPP, providing a parallel assessment of sound pressure calculations and computational demands between FEM and BEM. The findings highlight best practices for mesh design, boundary treatments, and coupling strategies, ultimately guiding the choice of simulation methodologies based on accuracy, computational cost, and ease of implementation. This work contributes to the advancement of acoustic modeling techniques, offering practical recommendations for sound pressure level calculation in industrial and environmental applications.

Acknowledgement

I would like to express my deepest gratitude to Mr. Oliver Eichelhard, who served as Expert Noise, Vibration, and Harshness (NVH) at Wölfel during my master's thesis, for his invaluable technical guidance, mentorship, and support. His expertise and insights were instrumental in shaping the direction and outcomes of this work. I would also like to extend my heartfelt thanks to Dr.-Ing. Manuel Eckstein, Head of Simulation at Wölfel, for providing me with the opportunity to work on this project.

I am also sincerely grateful to Ms. Oezge Akar, Wissenschaftliche Assistentin at the Institute of Applied Mechanics, FAU, for her guidance in writing this thesis, her advice on technical aspects, and for providing essential resources that greatly facilitated my work. I would also like to express my gratitude to Prof. Dr.-Ing. Julia Mergheim for facilitating my thesis at the Institute of Applied Mechanics and for her overall supervision and support.

I would like to thank Wölfel and Friedrich-Alexander-University Erlangen-Nuremberg for providing the necessary resources that enabled the successful completion of this thesis. I am grateful for the collaborative efforts and teamwork that have enhanced the quality of my work.

Finally, I would like to thank my family and friends for their unwavering support and encouragement throughout my academic pursuits. Their love and support have been a constant source of motivation and inspiration for me.

Contents

1	Introduction	2
1.1	Background	2
1.2	Objectives	3
1.3	Thesis Structure	4
2	Literature Review	7
2.1	Far-Field Acoustics and Infinite Elements	7
2.2	Fully and Sequentially Coupled Acoustic-Structural Analyses	8
2.3	Integration of Multibody Simulation (MBS) Data in Sequentially coupled acoustic analysis	9
2.4	FEM and BEM in Exterior Acoustics	10
2.4.1	Comparisons of Commercial and Open-Source Acoustic Solvers . .	11
2.5	Gaps in Current Research	11
2.6	Conclusion	12
3	Theoretical Background	13
3.1	Acoustics Fundamentals	13
3.2	Near and Far Field Acoustics	15
3.2.1	Near Field	16
3.2.2	Far Field	16
3.3	Numerical Methods in Acoustics	17
3.3.1	Finite Element Method (FEM)	17
3.3.2	Boundary Element Method (BEM)	18
3.3.3	From General Wave Equation to Harmonic Wave Equation	19
3.3.4	Free-Field and Sommerfeld Radiation Conditions	20
3.4	Acoustic Analysis Methodologies in Abaqus	20
3.4.1	Acoustic Analysis in Abaqus	21
3.4.2	Input(.inp) file structure of Abaqus	22
3.5	Coupled Exterior Acoustic-Structural Analysis in Abaqus	25
3.5.1	Real-Life Dynamics of Structural-Acoustic Interaction	25
3.5.2	Modeling in Abaqus	25
3.6	Harmonic Analysis	26
3.6.1	An Example of Harmonic Analysis	30
3.6.1.1	Mode Shapes and Modal Superposition	32
3.6.2	Material Damping in harmonic analysis	35
3.6.3	Mode-Based Steady-State Dynamic Analysis	38
3.6.4	Subspace-Based Steady-State Dynamic Analysis	41
3.6.5	Direct-Solution Steady-State Dynamic Analysis	42

3.7	Structural Elements in Coupled Acoustic Structural Analysis	47
3.7.1	Shell Elements	48
3.7.2	Solid Elements	49
3.8	Acoustic Medium	49
3.9	Acoustic Elements in Coupled Acoustic Structural Analysis	50
3.10	Modeling Infinite Domains in Abaqus for Exterior Problems	52
3.10.1	Acoustic Infinite Elements	53
3.11	Comparative Overview of Fully and Sequentially Coupled Analysis	56
3.12	Fully Coupled Acoustic-Structural Analysis	57
3.12.1	Structural Acoustic Coupling in Fully Coupled Analysis using surface-based tie constraint	58
3.12.2	Implementation of Surface-Based Tie Constraints in Simulation .	59
3.12.3	Output and Postprocessing in Fully Coupled Acoustic Structural Analyses	61
3.12.3.1	Sound Pressure Output	62
3.12.3.2	Total Energy Output Quantities	63
3.12.3.3	Equivalent Radiated Power (ERP)	63
3.12.3.4	Using Infinite Elements to project the results to a Far-Field	65
3.13	Sequentially Coupled Acoustic Structural Analysis	66
3.13.1	Submodeling in Sequential Coupling	67
3.13.2	Structural Acoustic Coupling in Sequentially Coupled Analysis using Acoustic Structural Interface Elements	68
3.13.3	Outputs in Sequentially Coupled Acoustic-Structural Analyses .	70
3.14	Boundary Element Method	70
3.14.1	Derivation of the Boundary Element Method for the Helmholtz Equation	72
3.15	The BEMPP Python Library: Architecture and Workflow	74
3.15.1	Null Field Approach and Representation Formulas in BEMPP .	77
4	Methodology	80
4.1	Comparative Analysis of Fully Coupled and Sequentially Coupled Acoustic Simulations in Abaqus	80
4.1.1	Objective	81
4.1.2	Model Setup for Fully Coupled Acoustic-Structural Analysis of the Prototype Cube	81
4.1.3	Mesh Resolution and Acoustic Cavity Dimensions	86
4.1.4	Acoustic-Structural Interface Using Structural Ties in Fully Coupled Analysis	88
4.1.5	Frequency Response Analysis in Fully Coupled Simulation	90
4.1.6	Output Definition	91
4.1.7	Model Setup for the Sequentially Coupled Acoustic-Structural Analysis of the Prototype Cube	93
4.1.8	Acoustic-Structural Interface with ASI Elements in Sequentially Coupled Analysis	93
4.1.9	Frequency Response Analysis in the Sequentially Coupled Simulation .	94
4.1.9.1	Submodel Run (Acoustic Cavity + ASI Elements + Infinite Elements)	95

4.2	Sequentially Coupled Acoustic Analysis of a Wind Turbine Gearbox Using Simpack and Abaqus	96
4.2.1	Wind Turbine Overview and Motivation for Gearbox Acoustic Analysis	96
4.2.2	Acoustic Cavity Modeling around the Gearbox Casing	98
4.2.3	Methods for Coupling Harmonic Displacements to Acoustic Cavity	101
4.2.3.1	Structural Tie Coupling Method	101
4.2.3.2	Acoustic-Structural Interface (ASI) Element Method	104
4.2.4	Converting Simpack Data into Abaqus Format	105
4.3	Acoustic Calculations for the Prototype Cube Model in the Boundary Element Method Python Package (BEMPP)	107
4.3.1	Steady-State Dynamic Analysis of the Cube	108
4.3.2	SPL Calculation in BEMPP	109
5	Results and Discussion	113
5.1	Comparison of Fully Coupled and Sequentially Coupled Acoustic Simulation Results for the Prototype Cube	113
5.1.1	Sound Pressure Level (SPL) Comparison	113
5.1.2	Comparison of Computational Times	114
5.1.3	Acoustic Radiated Energy Comparison	115
5.1.4	Validation Using Equivalent Radiated Power (ERP)	116
5.1.5	Visualization of Far-Field Results at User-Defined Distances	117
5.2	Sound Pressure Analysis of Sequentially Coupled Wind Turbine Gearbox	119
5.2.1	Acoustic Coupling Method Comparison	119
5.2.2	Spatial Sound Pressure Distribution Around the Gearbox	121
5.2.3	Structural Material Property Sensitivity and Effects of Remeshing-Induced Null Displacements	122
5.3	Comparison of Sound Pressure Level Results between BEMPP and Abaqus	126
5.3.1	Results	127
5.3.2	Validation of the Null-Field Approach	131
6	Conclusion	133
6.1	Summary of Key Findings	133
6.1.1	Comparative Analysis of Fully Coupled vs. Sequentially Coupled Approaches	133
6.1.2	Methodology Development for Gearbox Acoustic Analysis	134
6.1.3	Acoustic Calculations in BEMPP	134
6.1.4	Advancement of Computational Mechanics Knowledge Base	135
6.2	Recommendations and Future Work	135
6.3	Concluding Remarks	136
A	Derivation of Acoustic Power Formula from Energy	141
B	Python Script for Converting Simpack Displacement Data to Abaqus Format	142

List of Figures

3.6.1	Harmonic excitation illustrating amplitude and time period.	27
3.6.2	Harmonic excitation illustrating Phase shift.	28
3.6.3	Time-domain relationship between displacement and velocity. The 90° phase difference is illustrated.	29
3.6.4	Time-domain relationship between displacement and acceleration. The 180° phase difference is shown.	30
3.6.5	Relationship between mass-proportional and stiffness-proportional damping [1]	37
3.10.6	Reference point and node rays for acoustic infinite elements [2].	55
3.10.7	Defining the cosine for acoustic infinite elements [2].	55
3.13.8	Global Model. The structural model with elements and nodes is used to compute the displacement field. The boundary of the structure, shown as a line interface, will drive the acoustic submodel by transferring the computed structural displacements. The global model provides the input for the submodel, ensuring that the boundary conditions at the interface are accurately captured.	69
3.13.9	Submodel. The acoustic mesh with ASI elements along the structural interface is shown. The nodes along the ASI interface are driven by interpolated structural displacements from the global model. This allows the acoustic submodel to calculate the acoustic pressure field in response to the structure's vibrations. The correct orientation of the ASI element normals into the acoustic domain ensures the physical accuracy of the simulation.	69
4.1.1	Mesh of the prototype cube model used in both fully coupled and sequentially coupled analysis.	82
4.1.2	Illustration of the harmonic load of 100N applied to the prototype cube model.	83
4.1.3	XZ-plane section cut view of the acoustic cavity mesh surrounding the prototype cube model, showing the inner region meshed with tetrahedral elements and the outer region meshed with hexahedral elements.	84
4.1.4	XZ-plane section cut view of the acoustic cavity mesh showing the outermost layer of infinite elements (in red) and the reference point for these elements (yellow node) defined at the center of the sphere.	86
4.1.5	Translucent view of the complete model for the fully coupled acoustic-structural simulation setup, showing the cube structure at the center, surrounded by the inner and outer acoustic cavity.	87
4.1.6	str_acou surface pointing outward from the cube towards the acoustic cavity.	89

4.1.7	acou_str surface at the interface pointing inward towards the cube.	90
4.1.8	Structural Ties are used to tie the displacements between str_acou and acou_str surfaces.	91
4.1.9	XZ-plane section cut view of the submodel consisting of acoustic cavity mesh, infinite elements (in red) and the ASI elements (in green)	94
4.2.10	Schematic of a typical horizontal-axis wind turbine (Source: Chair of Machine Elements, TU Dresden, 2022) [3].	97
4.2.11	A sectional view of the acoustic cavity mesh around the gearbox.	100
4.2.12	A sectional view of the acoustic cavity mesh, highlighting the infinite elements (blue) at the outermost boundary.	101
4.2.13	Cross-sectional view of coarse acoustic cavity mesh assembly	103
4.2.14	Fine-resolution acoustic cavity mesh for ASI coupling	105
4.3.15	Prototype cube meshed with triangular elements for BEMPP.	108
4.3.16	BEMPP model: A 200 mm radius sphere around the cube. Both surfaces are discretized with triangular elements.	109
5.1.1	Comparison of SPL-dB obtained from fully coupled and sequentially coupled analyses for the prototype cube.	114
5.1.2	Comparison of acoustic radiated energy between fully coupled and sequentially coupled analyses.	116
5.1.3	Comparison of Radiated Power (RADPOW) and Equivalent Radiated Power (ERP) in Fully Coupled Analysis. The red curve represents RADPOW, and the blue curve represents ERP.	117
5.1.4	Visualization of sound pressure levels at 500 Hz in the far field at distances of 2000 mm and 2500 mm from the cube.	118
5.1.5	Visualization of sound pressure levels at 1000 Hz in the far field at distances of 2000 mm and 2500 mm from the cube.	118
5.2.6	SPL comparison at front position (Node 1859) showing < 1 dB deviation between methods	120
5.2.7	SPL comparison at Rear position (Node 930) with 2 dB maximum deviation	120
5.2.8	Spatial distribution of SPL at six far-field locations (2300 mm from the gearbox) over the frequency range of 90–200 Hz.	121
5.2.9	Magnified view of SPL distribution at six far-field locations in the frequency range of 180–200 Hz.	122
5.2.10	SPL at 95 Hz at the nodes of infinite elements for different structural materials.	124
5.2.11	SPL at 95 Hz at the nodes of infinite elements, comparing the effect of applying zero displacement to remeshed nodes.	125
5.2.12	Comparison of Radiated Power (RADPOW) and Equivalent Radiated Power (ERP) in the ties method. The red curve represents ERP, and the blue curve represents RADPOW.	125
5.3.13	Experiment 1: Velocity loaded to the single face perpendicular to the <i>y</i> -axis.	127
5.3.14	Experiment 2: Velocity loaded to the two faces perpendicular to the <i>y</i> -axis. The illustrated face is the opposite side of that shown in Figure 5.3.13.	128

5.3.15 Experiment 3: Velocity loaded to all faces of the cube.	129
5.3.16 SPL comparison between BEMPP and Abaqus when only one face (perpendicular to y -axis) is loaded.	130
5.3.17 SPL comparison between BEMPP and Abaqus when two opposite faces (perpendicular to y -axis) are loaded.	130
5.3.18 SPL comparison between BEMPP and Abaqus when all cube faces are loaded with velocities.	131
5.3.19 Contour plot of the sound pressure level around the cube at 500 Hz when two opposite faces are subjected to loading.	132

List of Tables

3.14.1 Comparison between Finite Element Method (FEM) and Boundary El-	
ement Method (BEM)	71
3.15.2 Boundary Operators for the Helmholtz Equation	76
3.15.3 Potential Operators for the Helmholtz Equation	77
4.1.1 Element and Node Count in the Acoustic Cavity Mesh of the Prototype	
Cube Model	85
4.2.2 Coarse Acoustic Cavity Mesh Statistics	103
4.2.3 Fine Acoustic Cavity Mesh Statistics	105
4.3.4 Mesh Statistics for the BEMPP Model of the Cube and Outer Sphere .	109
5.1.1 Comparison of computational time for fully coupled and sequentially	
coupled analyses	114
5.2.2 Comparison of Computational Resources for SSD Analysis Over the	
Frequency Range of 90 Hz to 200 Hz	119

About the Company

This thesis was conducted at Wölfel, a company specializing in vibrations, acoustics, structural mechanics, and emission protection.

The Wölfel Group, established in 1971, specializes in vibrations, acoustics, and environmental and emission protection. Over the past 50 years, the company has developed expertise as an engineering service provider in fields such as wind energy, structural dynamics, plant engineering, and power plant technology. By diversifying across these areas, Wölfel leverages synergy effects through knowledge transfer, offering comprehensive engineering services and customized products tailored to meet client requirements.

Wölfel's service portfolio in the field of vibroacoustics includes:

- Elastic modeling of the structural components
- Simulation of structure-borne sound and radiation behavior
- Subsequent simulation of airborne sound by modeling and calculating the air elements
- Extrapolation to the reference point and evaluation of influences on the total sound level

The company supports its clients throughout all project phases, from consulting and report preparation to project completion, drawing on decades of experience, engineering expertise, and in-house software solutions. With a strong emphasis on fundamental research and collaboration with universities, Wölfel ensures its solutions are informed by the latest scientific advancements and meet the highest standards.

Chapter 1

Introduction

Understanding and controlling noise emissions is a critical aspect of engineering applications, especially in industrial and environmental contexts. Excessive noise can lead to regulatory challenges, and operational inefficiencies. Computational methods for acoustic analysis enable engineers to predict and mitigate unwanted noise efficiently. This thesis explores numerical techniques for exterior acoustic simulations using Finite Element Method (FEM) and Boundary Element Method (BEM) to evaluate sound pressure under free-field boundary conditions.

This chapter provides the necessary background on acoustics, emphasizing the importance of numerical simulations in noise prediction and control. The objectives of this research are outlined, followed by an overview of the structure of the thesis.

1.1 Background

Sound is a mechanical vibration that travels as an acoustic wave through a transmission medium such as a gas, liquid, or solid. Humans typically hear sounds within the frequency range of 20 Hz to 20,000 Hz. The perception of sound depends on two primary factors: frequency, which determines the pitch, and loudness, which indicates the intensity of the sound. Frequency, measured in hertz (Hz), represents the number of pressure wave cycles per second, while loudness, measured in decibels (dB), quantifies the pressure level of the sound wave. A typical human ear can perceive sounds ranging from 0 dB to 140 dB, but prolonged exposure to levels above 85 dB can lead to hearing damage. Examples of common sources producing harmful sound levels are sirens, lawnmowers, and heavy machinery [4].

The impact of noise pollution from wind turbines, has become a topic of increasing environmental concern. Wind turbines produce a distinctive noise due to mechanical and aerodynamic sources, with the potential to affect both human populations and wildlife in their vicinity. Regulatory requirements for wind turbine installation highlight the need for rigorous acoustic simulations with far-field boundary conditions. For instance, the Ministry of Environment in Denmark mandates that noise emissions from wind turbines do not exceed 39 dB at wind speeds of 8 m/s and 37 dB at 6 m/s near residential areas [5]. Similarly, the state of Hesse in Germany recommends maintaining a precautionary

distance of 1,000 meters between wind turbines and residential zones to mitigate noise impact. These regulations necessitate the use of acoustic simulations that can accurately predict sound pressure levels at distances far from the source. Far-field boundary conditions in acoustic simulations ensure that the models reflect realistic scenarios where the sound has propagated and diffused over large distances, providing essential data to comply with these regulations while optimizing turbine placement and design.

Acoustic analysis extends beyond compliance with legal noise regulations; it also serves as a powerful diagnostic tool for identifying defects or performance issues in prototypes during the design phase. By simulating the conversion of vibrational energy into sound pressure around a structure, engineers can predict acoustic signatures and compare them against expected baselines. Deviations in resonance frequencies, amplitude levels, or sound pressure distributions may indicate changes in the prototype's stiffness, damping properties, or material behavior. This capability allows for early detection of design flaws, ensuring that the prototype functions as intended.

Acoustics is the science of sound, including its production, transmission, and effects [6, p. 1]. Acoustic analysis plays a crucial role in calculating sound pressure levels in various environments, from industrial settings to residential areas in tonality sensitive regions. Traditionally, experimental methods have been employed to measure sound levels. However, these methods are often costly, time-consuming, and require complex setups, making them less practical for iterative design processes. In contrast, numerical methods offer a cost-effective and efficient alternative, particularly when evaluating multiple design iterations. Unlike experimental approaches, which rely on physical measurements, numerical methods provide a predictive framework that simulates acoustic behavior under various conditions. This predictive capability enables engineers to identify and address potential issues early in the design phase, reducing the need for extensive prototyping and testing. As a result, numerical methods have gained prominence as a more feasible alternative. Finite Element Method (FEM) and Boundary Element Method (BEM) are two such numerical techniques widely used in the field of acoustics. FEM is extensively utilized for its versatility in handling complex geometries and material properties, while BEM is favored for problems involving infinite or semi-infinite domains, such as exterior sound radiation problems. Together, these methods provide comprehensive tools for predicting acoustic behavior and designing solutions that mitigate undesirable noise.

1.2 Objectives

This thesis aims to enhance understanding and methodologies in exterior acoustic calculations by focusing on free-field boundary conditions and employing both Finite Element Method (FEM) and Boundary Element Method (BEM). The tool used for FEM is the commercial software Abaqus, and for BEM, the open-source Python library Boundary Element Method Python Package (BEMPP) is utilized. The specific objectives are:

1. Comparative analysis of fully coupled and sequentially coupled acoustic simulations in Abaqus:

The aim is to evaluate two distinct simulation methodologies for a prototype cube model: fully coupled and sequentially coupled acoustic analyses. This objective involves explor-

ing both methodologies to understand their computational cost and how closely the results from the sequentially coupled method match those from the fully coupled approach. The goal is to determine if the sequentially coupled method can serve as an efficient yet accurate alternative in acoustic simulation scenarios where computational resources are constrained.

2. Methodology Development for Gearbox Acoustic Analysis:

Develop a robust simulation method for the acoustic analysis of a wind turbine gearbox in Abaqus. This involves integrating displacement results from time-domain multibody simulations in Simpack with Abaqus to perform sequentially coupled acoustic analyses. The integration addresses challenges such as data compatibility and conversion, aiming to establish a seamless workflow that enhances the practical applicability of these methods in industrial simulations.

3. Acoustic Calculations in BEMPP:

Perform acoustic simulations for the prototype cube model using BEMPP, and compare the results with those obtained from Abaqus. This objective aims to validate the effectiveness of BEMPP in handling free-field acoustic problems and to understand discrepancies, such as differences in solution accuracy and processing time, that may arise between FEM and BEM methodologies.

4. Advancement of Computational Mechanics Knowledge Base:

To meticulously document the challenges and solutions encountered across different simulation setups, offering a detailed scholarly review of the experimental processes, discrepancies observed, and theoretical justifications. This objective includes providing recommendations for improving simulation accuracy and efficiency, thereby facilitating the development of more refined acoustic modeling techniques that are applicable to both academic research and industrial practice.

These objectives collectively aim to contribute significantly to acoustic analysis and computational acoustics, fostering methodological advancements and innovation. By exploring and documenting the practical and theoretical aspects of employing FEM and BEM, this thesis serves as a comprehensive resource for future research, guiding the development of more accurate and efficient simulation practices tailored to industrial and academic needs.

1.3 Thesis Structure

This thesis is organized into six main chapters, each addressing a different facet of the research on free-field acoustic simulations using finite and boundary element methods. Below is a concise overview of the contents and objectives of each chapter:

1. Chapter 1: Introduction

This chapter outlines the motivation for studying exterior acoustics, highlighting the health, safety, and regulatory considerations that drive the need for accurate noise prediction. Section 1.1 presents the *Background*, discussing essential concepts of sound propagation and noise hazards in industrial and environmental contexts. Section 1.2 states the *Objectives* of the research, emphasizing comparative analyses of various coupling and modeling strategies. Section 1.3 provides an overview of the thesis organization.

2. Chapter 2: Literature Review

An extensive survey of prior work in far-field acoustics is offered here. Section 2.1 details *Far-Field Acoustics and Infinite Elements*, focusing on boundary treatments for unbounded domains. Section 2.2 explains the difference between *Fully and Sequentially Coupled Acoustic-Structural Analyses*, followed by Section 2.3, which explores *Integration of Multibody Simulation (MBS) Data in Sequentially Coupled Acoustic Analysis* for enhanced realism. Section 2.4 turns to *FEM and BEM in Exterior Acoustics*, including Section 2.4.1 on *Comparisons of Commercial and Open-Source Acoustic Solvers*. Sections 2.5 and 2.6 identify research *Gaps* and conclude the literature survey.

3. Chapter 3: Theoretical Background

This chapter establishes the fundamental acoustics and numerical methods underpinning the research. Section 3.1 introduces *Acoustic Fundamentals*, while Sections 3.2.1 and 3.2.2 clarify the distinction between *Near Field* and *Far Field* behavior. Section 3.3 surveys *Numerical Methods in Acoustics*, contrasting FEM and BEM approaches. In Section 3.4 and onward, the focus shifts to *Acoustic Analysis Methodologies in Abaqus*, addressing how the software handles fluid-structure coupling via finite elements and infinite elements. Sections 3.6–3.10 delve into harmonic analysis, material damping, and infinite-domain modeling, culminating in *Fully Coupled* vs. *Sequentially Coupled* formulations (Sections 3.11–3.13). Finally, Sections 3.14 and 3.15 introduce the *Boundary Element Method* and the *BEMPP Python Library*, including a discussion of the null-field approach and representation formulas.

4. Chapter 4: Methodology

This chapter describes the *practical* modeling steps and simulation workflows used throughout the thesis. Section 4.1 focuses on the *Comparative Analysis of Fully Coupled and Sequentially Coupled Acoustic Simulations in Abaqus*, detailing the model setup, mesh resolution requirements, and frequency response steps. It covers both structural ties and acoustic-structural interface (ASI) elements. In Section 4.2, the *Sequentially Coupled Acoustic Analysis of a Wind Turbine Gearbox* is presented, illustrating how displacement data from a Simpack multibody dynamics run feed into Abaqus for acoustic predictions. Section 4.3 discusses *Acoustic Calculations for the Prototype Cube Model in BEMPP*, providing insight into the boundary-element-based SPL calculations.

5. Chapter 5: Results and Discussion

This chapter synthesizes and interprets the findings from the computational studies. Section 5.1 reports a *Comparison of Fully Coupled and Sequentially Coupled*

Acoustic Simulation Results for the prototype cube, including sound pressure level (SPL) comparisons, computational cost analyses, radiated energy measurements, and validation using the Equivalent Radiated Power (ERP). Section 5.2 shifts to the *Sound Pressure Analysis of the Sequentially Coupled Wind Turbine Gearbox*, contrasting coupling methods and examining spatial SPL distributions. Finally, Section 5.3 compares *BEMPP and Abaqus Results*, highlighting discrepancies, resonance captures, and the role of geometry and mesh resolution in affecting solution accuracy.

6. Chapter 6: Conclusion

The thesis concludes with a summary of the key findings and contributions, reiterating the efficacy of various acoustic modeling methodologies in different scenarios. It also identifies open questions and suggests pathways for future research, including more advanced mesh convergence studies, refined handling of non-smooth geometries, and broader validation in industrial settings.

Overall, this structure first situates the research in relevant literature, then introduces the theoretical foundations of acoustic modeling, and finally applies these methods to systematically examine the performance of fully coupled, sequentially coupled, and boundary element approaches for free-field acoustic simulations.

Chapter 2

Literature Review

This chapter provides an overview of existing literature on far-field acoustic simulations, focusing on numerical approaches using the Finite Element Method (FEM) and Boundary Element Method (BEM). The discussion encompasses:

1. Studies employing infinite or infinite-like elements to model unbounded domains in exterior acoustics;
2. Studies on fully and sequentially coupled acoustic–structural approaches;
3. Research integrating multibody simulation (MBS) data for acoustic analyses;
4. Investigations into the relative merits of FEM and BEM for exterior acoustics.

Finally, key research gaps are identified, motivating this thesis’s objectives in bridging industrial applications (e.g. wind turbines) and advanced simulation techniques for accurate far-field noise predictions.

2.1 Far-Field Acoustics and Infinite Elements

Far-field acoustics frequently requires modeling an unbounded domain in which sound waves propagate without reflecting at finite boundaries. One standard solution is to use infinite (or absorbing) elements. Astley [7] presents an extensive review of infinite element formulations for exterior wave problems, highlighting the use of orthogonal functions for transverse interpolation within the infinite element domain. This work underscores the mathematical foundation for coupling finite and infinite element formulations to capture wave decay accurately.

The practical benefits of infinite elements are demonstrated by Dassault Systèmes SIMULIA [8], where sound radiation from an engine valve cover is analyzed. The study compares impedance-based methods with infinite elements and observes that infinite elements significantly reduce computational costs (over an order of magnitude in some cases) while accurately capturing near-field and far-field acoustics. Notably, the mesh

size dropped from 391,644 elements to 18,474, and computational time decreased to one-tenth of the original. This result is directly relevant to industrial noise studies, including wind turbine components, where large-scale meshing can inflate solver times.

Stoyanova [9] investigated noise emissions from an electric drive unit (EDU) in heavy trucks, employing forward-coupled structural-acoustic analysis in Abaqus. The work highlights the importance of carefully selecting acoustic boundary conditions (e.g. non-reflective acoustic infinite elements) and justifies the use of direct-solution steady-state dynamic analyses for accurate exterior acoustic predictions. Despite high fidelity, the computational expense of such analyses emerges as a pressing concern. In the context of wind turbine gearbox simulations, similar trade-offs between accuracy and solver run times must be managed, supporting the idea that advanced boundary conditions and optimized frequency partitions are vital for balancing efficiency and robustness.

2.2 Fully and Sequentially Coupled Acoustic–Structural Analyses

Fully coupled simulations solve structural and acoustic equations simultaneously, capturing two-way fluid-structure interactions (FSI) [10]. Though this approach may yield high accuracy, the associated computational burden can be significant. Alternatively, sequentially coupled simulations compute the structural response first, then use it as a boundary condition in the acoustic domain.

Benra et al. [11] investigate the differences between one-way and two-way coupling methods for solving FSI problems. Their study highlights that one-way coupling, where the fluid influences the structure without feedback, significantly reduces computational effort but may lead to inaccuracies in cases with strong interactions. Through various case studies, including plate deflection under fluid loads and single-blade pump simulations, the authors demonstrate that while one-way coupling provides reasonable approximations when the vortex shedding frequency is close to the natural frequency, it underestimates deflections compared to experimental results. In contrast, two-way coupling, which accounts for mutual interactions between the fluid and the structure, offers more accurate predictions at the cost of higher computational demand. Their findings underscore that the choice between one-way and two-way coupling should be based on the problem characteristics, with two-way coupling being preferable for cases requiring high fidelity in capturing dynamic structural responses to fluid forces.

In the study by [12], wind-induced noise transmission is investigated for vehicle cabins. The coupling of Large-Eddy Simulation for fluid flows and FE-based structural-acoustic analysis parallels the complexities found in rotor-driven turbines. The findings illustrate how structural modes and acoustic excitations collaboratively shape interior sound levels. Translated to wind turbine gearboxes, it suggests that both structural resonance and acoustic boundary conditions can profoundly influence noise radiation, reinforcing the importance of robust coupling strategies.

Schäfer [13] provides a comprehensive survey on the numerical simulation of coupled fluid-solid interaction problems, classifying them based on different coupling mechanisms. The study discusses the modeling framework within continuum mechanics and

highlights key numerical challenges related to discretization and solution strategies. Various numerical examples are presented to illustrate different coupling mechanisms, along with an evaluation of numerical accuracy and computational efficiency. This work serves as a foundational reference for understanding the complexities involved in solving fluid-solid interaction problems and the trade-offs between accuracy and computational cost in numerical simulations. The study reaffirms that the choice between fully coupled or sequentially coupled methods depends on the required fidelity and computational resources. This thesis extends these considerations, especially within the realm of rotating machinery acoustics (e.g. gearboxes), where sequential coupling could offer a pragmatic balance between accuracy and efficiency.

CALFEM's framework [14] provides a versatile implementation of acoustic finite elements for both two-dimensional and three-dimensional analysis, along with structure-acoustic interaction capabilities. It includes triangular and quadrilateral elements for 2D acoustics, as well as three-dimensional isoparametric elements, enabling coupled acoustic-structural simulations. Interface elements are available for modeling interactions between acoustic and solid domains, facilitating modal decomposition of the fluid and structural domains. The study presents the finite element formulations based on acoustic pressure or fluid displacement potential and discusses the computation of coupling element matrices for structure-acoustic interaction. Although the numerical comparisons among different coupling formulations are limited, the insights on building an interface between acoustic and structural domains inform the coupling strategies explored in this thesis.

2.3 Integration of Multibody Simulation (MBS) Data in Sequentially coupled acoustic analysis

Automotive chassis components play a crucial role in vehicle safety and must meet durability and strength requirements under extreme loading conditions. Traditional finite element (FE) simulations rely on load inputs from multi-body dynamics (MBD) models, which do not account for energy dissipation due to plastic deformation during impact events such as driving over potholes or sliding into a curb. Behera et al. [15] propose a tightly coupled co-simulation approach integrating Simpack for MBD and Abaqus for FE analysis. This method enhances accuracy by capturing both the global vehicle dynamics and local nonlinear material behavior, overcoming limitations of standalone FE-based full vehicle models. The study demonstrates the effectiveness of the Simpack-Abaqus co-simulation framework through case studies on chassis components subjected to extreme loading, highlighting its potential for optimizing vehicle design while reducing physical testing requirements.

In many industrial applications structural vibrations arise from complex dynamic interactions that may not be well-represented by static or simplified load assumptions. Multibody softwares have the ability to capture gear meshing forces, bearing stiffness, and transient phenomena. Introducing MBS data into an acoustic solver such as Abaqus can significantly enhance realism by including transient and nonlinear effects absent in simpler load assumptions.

2.4 FEM and BEM in Exterior Acoustics

The Finite Element Method is typically favored for its capacity to handle complicated interior domains and heterogeneous materials, while the Boundary Element Method can be more efficient for exterior problems due to the reduced dimensionality of its mesh [16]. Studies have illustrated that FEM requires a properly formulated far-field boundary (using infinite or absorbing elements) to avoid artificial reflections [8], whereas BEM intrinsically satisfies the Sommerfeld radiation condition at infinity [17].

Huang et al. [18] present the development and implementation of finite element and boundary element methods for solving vibro-acoustic problems in LS-DYNA¹. The study reviews the theoretical foundations of these methods and demonstrates their application in automotive, naval, and civil industries where noise control is critical. A benchmark example involving a vibrating plate subjected to an impulsive force is analyzed using BEM, the Kirchhoff method, and the Rayleigh method, providing cross-validation of these approaches. Additionally, the paper addresses the issue of non-uniqueness in conventional BEM solutions for exterior acoustic problems at eigenfrequencies and proposes a dual BEM formulation based on the Burton-Miller method to mitigate this issue. The results confirm that the dual BEM approach effectively resolves irregular frequency problems, ensuring accurate predictions of sound pressure fields. These advancements highlight the potential of FEM and BEM in addressing complex acoustic challenges in frequency-domain simulations.

Herrin [19] explores the application of the inverse Boundary Element Method (BEM) for predicting far-field sound pressure using near-field measurements. The study demonstrates that by estimating the vibration of a radiating surface based on near-field sound pressure data, it is possible to reconstruct the far-field sound using a forward BEM analysis. The methodology is validated through two case studies—a generator set and an engine cover—where the inverse BEM approach provided accurate far-field predictions, with minor discrepancies observed at low frequencies (below 250 Hz). Additionally, the study highlights the potential for computational efficiency improvements by employing a patch-based BEM model. The paper suggests that inverse BEM can serve as a viable alternative to traditional source reconstruction methods, such as near-field acoustic holography and Helmholtz equation least squares, and can aid in ranking noise contributions from different components for targeted noise reduction strategies.

Jelich [20] advances BEM-based methods further, introducing fast multipole techniques for large-scale periodic structure analysis, which is a faster solver but demands a very high memory. The work also explores iterative solvers for handling multiple load cases in boundary element discretized acoustic problems, demonstrating their effectiveness in aeroacoustic noise prediction and eigenvalue analysis of acoustic metamaterials. These advancements significantly enhance the feasibility of large-scale acoustic simulations, offering a robust framework for optimizing acoustic designs in engineering applications.

[21] conducted a comparative study on the computational costs associated with the Finite Element Method (FEM) and the Boundary Element Method (BEM) for acoustical problems. The study analyzed the variational-collocative BEM (DBEM) and the variational BEM (IBEM) in terms of matrix composition costs and system solution costs. The

¹<https://lsdyna.ansys.com/>

findings indicate that FEM can be more computationally efficient than BEM, particularly for three-dimensional problems involving large models. The study also highlights that the computational cost of BEM is strongly dependent on the order of quadrature, with IBEM generally being more computationally intensive than DBEM, except in certain cases where two-dimensional models with parabolic elements are considered. Additionally, the research suggests that while BEM is beneficial for handling unbounded domains, FEM may be preferable for large-scale models due to its lower memory requirements and computational efficiency. These insights provide valuable guidelines for selecting the most cost-effective numerical approach depending on problem complexity and computational resources.

2.4.1 Comparisons of Commercial and Open-Source Acoustic Solvers

Despite the widespread use of commercial solvers, peer-reviewed literature offering direct comparisons with open-source codes (e.g. BEMPP) is limited.

AAussal et al. [22] present the GypsilAB framework, an open-source MATLAB library designed for solving complex vibro-acoustic problems using both the Finite Element Method (FEM) and the Boundary Element Method (BEM). The study focuses on the strong coupling of incoming sound waves with vibrating finite structures, leveraging FEM for structural computations due to its suitability for non-homogeneous and anisotropic media, and BEM for acoustic propagation in infinite domains. [23] similarly compares semi-analytical approaches with FEM/BEM to evaluate composite structures but stops short of investigating open-source vs. commercial codes.

Hence, it remains unclear how solutions from BEMPP or other open-source frameworks fare against commercial codes like Abaqus exterior-acoustic problems. This shortfall partially motivates our thesis's dual approach to using both a commercial FEM platform (Abaqus) and an open-source BEM library (BEMPP) for cross-validation.

2.5 Gaps in Current Research

From the surveyed studies, several key limitations become evident:

- **Fully vs. Sequentially Coupled Validation:** Although the advantages of fully coupled methods are well-documented, direct comparisons with sequentially coupled analyses remain sparse.
- **Integration of MBS Outputs:** Existing literature showcases the benefits of MBS in capturing realistic loads, but no comprehensive workflow is detailed for importing time-domain Simpack displacement data into an acoustic solver (Abaqus) under far-field boundary conditions.
- **Comparisons of Open-Source vs. Commercial Codes:** Although BEMPP and other open-source solvers appear in some references, robust benchmarks

against commercial platforms such as Abaqus are rare, especially for large-scale far-field scenarios common.

Addressing these gaps could substantially advance numerical acoustics for industrial design and noise reduction.

2.6 Conclusion

Far-field acoustic simulations have been investigated using both FEM and BEM, each with distinct advantages based on problem geometry, frequency range, and available computational resources. The literature indicates that fully coupled vibro-acoustic methods yield high fidelity but can be prohibitively expensive for large industrial problems, whereas sequential coupling offers cost savings but remains under-validated. Incorporating MBS data—such as from Simpack—emerges as a critical step to ensuring wind turbine gearboxes' real operational behaviors are reflected in acoustic analyses.

Consequently, this thesis aims to:

- Quantify the trade-offs between fully and sequentially coupled approaches in Abaqus,
- Demonstrate a robust sub-workflow for applying MBS-derived displacements to an acoustic domain,
- Investigate the potential of an open-source BEM implementation (BEMPP) as a complement or alternative to established commercial FEM tools.

Chapter 3

Theoretical Background

Accurate acoustic simulations require a strong foundation in wave propagation principles, numerical methods, and computational modeling techniques. This chapter introduces the essential concepts necessary for understanding exterior acoustic simulations and their implementation in commercial and open-source solvers.

The chapter begins by discussing the fundamentals of acoustics, including the distinction between near-field and far-field acoustics and their relevance to engineering applications. This is followed by an overview of numerical methods in acoustics, focusing on the Finite Element Method (FEM) and the Boundary Element Method (BEM), which are widely used for solving acoustic problems in bounded and unbounded domains, respectively.

Subsequent sections explore acoustic-structural coupling methods, which are crucial in analyzing noise radiation from vibrating structures. The chapter explains different acoustic analysis methodologies in Abaqus, including harmonic analysis and the use of far-field boundary conditions through infinite elements. The mathematical formulation of fully coupled and sequentially coupled acoustic-structural analyses is also presented, providing insight into the computational trade-offs between the two approaches.

The final sections focus on modeling aspects specific to coupled acoustic-structural problems, covering the selection of structural and acoustic elements, damping considerations, and post-processing techniques such as sound pressure level (SPL) calculations, radiated acoustic power, and equivalent radiated power (ERP). These theoretical foundations serve as the basis for the methodology and simulations conducted in this thesis.

3.1 Acoustics Fundamentals

The following discussion on sound waves and their characteristics is summarized from the work of Pierce [6].

Acoustics is the branch of physics that deals with the study of all mechanical waves in gases, liquids, and solids including topics such as vibration, sound, ultrasound, and infrasound. A sound wave is typically produced by a vibrating object and propagates through a transmission medium such as air, water, or steel. Understanding how sound waves travel and interact with their environments is crucial for numerous applications,

ranging from architectural design to noise reduction in transportation.

Sound Propagation:

Sound waves propagate as fluctuations in pressure and particle displacement within a medium. These waves can be characterized as longitudinal waves where the displacement of the medium is parallel to the direction of wave propagation. The speed of sound varies depending on the medium through which it travels and is influenced by the medium's properties such as density and elasticity. The general formula for the speed of sound in a medium is given by:

$$c = \sqrt{\frac{K}{\rho}}$$

where c is the speed of sound, K is the stiffness of the medium (bulk modulus), and ρ is the density of the medium.

Mechanics of Sound Waves:

Typically, waves are termed 'acoustic' when they can be characterized primarily by compression and expansion of the medium, excluding any shear effects. These waves are classified as longitudinal because the displacement of the medium is parallel to the direction of wave propagation. When particles in the medium deviate from their stress-free configuration, they generate internal forces due to dilatation. These forces, known as acoustic pressures, are linearly proportional to the volumetric strain. Sound waves result from small vibrations within a medium that lacks shear stiffness, leading to dilatational (volumetric) changes in the medium. The medium's inertia opposes these dilatational accelerations, a fundamental aspect of acoustic waves.

Viscosity and Wave Attenuation:

While primarily dilatational, acoustic waves can also exhibit effects of bulk and shear viscosity, which attenuate the wave as it propagates through the medium. In addition to viscosity, acoustic waves can diminish in amplitude due to interactions with thin, reactive layers such as carpets or specially designed 'acoustic layers'. These interactions are critical in environments where sound control is necessary, influencing the design of materials and structures to achieve desired acoustic properties.[24]

The Wave Equation:

The behavior of sound waves can be described by the acoustic wave equation, which is a second-order partial differential equation that relates the pressure or displacement of the wave at any point in the medium to the time and spatial derivatives. The wave equation in one dimension can be expressed as:

$$\begin{aligned} \frac{\partial^2 p}{\partial t^2} &= c^2 \Delta p \\ \Delta p &= \frac{\partial^2 p}{\partial x^2} + \frac{\partial^2 p}{\partial y^2} + \frac{\partial^2 p}{\partial z^2} \end{aligned}$$

where p represents the sound pressure, c is the speed of sound, t is time, Δp is the Laplacian and x, y, z are the spatial coordinates. This equation assumes the sound wave is moving through a non-dissipative medium without any interference from boundaries or other objects.

Characteristics of Sound Waves:

Key characteristics of sound waves include their frequency, wavelength, amplitude, and speed:

- **Frequency (f):** The number of times the wave oscillates per second, measured in Hertz (Hz).
- **Wavelength (λ):** The distance between successive crests or troughs in a wave.
- **Amplitude:** The height of the wave crest or depth of the trough from the rest position, which correlates with the loudness of the sound.
- **Speed (c):** As discussed, this depends on the medium.

The relationship between wavelength, frequency, and speed of sound is given by[6]:

$$\lambda = \frac{c}{f}$$

Understanding sound propagation is essential for applications such as architectural acoustics, where sound behavior within a room or building must be controlled, or in environmental acoustics, where the impact of sound on human health and well-being is of concern. Numerical methods like the Finite Element Method (FEM) and Boundary Element Method (BEM) are commonly used to solve the wave equation for complex boundary conditions and irregular geometries that cannot be easily addressed analytically.

Coupled Acoustic-Structural Analysis: Coupled acoustic-structural analysis involves the study of interactions between structural dynamics and acoustic phenomena, primarily focusing on how vibrations in structures generate and influence sound waves. This field is essential for understanding the noise emissions of various mechanical systems, vehicles, and building components under vibrational stress. It examines the transmission of sound through different materials and structures, assessing how vibrations from these structures generate acoustic waves that propagate through the surrounding environment. Such analyses are crucial for designing quieter and more comfortable living and working spaces, as well as for improving the sound quality of products and enhancing noise control measures.

3.2 Near and Far Field Acoustics

Understanding the distinction between near and far field acoustics is crucial in the analysis of acoustic phenomena, when assessing the interaction of sound waves with structures or in open environments. This distinction affects how acoustic simulations and measurements are approached, especially in computational acoustics where the accuracy of the mesh density and the applicability of boundary conditions are influenced by these regions.

3.2.1 Near Field

The near field is defined as the region within one wavelength from the source or structure. Characteristics of the near field are:

- High complexity in acoustic pressure and velocity fields due to the proximity to the source.
- Presence of evanescent waves, which decay exponentially with distance from the source, and do not contribute significantly to sound propagation at larger distances.
- Significant influence of the structural interactions, such as added mass effects, where the motion of the structure interacts dynamically with the surrounding acoustic medium.
- Mesh density and quality in this region crucially affect the accuracy of simulation results, necessitating finer meshes to capture the detailed acoustic phenomena accurately.

The near-field region diminishes in size as the frequency increases because the structural wavelengths decrease. Consequently, the acoustic properties and the computational requirements change rapidly over small distances.

3.2.2 Far Field

Beyond one wavelength from the source or structure, the region is considered as the far field. In this region:

- The complexities associated with the near field significantly diminish, leading to simpler and more predictable acoustic behavior.
- Evanescent effects are negligible, and the acoustic waves propagate without the rapid spatial variations observed in the near field.
- The influence of the near-field mesh on simulation results becomes less critical, allowing for coarser meshes compared to the near field.
- Simulation requirements focus more on capturing the propagative aspects of the acoustic waves and less on the intricate interactions close to the source.

It is important to note that while the near-field mesh can have a limited impact on the far-field results, the boundary conditions applied at the far-field boundary must be chosen carefully to ensure accurate simulation of wave propagation and absorption. This often involves different strategies than those used at the near-field boundary, emphasizing the need for appropriate far-field boundary conditions that prevent reflections and simulate an open domain effectively.

These distinctions guide the setup of computational models in acoustic simulations, influencing everything from the choice of element types and sizes to the strategies for implementing boundary conditions and assessing simulation fidelity [25].

3.3 Numerical Methods in Acoustics

Numerical methods in acoustics are essential for solving problems that are too complex for analytical solutions. These methods allow for the accurate simulation of acoustic phenomena under a variety of conditions and constraints. While analytical methods provide solutions in idealized scenarios, numerical methods can handle the irregular geometries, complex boundary conditions, and material properties often encountered in real-world applications.

3.3.1 Finite Element Method (FEM)

The Finite Element Method (FEM) is widely used in acoustic simulations due to its flexibility in modeling complex materials and geometries. It involves dividing a large system into smaller, simpler parts that are called finite elements. The equations that model these elements are then assembled into a larger system of equations that models the entire problem. FEM is particularly effective in Coupled Acoustic-Structural Analysis where structural vibrations interact with surrounding acoustic fields. This method is used in commercial software such as Abaqus, which provides advanced capabilities for simulating acoustic behavior in engineering applications.

FEM excels in handling complex materials and geometrical configurations by breaking down a large system into smaller, manageable sub-domains known as finite elements. This method transforms a complex partial differential equation (PDE) that represents the physics of the problem into a set of algebraic equations that can be solved computationally.

From PDEs to Algebraic Equations:

The essence of the Finite Element Method involves transforming the strong form of a partial differential equation (PDE) into its weak form. This transformation begins by multiplying the PDE by a test function v (also known as the weight function) and integrating over the domain. This step is crucial in reducing the order of derivatives required for a numerical solution.

Integration by parts is utilized to shift derivatives from the solution function, known as the trial function u , to the test function v . This process, illustrated for a second-order differential operator, is shown below [26]:

$$\int_0^\ell v(x)u''(x) dx = [v(x)u'(x)]_0^\ell - \int_0^\ell v'(x)u'(x) dx$$

This equation demonstrates how boundary terms emerge and the derivative orders are reduced. The trial function u and the test function v belong to appropriate function spaces that satisfy the boundary conditions of the problem, ensuring the validity of the integration by parts.

Transforming the problem from its original strong form to the integral weak form allows for the approximate numerical solution by discretizing the domain and applying the finite element method. This methodology is fundamental in engineering applications

facilitated by commercial software like Abaqus, where such numerical techniques are implemented to solve complex real-world problems.

Discretization and Assembly

The weak form equations are discretized into a system of linear equations by subdividing the domain into finite elements, often using a mesh. Each element is associated with a set of shape functions that approximate the field variables within the element. The global system of equations is assembled from the contributions of all elements:

$$[K]\{u\} = \{F\} \quad (3.3.1)$$

where $[K]$ is the global stiffness matrix, $\{u\}$ the vector of unknown nodal displacements, and $\{F\}$ the vector of forces.

Three Stages of FEM in Software:

In software like Abaqus, FEM involves three key stages:

1. **Pre-processing:** Includes defining the geometry, generating the mesh, applying material properties, and setting boundary conditions. This stage sets up the problem for analysis.
2. **Solution:** The solver computes the unknowns using numerical methods to solve the assembled system of equations. This phase may involve linear or nonlinear, static or dynamic analyses.
3. **Post-processing:** The results are visualized and analyzed. This includes reviewing displacements, stresses, or other relevant physical quantities to evaluate the behavior of the model under specified conditions.

FEM is particularly effective for Coupled Acoustic-Structural Analysis in Abaqus, where the interaction between structural vibrations and acoustic fields is critical. The method's flexibility in modeling diverse physical phenomena makes it indispensable for predicting acoustic behavior in various engineering applications.

3.3.2 Boundary Element Method (BEM)

The Boundary Element Method (BEM) is another powerful numerical technique used in acoustics, especially suited for problems involving infinite or semi-infinite domains, like exterior sound radiation problems. BEM reduces the dimensionality of a problem by one, as it only requires discretization of the boundary rather than the entire volume. This can significantly decrease computational effort in cases where the boundary is simpler than the volume. Unlike the Finite Element Method, which requires artificial boundary conditions to model infinite domains, BEM naturally satisfies far-field boundary conditions through the use of fundamental solutions. In acoustics, the fundamental solution of the Helmholtz equation inherently satisfies the Sommerfeld radiation condition, ensuring that waves radiate outward to infinity without reflection. BEM's implementation in open-source software like BEMPP allows for detailed exploration and modification of

acoustic simulations, facilitating the advancement of research and application in acoustic analysis.

Harmonic Analysis in Vibro-Acoustics

In Coupled Acoustic-Structural Analysis problems focusing on steady-state responses to harmonic excitation, the harmonic wave equation becomes essential. This equation, distinct from the standard time-dependent wave equation, is pivotal in understanding how sound waves behave under steady-state excitation and is extensively used in simulations that aim to predict noise generated by vibrating structures in a fluid medium, such as a gearbox surrounded by air.

3.3.3 From General Wave Equation to Harmonic Wave Equation

The general wave equation for sound in a medium is given by:

$$\frac{\partial^2 p}{\partial t^2} = c^2 \Delta p \quad (3.3.2)$$

where p represents the pressure field, c the speed of sound in the medium, and Δ denotes the Laplacian operator.

Assuming the pressure varies harmonically with time, $p(\mathbf{x}, \mathbf{y}, \mathbf{z}, t) = \text{Re}\{p(\mathbf{x}, \mathbf{y}, \mathbf{z})e^{-i\omega t}\}$, and substituting into the general wave equation leads to a simplification where time derivatives are transformed into algebraic terms:

$$\frac{\partial^2}{\partial t^2} (p(\mathbf{x}, \mathbf{y}, \mathbf{z})e^{-i\omega t}) = -\omega^2 p(\mathbf{x}, \mathbf{y}, \mathbf{z})e^{-i\omega t} \quad (3.3.3)$$

Substituting equation (3.3.3) into equation (3.3.2), we get:

$$-\omega^2 p = c^2 \Delta p$$

or, rearranging terms,

$$\Delta p + \frac{\omega^2}{c^2} p = 0$$

Defining the wave number k as $k = \frac{\omega}{c}$, we obtain the Helmholtz equation:

$$\Delta p + k^2 p = 0$$

Significance of the Wave Number k

The wave number k represents the spatial frequency of the wave and is directly proportional to the frequency of the sound and inversely proportional to the speed of sound in the medium. It determines the wavelength λ of the sound wave through the relationship $\lambda = \frac{2\pi}{k}$. The wave number's magnitude affects how sound waves propagate through different media; a higher k implies a shorter wavelength, which affects the wave's ability to diffract around obstacles and interact with the medium.

Additionally, the sign of k in the Helmholtz equation influences the nature of the solution. A positive k^2 leads to oscillatory solutions, indicative of propagating waves. In contrast, a negative k^2 would lead to exponentially decaying solutions.

This section of the thesis provides the theoretical foundation necessary for the ensuing discussion on specific vibro-acoustic simulation techniques applied to the study cases in later chapters.

3.3.4 Free-Field and Sommerfeld Radiation Conditions

Free-Field Conditions

Free-field conditions are typically assumed in acoustic problems to simulate an environment devoid of any reflecting boundaries or obstacles. This setup is essential for examining the inherent propagation characteristics of sound waves from a source, as it suggests that the medium extends infinitely in all directions and that sound waves do not encounter any barriers that would reflect or scatter the sound back toward the source.

Sommerfeld Radiation Condition

The Sommerfeld radiation condition for time-harmonic waves, is a mathematical formulation used to ensure that the solution to a wave equation represents outgoing waves at infinity. This condition is essential in numerical simulations to prevent any artificial reflection of waves at the boundary of the computational domain:

$$\lim_{r \rightarrow \infty} r \left(\frac{\partial p}{\partial r} - ikp \right) = 0 \quad (3.3.4)$$

where p is the pressure field, r is the distance from the source, and k is the wave number. The condition states that the spherical wave amplitude decreases proportionally to $\frac{1}{r}$ and the derivative of the wave is predominantly outgoing.

Comparison and Application

While both conditions are used to describe wave behavior in unbounded domains, they serve different purposes in acoustic modeling. Free-field conditions are more of a physical assumption about the environment, while the Sommerfeld radiation condition is a mathematical tool to enforce the correct behavior at the computational domain's boundaries. In practical simulations, these conditions help to accurately predict the physical behavior of acoustic waves in free space and are crucial for validating theoretical models with experimental data [17].

3.4 Acoustic Analysis Methodologies in Abaqus

Abaqus¹, developed by Dassault Systemes, is a comprehensive suite of software solutions for finite element analysis and computer-aided engineering. Known for its robust capabilities in simulating the physical behavior of materials and products under load,

¹Abaqus: <https://www.3ds.com/products/simulia/abaqus/standard>

Abaqus offers two main solvers: Abaqus/Standard and Abaqus/Explicit. Abaqus/Standard uses an implicit integration scheme, well-suited for static and low-speed dynamic events where highly accurate stress solutions are critical. Conversely, Abaqus/Explicit is designed to handle highly nonlinear problems with complex contacts and large deformations where transient dynamic phenomena are significant. It uses an explicit time integration method, which is more suitable for cases where very rapid transient events occur, such as crashes or explosions.

For the purposes of this thesis, Abaqus/Standard is employed primarily for its proficiency in handling linear dynamic simulations and small-scale deformations efficiently within coupled acoustic-structural analyses under steady-state harmonic excitation. This solver is particularly suitable due to its robust computational stability and precise handling of acoustic phenomena, which are central to this research. Additionally, it is preferred for its ability to handle frequency domain solutions effectively, which is crucial for understanding the behavior of structures subjected to sinusoidal or harmonic loads over time [27].

Overview

Acoustic analysis in Abaqus is utilized to simulate various engineering phenomena that involve interactions between fluids (such as air and water) and structures. These phenomena range from low-amplitude wave propagation in acoustic mediums, such as the sound waves generated by musical instruments in air, to high-amplitude shock analyses, where fluids interact dynamically with structural boundaries, such as the impact of underwater explosions on ship hulls. Shock analysis typically involves wave amplitudes that are significantly higher than those found in standard acoustic problems and requires specific consideration regarding the intensity of fluid-structure interactions, which is not the focus of this thesis.

3.4.1 Acoustic Analysis in Abaqus

Acoustic analysis is employed to address a broad spectrum of problems, including:

- Sound propagation, emission, and radiation in various environments.
- The natural frequencies of vibration within cavities filled with acoustic fluids.
- Noise levels inside vehicles or other enclosed structures through coupled acoustic-structural systems.
- Transmission of sound through structural barriers.

The simulation of problems focusing on steady-state responses to harmonic excitation in Abaqus can be conducted using various dynamic procedures:

- Mode-Based Steady-State Dynamic Analysis
- Subspace-Based Steady-State Dynamic Analysis
- Direct-Solution Steady-State Dynamic Analysis

These procedures are applicable to:

- Acoustic media in isolation, which are useful for studying phenomena such as the natural resonance of fluid-filled cavities.
- Coupled acoustic-structural systems, which are crucial for assessing sound transmission and noise levels within coupled environments.

Modeling Considerations in Abaqus:

- Acoustic elements are required for simulating the fluid medium.
- Surface-based interactions, such as tie constraints or acoustic interface elements, are employed for modeling coupled systems.
- Both interior and exterior acoustic problems can be addressed, facilitating the study of structures that either enclose or are situated within infinite acoustic domains.

In this thesis, the Direct-Solution Steady-State Dynamic Analysis procedure has been employed to address exterior acoustic problems, focusing on structures located within an infinitely extending fluid medium, specifically atmospheric air. This method aligns with the need to evaluate acoustic phenomena under steady-state harmonic excitation and is suited to scenarios where shear stress effects are negligible. Detailed discussions on each analysis procedure used in this study are presented in the following sections, offering insights into their operational mechanisms and applications.

3.4.2 Input(.inp) file structure of Abaqus

The Abaqus input file (.inp) is crucial for defining the complete model and analysis settings in a text format, which can be executed using the Abaqus solver without the need for the graphical user interface (GUI). This capability is particularly useful for automating repetitive tasks or running batch analyses in high-performance computing environments.

General Structure of an input File

An input file in Abaqus is typically structured in several sections, each defining specific aspects of the simulation [28]:

- **Heading:** Describes the analysis or provides comments for user reference.
- **Preprocessor:** Defines material properties, element types, and model geometry.
- **Assembly:** Specifies the assembly of the model components if multiple parts or instances are involved.
- **Boundary Conditions:** Applies constraints and loads to the model.

- **Step:** Defines the analysis steps, including the type of analysis (static, dynamic, etc.), time settings, and specific solution controls.
- **Output Requests:** Specifies the results to be outputted for post-processing.
- **End Step:** Marks the completion of an analysis step.

Example input file for a frequency extraction Analysis

```
*Heading
** Job name: AcousticExample
*Material, name=Steel
*Elastic
210000, 0.3
*Density
7800
*Node
1, 0.0, 0.0, 0.0
2, 1.0, 0.0, 0.0
*Element, type=B31, ELSET=BeamElements
1, 1, 2
*BEAM SECTION, ELSET=BeamElements, SECTION=RECT, MATERIAL=Steel
0.1, 0.1
*Nset, nset=FixedEnd, generate
1, 1
*Nset, nset=LoadEnd
2, 2
*Boundary
FixedEnd, ENCASTRE
*Step, name=FrequencyResponse, nlgeom=N0, perturbation
*Frequency, eigensolver=Lanczos, acoustic coupling = on
10
*Node Print, nset=LoadEnd
U, FREQUENCY
*End Step
```

The above input file for Abaqus sets up a basic structural analysis using beam elements to determine the frequency response of a simple structure. It defines a material named 'Steel' with elastic properties and a density typical for steel. Nodes and elements are specified to construct the geometry, with one end of the beam fixed in all directions (ENCASTRE boundary condition). The beam's cross-sectional properties are defined using a rectangular section, specified in the *BEAM SECTION entry, which determines the structural characteristics such as moment of inertia and section modulus necessary for the analysis. The analysis step named 'FrequencyResponse' is configured to use the Lanczos eigensolver for frequency extraction, emphasizing the coupling effect of acoustic phenomena. The output request is set up to print the displacement and frequency at the load-applied node, indicating the focus on how the structure's frequency response is analyzed under fixed-end conditions.

3.5 Coupled Exterior Acoustic-Structural Analysis in Abaqus

Coupled acoustic-structural analysis enables engineers to predict how vibrations in solid structures produce sound in the adjacent air. This section presents the fundamental principles of structural-acoustic interaction and details how it is implemented in Abaqus. The discussion includes real-life structural-acoustic interaction, describing how mechanical vibrations generate sound waves in practical applications and modelling strategies in Abaqus,

3.5.1 Real-Life Dynamics of Structural-Acoustic Interaction

In the real world, sound is often generated by the vibration of structures. For instance, when a structure like a building facade or a machine casing vibrates due to external forces (e.g., wind, operational loads), these vibrations transfer energy to the surrounding air, creating sound waves. This transmission occurs because the mechanical vibrations of the structure induce movements in the air particles, leading to variations in air pressure which propagate as sound. The intensity and characteristics of this sound depend on the vibration frequency of the structure, its material properties, and how these vibrations interact with the air [29].

3.5.2 Modeling in Abaqus

In Abaqus, coupled exterior acoustic-structural analysis is used to simulate this interaction between structural vibrations and surrounding air. Initially, the structural model is meshed and assigned appropriate material properties such as Young's modulus, Poisson's ratio, damping coefficient and density. A separate acoustic mesh, representing the air, surrounds the structural model. This acoustic domain is assigned properties like air density and bulk modulus to simulate the air's resistance to compression under sound wave propagation.

In Abaqus, the connection between the structural and acoustic meshes is typically managed via coupling elements that ensure the transfer of vibrational energy from the structural boundaries to the acoustic field. The structural model's displacements, which result from applied harmonic loads, are transmitted to the nodes of acoustic mesh. These movements simulate the vibrational energy that would cause sound waves in real life. The analysis does not connect rotational degrees of freedom because sound waves in air are purely compressional and do not involve shear.

To accurately capture the dynamic response, Abaqus uses various steady-state dynamic analysis procedures. These analyses help predict how the structure will respond to different frequencies of excitation and how these responses lead to sound radiation in the adjacent air. The solver computes the response of the system over a range of frequencies, typically focusing on the natural frequencies of the structure, which are the frequencies at which the structure would naturally tend to vibrate most strongly. By simulating this process, engineers can predict the sound levels generated by the structure and assess

potential impacts on the environment and human comfort.

This approach in Abaqus provides a comprehensive tool for engineers to study the vibratory and acoustic behavior of structures within their operational environments, enabling the design and implementation of noise mitigation strategies where necessary [24].

3.6 Harmonic Analysis

Harmonic analysis, also known as steady-state dynamic analysis, is used to evaluate how structures behave when subjected to continuous, sinusoidal forces. This type of analysis helps determine how the structure responds once the initial effects of the force have settled, and the behavior becomes consistent over time. It is crucial for identifying whether the structure experiences resonance - a phenomenon where certain frequencies cause excessive vibrations, stress, noise, or motion. A key characteristic of harmonic analysis is that if a system is subjected to a steady, sinusoidal input, the resulting output will also be sinusoidal, but its amplitude and phase may differ depending on the system's properties. In the context of acoustics, harmonic analysis becomes especially significant. By applying it to a structure coupled with an acoustic cavity, it is possible to predict how sound waves propagate through and around the structure.

Dynamic problems can be analyzed in two principal ways:

- **Time Domain:** This method studies how a system responds to any type of input over time, including sudden or changing forces (known as transient responses). However, finding the system's stable behavior (steady state) using this approach can take a lot of time and computing power, as the entire process needs to be calculated step by step.
- **Frequency Domain:** This method focuses on how the system behaves when subjected to steady, repeating forces at a specific frequency (sinusoidal inputs). Instead of analyzing the entire process, it simplifies the calculation by directly solving for the system's response at one frequency at a time. By analysing different frequencies, steady-state behavior could be found efficiently across a frequency range of interest, saving time and computational effort.

Harmonic excitation refers to sinusoidal forces or loads applied to a system. The harmonic response is primarily determined by three main variables: frequency, amplitude, and phase angle. These components are explained below:

- **Frequency (f):**

Frequency represents how many oscillations occur in one second and is measured in Hertz (Hz). It is related to the circular frequency (ω) and the time period (T_f) as follows:

$$\omega = 2\pi f, \quad f = \frac{1}{T_f}$$

Here, ω is the imposed circular frequency in radians per second, f is the frequency in Hz, and T_f is the time period of one oscillation.

- **Amplitude (F_i):**

Amplitude is the maximum magnitude of the applied force or load during an oscillation. It dictates the peak value of the excitation, both in positive and negative directions. The amplitude plays a significant role in determining the intensity of the system's response to harmonic excitation.

- **Phase Angle (θ_i):**

The phase angle defines the timing difference between the applied load and the system's response. This becomes critical when multiple forces are applied, as the relative phase determines how the different excitations interact. For example, phase differences can amplify or cancel out responses depending on their alignment.

The harmonic excitation function is expressed as:

$$F = F_i \sin(\omega_i t + \theta_i)$$

Where:

- ω_i : Imposed circular frequency
- F_i : Amplitude of excitation
- θ_i : Phase angle
- t : Time
- F : The instantaneous force at time t

By substituting specific values for t , the force F at any given moment can be calculated. This sinusoidal nature of the excitation ensures that the behavior remains consistent over time in steady-state conditions.

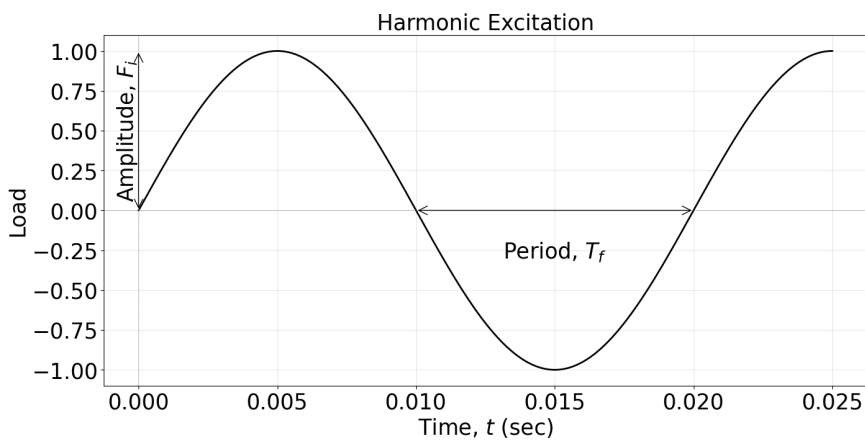


Figure 3.6.1: Harmonic excitation illustrating amplitude and time period.

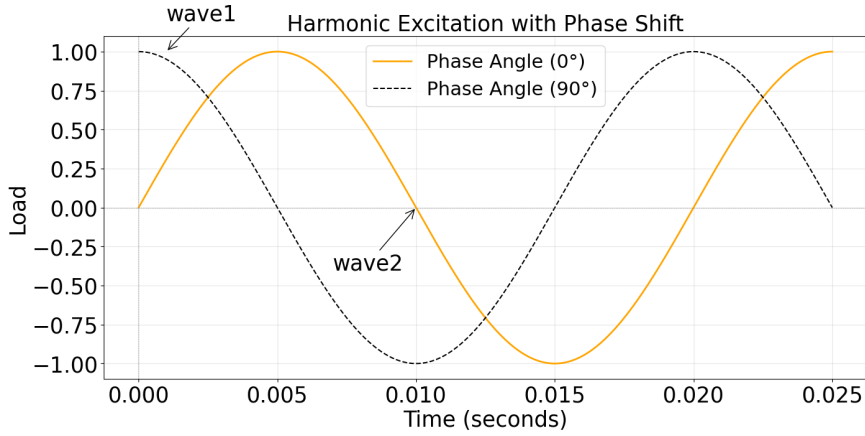


Figure 3.6.2: Harmonic excitation illustrating Phase shift.

Complex Notation and Analysis

The use of complex variables simplifies the mathematics of harmonic analysis. By representing sinusoidal functions in complex exponential form, the analysis can directly deal with the phase and amplitude changes across the system. The general form of a sinusoidal function in complex notation is:

$$z = Ae^{i\phi} = A(\cos \phi + i \sin \phi)$$

where A is the amplitude, and ϕ is the phase angle. This formulation allows for an elegant and compact representation of sinusoidal functions.

Displacement, Velocity, and Acceleration

In the context of harmonic analysis, while force and displacement have been discussed, it is equally important to understand other related quantities, such as velocity and acceleration. These quantities also offer insights into the dynamic behavior of a structure under sinusoidal loading.

From basic physics, the relationships for velocity and acceleration can be expressed as:

$$\dot{u} = \frac{du}{dt} \quad (\text{Velocity}), \quad \ddot{u} = \frac{d\dot{u}}{dt} = \frac{d^2u}{dt^2} \quad (\text{Acceleration}).$$

Assuming a sinusoidal displacement of the form:

$$u = Ae^{i\Omega t},$$

the velocity and acceleration can be computed by differentiating this expression:

$$\dot{u} = i\Omega Ae^{i\Omega t}, \quad \ddot{u} = -\Omega^2 Ae^{i\Omega t}.$$

For visualization purposes, reverting to the trigonometric form of the equations provides:

$$u = A(\cos(\Omega t) + i \sin(\Omega t)),$$

$$\dot{u} = \Omega A (-\sin(\Omega t) + i \cos(\Omega t)),$$

$$\ddot{u} = -\Omega^2 A (\cos(\Omega t) + i \sin(\Omega t)).$$

These equations highlight the phase relationships between displacement, velocity, and acceleration:

- Velocity is shifted 90° out of phase with displacement.
- Acceleration is shifted 180° out of phase with displacement (or 90° from velocity).
- **Displacement and velocity:** When the displacement is at its maximum or minimum, the velocity is zero. Conversely, when velocity is at its maximum, displacement passes through zero. This 90° phase difference is crucial in harmonic motion.
- **Displacement and acceleration:** The acceleration is at its maximum when the displacement is at its minimum, and vice versa. This demonstrates a 180° phase shift.

These relationships can be visualized in Figure 3.6.3 and Figure 3.6.4, which depict the time-domain variations of these quantities.

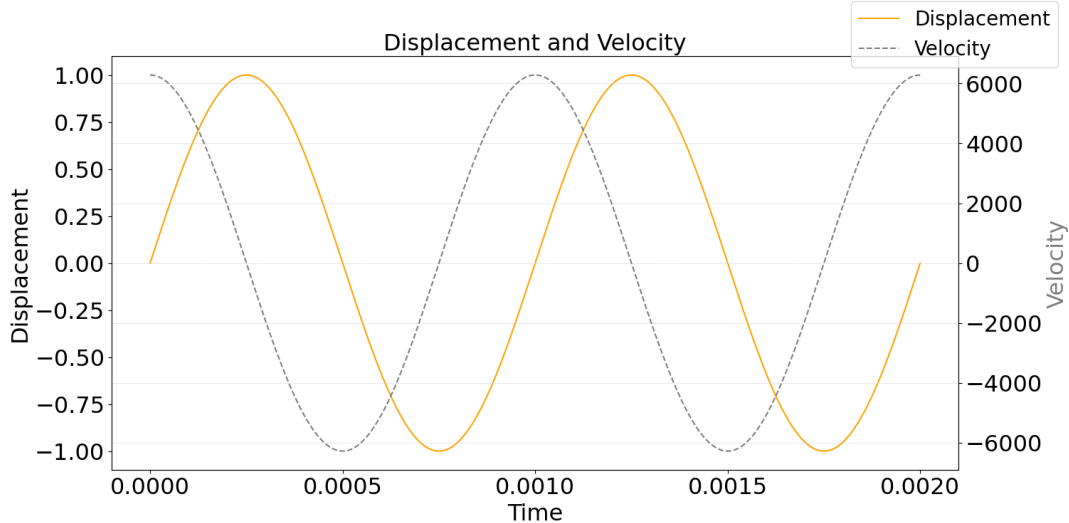


Figure 3.6.3: Time-domain relationship between displacement and velocity. The 90° phase difference is illustrated.

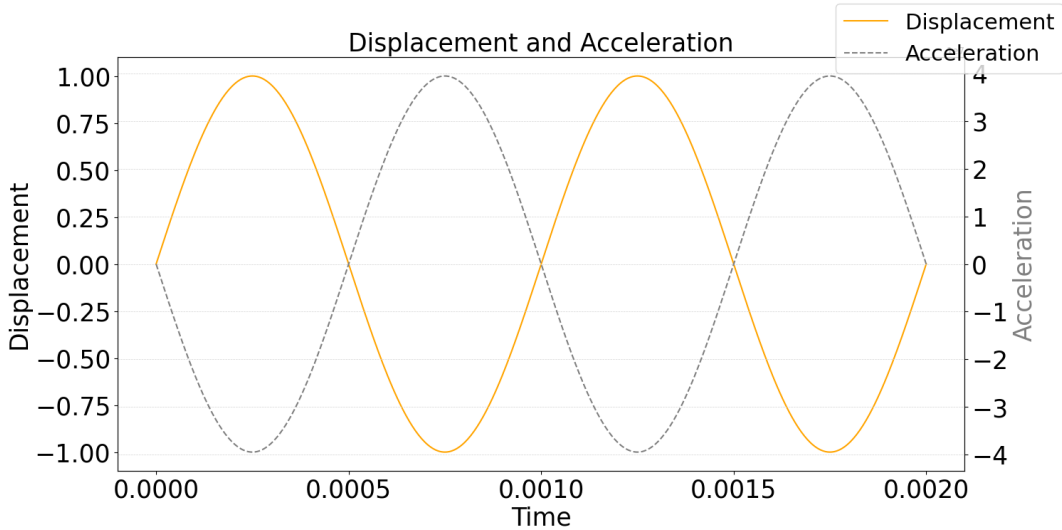


Figure 3.6.4: Time-domain relationship between displacement and acceleration. The 180° phase difference is shown.

3.6.1 An Example of Harmonic Analysis

A Harmonic solution to the equation below has been discussed in this section. The equation expresses the governing equations of motion in matrix form, which describes the behavior of a dynamic system under harmonic excitation. This equation can be written as:

$$[M]\{\ddot{u}\} + [C]\{\dot{u}\} + [K]\{u\} = \{F\}$$

Here, $[M]$ represents the mass matrix, $[C]$ is the damping matrix, $[K]$ is the stiffness matrix, and $\{F\}$ is the forcing function. The terms $\{\ddot{u}\}$, $\{\dot{u}\}$, and $\{u\}$ denote acceleration, velocity, and displacement vectors, respectively.

Since the input and output are harmonic, the forcing function $\{F\}$ and the displacement vector $\{u\}$ are expressed as sinusoidal functions, represented in complex form:

$$\{F\} = \{F_{\max}e^{i\psi}\}e^{i\Omega t}, \quad \{u\} = \{u_{\max}e^{i\phi}\}e^{i\Omega t}$$

where:

- ψ is the force phase shift,
- ϕ is the displacement phase shift,
- Ω is the imposed circular frequency, and
- t is time.

The sinusoidal representation of displacement is substituted into the equation:

$$\{u\} = \{u_{\max}e^{i\phi}\}e^{i\Omega t}.$$

Differentiating this expression gives:

$$\begin{aligned}\{\dot{u}\} &= \frac{d}{dt}\{u\} = i\Omega\{u_{\max}e^{i\phi}\}e^{i\Omega t}, \\ \{\ddot{u}\} &= \frac{d}{dt}\{\dot{u}\} = (i\Omega)^2\{u_{\max}e^{i\phi}\}e^{i\Omega t} = -\Omega^2\{u_{\max}e^{i\phi}\}e^{i\Omega t}.\end{aligned}$$

Simplification and Rearrangement

Substitute $\{\ddot{u}\}$, $\{\dot{u}\}$, and $\{u\}$ into the governing equation:

$$[M](-\Omega^2\{u_{\max}e^{i\phi}\}e^{i\Omega t}) + [C](i\Omega\{u_{\max}e^{i\phi}\}e^{i\Omega t}) + [K](\{u_{\max}e^{i\phi}\}e^{i\Omega t}) = \{F_{\max}e^{i\psi}\}e^{i\Omega t}.$$

Since $e^{i\Omega t}$ is common across all terms and non-zero, divide through by $e^{i\Omega t}$ to obtain:

$$(-\Omega^2[M] + i\Omega[C] + [K])\{u_{\max}e^{i\phi}\} = \{F_{\max}e^{i\psi}\}.$$

Separating Real and Imaginary Components

Represent the displacement and force in terms of their real and imaginary components:

$$\{u_{\max}e^{i\phi}\} = \{u_1\} + i\{u_2\}, \quad \{F_{\max}e^{i\psi}\} = \{F_1\} + i\{F_2\}.$$

Substituting these into the equation gives:

$$(-\Omega^2[M] + i\Omega[C] + [K])(\{u_1\} + i\{u_2\}) = (\{F_1\} + i\{F_2\}).$$

This is the harmonic equation of motion in the frequency domain. The frequency domain formulation reduces the time-dependent problem to a steady-state analysis for a given frequency Ω . The terms in the equation represent:

- $-\Omega^2[M]$: Inertial forces.
- $i\Omega[C]$: Damping forces.
- $[K]$: Stiffness forces.

The real ($\{u_1\}, \{F_1\}$) and imaginary ($\{u_2\}, \{F_2\}$) components describe the phase relationships in the system's response. By solving this equation, one can analyze the system's resonance, phase shifts, and response amplitude to ensure it operates safely and efficiently under dynamic conditions.

3.6.1.1 Mode Shapes and Modal Superposition

Mode shapes represent the characteristic deformation patterns of a structure vibrating at its natural frequencies. Each mode shape corresponds to a specific natural frequency and depicts how the structure deforms spatially when oscillating in that mode [30]. Analyzing mode shapes provides insight into how different parts of a structure move relative to each other during vibration, helping identify regions prone to high stress or displacement. This understanding is critical for designing and optimizing structures subject to dynamic loading.

To efficiently solve the governing equations of motion in harmonic analysis, the modal superposition method is employed. This approach leverages the orthogonality of mode shapes to decouple the equations into independent modal equations, significantly reducing computational complexity.

Steps to Derive Modal Equations

The governing equation of motion for a system under harmonic loads and displacements is given by:

$$(-\Omega^2[M] + i\Omega[C] + [K])\{u\} = \{F\},$$

To transform this into modal form, the following steps are performed:

- 1. Mode Shape Decomposition:** The displacement vector $\{u\}$ is expressed as a linear combination of mode shapes:

$$\{u\} = \sum_{j=1}^n \{\phi_j\} y_{jc}, \quad \text{or equivalently, } \{u\} = [\Phi]\{y_c\},$$

where:

- $[\Phi]$ is the matrix of mode shapes, with each column representing a mode shape $\{\phi_j\}$,
- $\{y_c\}$ is the vector of modal coordinates, and y_{jc} is the modal coordinate for mode j .

- 2. Orthogonal Transformation:** The mode shapes satisfy orthogonality conditions with respect to the mass, damping, and stiffness matrices:

$$[\Phi]^T[M][\Phi] = [I], \quad [\Phi]^T[K][\Phi] = [\Lambda], \quad [\Phi]^T[C][\Phi] = [\Gamma],$$

where:

- $[I]$ is the Identity matrix
- $[\Lambda]$ is a diagonal matrix containing the eigenvalues ω_j^2 , and
- $[\Gamma]$ is a diagonal matrix representing the damping terms.

3. Decoupling the Equations: Substituting $\{u\} = [\Phi]\{y_c\}$ into the governing equation and premultiplying by $[\Phi]^T$ results in:

$$(-\Omega^2[I] + i\Omega[\Gamma] + [\Lambda])\{y_c\} = \{f_c\},$$

where $\{f_c\} = [\Phi]^T\{F\}$ is the modal force vector.

Since $[\Lambda]$, $[\Gamma]$, and $[I]$ are diagonal matrices, the equations decouple into independent equations for each mode:

$$(-\Omega^2 + i2\omega_j\zeta_j\Omega + \omega_j^2)y_{jc} = f_{jc},$$

where:

- ω_j is the natural circular frequency of mode j ,
- ζ_j is the damping ratio for mode j ,
- y_{jc} is the complex modal coordinate, and
- f_{jc} is the modal force for mode j .

Solution and Reconstruction

The solution for each modal coordinate y_{jc} is obtained as:

$$y_{jc} = \frac{f_{jc}}{\omega_j^2 - \Omega^2 + i(2\omega_j\zeta_j\Omega)}.$$

Once the modal coordinates are computed, the total displacement vector $\{u\}$ is reconstructed by summing the contributions of all modes:

$$\{u\} = \sum_{j=1}^n \{\phi_j\} y_{jc}.$$

Intuition Behind the Approach

The modal superposition method decomposes the system's response into contributions from individual modes, offering several advantages. The orthogonality of mode shapes transforms the coupled system of equations into independent equations for each mode, simplifying the computation and enabling decoupling. This approach is computationally efficient, as only the dominant modes - those with significant contributions to the response - need to be considered, thereby reducing computational cost. Moreover, it provides physical insight by representing each mode as a specific vibration pattern and analyzing its contribution to the overall response, which helps engineers identify resonances and assess the effects of damping. Additionally, the use of complex numbers allows for a compact representation of sinusoidal motion by encapsulating both amplitude and phase information, making the analysis straightforward. This method is particularly advantageous for systems with a large number of degrees of freedom, enabling efficient and accurate analysis of steady-state responses to harmonic excitations. Widely applied in structural dynamics, acoustics, and vibration analysis, modal superposition is a cornerstone for understanding and addressing harmonic loads.

Discussion on Damping and Resonance

The behavior of modal coordinates can be understood by analyzing the following equation:

$$y_{jc} = \frac{f_{jc}}{\omega_j^2 - \Omega^2 + i(2\omega_j\zeta_j\Omega)},$$

where y_{jc} represents the modal coordinate, Ω is the excitation frequency, ω_j is the natural frequency, and ζ_j is the damping ratio.

A few key observations can be made:

- When the excitation frequency (Ω) equals the natural frequency (ω_j), and the damping ratio (ζ_j) is zero, the denominator of the equation becomes zero, causing the modal coordinate (y_{jc}) to become infinite. This theoretical scenario, known as resonance, highlights the importance of damping in real-world systems to prevent non-physical infinite responses.
- In practical systems, resonance ($\Omega = \omega_j$) can lead to significant vibrations if damping is insufficient. Introducing appropriate damping ensures the response remains physically realistic and avoids structural damage.
- Additionally, at resonance ($\Omega = \omega_j$), the phase angle of the system's response to the input shifts by 90 degrees. This phenomenon occurs because, at resonance, the inertial and elastic forces balance each other, leaving the damping force as the dominant term in the system's response. Mathematically, the imaginary component of the denominator ($i(2\omega_j\zeta_j\Omega)$) dominates, leading to a phase angle of approximately $\phi = 90^\circ$. This phase shift indicates that the displacement reaches its maximum when the driving force is at its peak velocity, rather than being in sync with the force itself. The implications of this phase shift are significant: at resonance, the system absorbs energy most efficiently from the excitation, resulting in maximum response amplitude, which can lead to large oscillations and potential structural damage if not properly damped. The 90-degree phase shift highlights the inherent lag between the driving force and the system's displacement, a key characteristic of resonance. This phase relationship must be carefully considered during system design to ensure stability and minimize undesirable effects. In practical applications such as vibration isolation or noise control, understanding this phase behavior enables engineers to design effective damping mechanisms or tuning systems to mitigate resonance effects and protect the structure from harm.

Amplitude and Phase in Relation to Real and Imaginary Components

The result of the harmonic analysis is the complex displacement vector:

$$\{u_c\} = \sum_{j=1}^n \{C_j\},$$

where $\{C_j\}$ represents the contribution of mode j to the total displacement.

The output of this analysis provides both real and imaginary components, which are often less intuitive to interpret. Instead, the amplitude and phase are more meaningful metrics:

- The amplitude (A) represents the magnitude of the response and can be computed from the real (x) and imaginary (y) components using the relationship:

$$A = \sqrt{x^2 + y^2}.$$

- The phase angle (ϕ) indicates the temporal shift of the response relative to the input and is calculated as:

$$\phi = \tan^{-1} \left(\frac{y}{x} \right).$$

Using these relationships, the amplitude of the steady-state response can be determined, providing valuable insight into the system's behavior under harmonic excitation. This interpretation is particularly helpful in identifying resonant frequencies and understanding the phase relationship between the applied force and the resulting displacement.

The real and imaginary components of the response can also be understood as varying contributions of the cosine (cos) and sine (sin) components of the motion over time. For a given time t , the displacement can be represented as:

$$\{u\} = \{u_{\max} e^{i\phi}\} e^{i\Omega t}.$$

This equation encapsulates both the amplitude and phase of the response, highlighting the sinusoidal nature of the displacement. By considering the complex displacement vector, engineers can easily analyze and predict the steady-state behavior of systems under harmonic loads [31].

This discussion emphasizes the critical role of damping in controlling resonance and avoiding unbounded responses in dynamic systems. It also underscores the importance of amplitude and phase in comprehending the system's behavior. While the real and imaginary components provide a mathematical basis, their transformation into amplitude and phase offers a more intuitive understanding of the response. This approach bridges the gap between mathematical rigor and practical application, making it a cornerstone of harmonic analysis.

This overview sets the stage for detailed discussions on dynamic procedures in Abaqus available for acoustic analysis such as Mode-Based, Subspace-Based and Direct-Solution Steady-State Dynamic Analysis, which will be elaborated in subsequent sections.

3.6.2 Material Damping in harmonic analysis

Material damping in Abaqus is critical for simulating the energy dissipation mechanisms inherent in materials or structures when subjected to dynamic loading. This damping can be configured for different types of dynamic analysis, including direct-solution, subspace-based steady-state dynamics and mode-based dynamic analysis in Abaqus/Standard.

Rayleigh Damping: Rayleigh damping in Abaqus provides a mechanism to introduce general damping into the system, which is especially useful when other forms of energy dissipation like dashpots or inelastic material behavior are absent. It is defined using two coefficients:

- α_R (mass proportional damping) affects the lower frequencies more because it adds a damping force that is proportional to the mass-related terms in the system's equations of motion. Since mass effects dominate the system's inertia at lower frequencies, α_R helps in controlling excessive motion where inertia is significant, thus dampening the lower frequency vibrations more effectively.
- β_R (stiffness proportional damping) impacts higher frequencies to a greater extent as it introduces damping that is proportional to the stiffness of the system. At higher frequencies, the stiffness-related forces are predominant due to the stiffer response of materials to faster oscillations. This makes β_R particularly effective in attenuating vibrations where stiffness governs the dynamic behavior.

These coefficients are adjustable and allow for the damping effects to be tailored according to specific dynamic characteristics of the system being modeled. This form of damping is especially beneficial in simulations of engineered systems where damping needs to be incorporated to predict physical behavior accurately under dynamic loading conditions.

Mathematically, the critical damping ratio ξ_i for a given mode i is calculated as:

$$\xi_i = \frac{\alpha_R}{2\omega_i} + \frac{\beta_R\omega_i}{2} \quad (3.6.5)$$

where ω_i represents the natural frequency of mode i . This formula highlights the respective influences of mass and stiffness proportional damping by modulating the contribution of each based on the frequency. Lower frequencies see a higher impact from α_R due to the division by ω_i , and higher frequencies are more affected by β_R as its influence grows with ω_i as shown in the Figure 3.6.5. This dual mechanism ensures that damping is appropriately applied across the spectrum of vibrational modes, enhancing both the stability and accuracy of dynamic simulations.

Input File Usage: Material damping properties are set in the input file as follows:

```
*Material, name=Steel
*Damping, alpha=0.005, beta=1.2e-4
```

This input specifies both mass-proportional and stiffness-proportional Rayleigh damping for a material named "Steel", ensuring that both low and high-frequency responses are appropriately damped based on the defined α_R and β_R values.

Applications and Implications

Incorporating material damping is crucial for accurately predicting the dynamic response of structures to operational loads, especially in environments where energy dissipation influences overall structural integrity and service life. It also plays a significant role in the design and analysis of acoustic environments, where damping directly affects sound propagation and noise levels.

Understanding and implementing material damping correctly in simulations helps engineers design safer and more reliable structures by accurately predicting how they respond to dynamic stresses and environmental interactions [32].

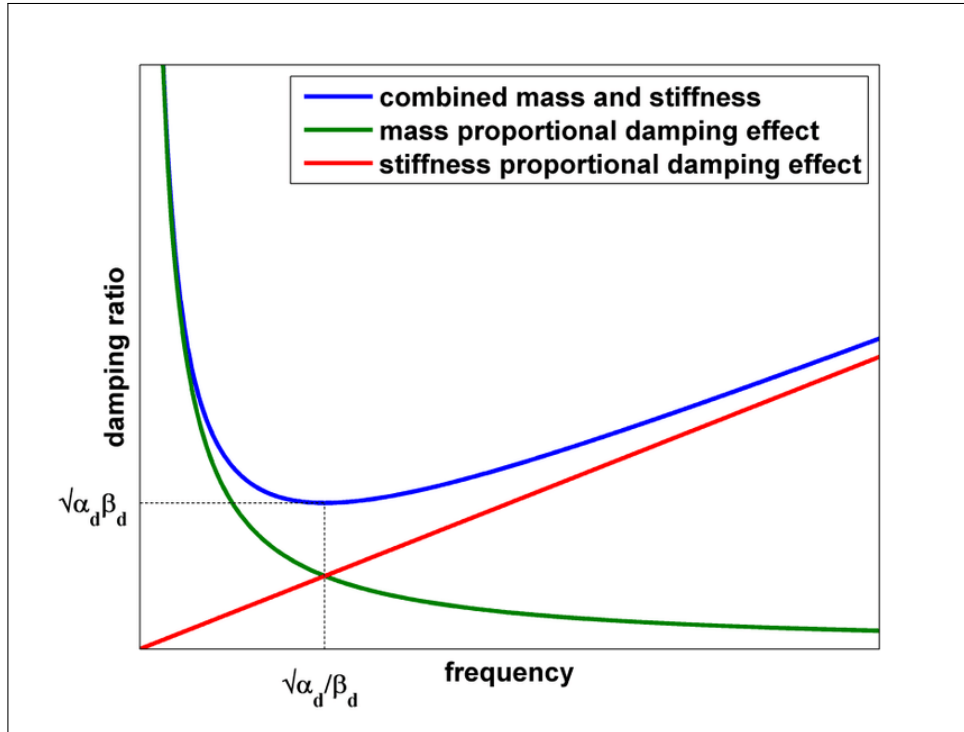


Figure 3.6.5: Relationship between mass-proportional and stiffness-proportional damping [1]

Structural Damping:

Structural damping is a type of damping mechanism where the damping forces are proportional to the forces induced by the structural stresses and are directionally opposed to the velocity. This relationship necessitates that the displacement and velocity are out of phase by exactly 90° . Such a characteristic makes structural damping particularly effective in frequency domain dynamic analyses, where the interactions of forces and movements are predominantly cyclic and predictable.

Mathematical Representation: Structural damping models the damping forces as directly proportional to the forces induced by structural stresses but phase-shifted by 90 degrees. This phase shift implies that the damping forces act in opposition to the velocity, characteristic of how frictional forces behave in dynamic systems. The mathematical expression for the damping forces is given by:

$$F_D^N = i s I^N, \quad (3.6.6)$$

where F_D^N represents the damping forces, $i = \sqrt{-1}$ introduces a phase shift of 90 degrees (making the damping forces orthogonal to the velocity vector), s is the user-defined structural damping factor, and I^N denotes the internal forces generated by stressing the structure. This representation is effective in scenarios where damping closely resembles frictional behavior, such as in joints within a mechanical system or in materials exhibiting significant internal friction. The application of this damping type is crucial in the analysis of systems where traditional viscous damping models (proportional to velocity) do not adequately describe the energy dissipation behavior.

Applications: Structural damping is suitable for systems that exhibit significant frictional interactions, such as the dry rubbing of joints in a multi-link mechanism or materials that inherently demonstrate frictional characteristics. This form of damping can also be represented in simulation models by using mechanical dampers, such as connectors with damping properties, or by defining a complex stiffness in spring elements. It is particularly utilized in steady-state dynamic analyses where nondiagonal damping matrixes are allowed, enabling a more accurate representation of the structural behavior under cyclic loads.

Input File Specification: To define structural damping in a simulation, the following syntax is used in the input file:

```
DAMPING, STRUCTURAL=s
```

where s specifies the damping factor, tuning the degree of damping applied to the structure based on the anticipated frictional effects.

This form of damping is instrumental in managing the dynamic response of structures, ensuring that the simulations reflect realistic behavior under operational conditions. It is crucial for engineers to carefully select the damping parameters to align with the physical properties and expected dynamic interactions within the modeled system [32].

3.6.3 Mode-Based Steady-State Dynamic Analysis

Mode-based steady-state dynamic analysis is employed to compute the linear response of a structure to harmonic loads, leveraging the system's eigenmodes. This approach is a linear perturbation procedure, meaning it assumes small deviations from an undeformed state, and it requires pre-calculation of the system's natural frequencies and mode shapes through an eigenfrequency extraction procedure.

- **Procedure Overview:** Mode-based steady-state dynamic analysis leverages the concept of modal superposition, where the total response of a system to harmonic excitation is approximated by summing the individual responses of each mode. Each mode's response is scaled by its *mode participation factor*, which quantifies how much that mode contributes to the response at a particular excitation frequency. Essentially, the system's response at any given frequency is constructed by combining the effects of each eigenmode.
- **Computational Efficiency:** This method is generally more efficient in terms of processing time compared to direct-solution methods. It reduces computational complexity by focusing on a subset of the total degrees of freedom-those defined by the selected eigenmodes-thereby typically requiring less computational power. However, it is important to note that the initial frequency extraction step in mode-based analysis, where eigenmodes up to at least 1.5 times the maximum frequency of interest should be extracted to ensure accuracy, may require significant memory usage. While this initial step can be memory-intensive, ensuring all relevant dynamic behaviors of the system are captured, the subsequent modal analysis steps are less demanding in terms of memory and computational power. This

makes mode-based SSD suitable for many scenarios; however, if memory is constrained during the frequency extraction step, a direct-solution SSD approach may be preferable as it bypasses the need for extensive mode extraction.

- **Accuracy and Limitations:** The accuracy of mode-based analysis may diminish under certain conditions:
 - **Material Damping:** Significant damping can alter the energy dissipation characteristics of the modes, which may not be accurately captured if damping is not properly modeled.
 - **Close to Natural Frequencies:** If the excitation frequency approaches one of the system's natural frequencies (resonance), the response prediction may become overly sensitive to small perturbations in input data or modeling assumptions, leading to potential inaccuracies.
- **Applications:** Mode-based analysis is useful for evaluating the vibrational behavior of structures under operational loads, such as machinery at work or buildings subjected to environmental vibrations. It also facilitates the calculation of *acoustic contribution factors*, which help identify and quantify the contributions of different structural modes to overall acoustic emissions. This is crucial for designing quieter and more harmoniously operating machines and structures.

Prior to performing mode-based steady-state dynamic analysis, it is crucial to determine the system's eigenfrequencies. This process typically involves an eigenfrequency extraction step, where both eigenmodes. Eigenmodes represent the natural vibration patterns of the system at specific frequencies. The number of modes to be extracted depends on the required accuracy and the specific dynamic characteristics of the system.

In defining a mode-based analysis within a simulation environment such as Abaqus, you specify:

- The frequency range of interest.
- The number of frequencies within this range for which responses are needed, including the bounding frequencies.

The analysis can account for initial stress effects if stress-stiffening (due to nonlinear geometric effects) was considered in any prior general analysis step [33].

Example input File Snippet: The following example illustrates the setup for a mode-based steady-state dynamic analysis in an Abaqus input file. This setup focuses on specifying the frequency range and modal analysis parameters, critical for assessing the dynamic response of a structure under harmonic excitation.

```
*Heading
** Job Name: ModalBasedDynamicAnalysis
*Material, name=Steel
*Elastic
210E3, 0.3
```

```
*Density
7800
*Node, nset=AllNodes
1, 0, 0, 0
2, 1, 0, 0
*Element, type=B31, elset=BeamElements
1, 1, 2
*BEAM SECTION, ELSET=BeamElements, SECTION=RECT, MATERIAL=Steel
0.1, 0.1
*Nset, nset=FixedEnd
1,
*Nset, nset=LoadEnd
2,
*Boundary
FixedEnd, ENCASTRE
*STEP
*FREQUENCY,eigensolver=lanczos,
10,30,5
*END STEP
*STEP
*STEADY STATE DYNAMICS,FREQUENCY SCALE=LINEAR
10,20,6
*CLOAD, OP=NEW
LoadEnd,1,100.0
*END STEP
```

This setup initiates a modal dynamic analysis step, focusing on the frequency range from 10 to 30 Hz. It is designed to calculate responses at five frequencies within this range to adequately capture the steady-state behavior under harmonic excitation. This frequency extraction is crucial as it determines the modal information that will be used in the subsequent steady-state dynamic analysis step. The analysis between 10 to 20 Hz utilizes these extracted modes to assess the dynamic response of the structure under operational conditions. To ensure comprehensive coverage and accuracy in the steady-state response, a frequency extraction up to 30 Hz is performed, following a thumb rule of using 1.5 times the maximum frequency of interest in the steady-state dynamic analysis. This approach ensures that the modal contributions to the dynamic response are fully captured, particularly near the higher end of the frequency range.

The ‘CLOAD’ command within the steady-state dynamic analysis step specifies a harmonic load applied at the ‘LoadEnd’ node. Although ‘CLOAD’ typically defines a point load, within the context of steady-state dynamics, it assumes a harmonic characteristic with a defined amplitude. Here, the amplitude is set at 100 units, and the frequency of excitation is defined by the frequencies specified in the dynamic step. This setup allows for the analysis of how the structure responds under varying sinusoidal load conditions, capturing essential dynamics such as resonance and acoustic behavior within the structure.

3.6.4 Subspace-Based Steady-State Dynamic Analysis

Overview: Subspace-based steady-state dynamic analysis is employed to compute the steady-state response of structures to harmonic excitations. Unlike direct-solution methods that consider all physical degrees of freedom, this method projects the dynamic equations onto a selected subspace of modes from the undamped system, combining efficiency with the ability to model frequency-dependent phenomena like damping and viscoelastic effects.

Procedure: The process begins with an eigenfrequency extraction to identify the undamped system's modes, including both eigenmodes and optional residual modes. These modes form a basis for the subspace onto which the dynamic equations are projected. This projection simplifies the equations to a smaller system, which is computationally less demanding to solve.

Mathematical Formulation: The steady-state dynamic response equations are projected onto a subspace defined by the extracted modes, resulting in a reduced set of complex equations:

$$\mathbf{K}_{\text{red}} \mathbf{u} = \mathbf{F}_{\text{red}} \quad (3.6.7)$$

where \mathbf{K}_{red} represents the reduced stiffness matrix and \mathbf{F}_{red} the reduced force vector, both of which depend on the selected modes. The solution of these equations provides modal amplitudes, which are then used to compute nodal displacements, stresses, and other quantities.

Computational Advantages: This method is particularly effective when dealing with nonsymmetric systems or when incorporating complex material behaviors such as viscoelasticity. It allows for the inclusion of non-modal forms of damping and captures frequency-dependent effects more accurately than mode-based methods, though it is typically more computationally intensive than mode-based but less so than direct-solution approaches.

Application Scope: Ideal for systems where the dynamic response is influenced by significant damping or viscoelastic behaviors. It is also suitable for analyses where the stiffness matrix is nonsymmetric, often due to complex loading or boundary conditions.

Key Considerations: While the subspace-based method simplifies the computation by reducing the number of equations, the accuracy of the results heavily depends on the correct selection of modes. Adequately capturing the dynamics of the system requires careful consideration of the mode coverage, particularly around the frequencies of interest [34].

Example Input File: Below is an example of how to set up a subspace-based steady-state dynamic analysis in an Abaqus input file:

```
*Heading
** Job Name: SubspaceBasedAnalysis
*Material, name=Steel
*Elastic
210E3, 0.3
*Density
7800
```

```

*Node, nset=AllNodes
1, 0, 0, 0
2, 1, 0, 0
*Element, type=B31, elset=BeamElements
1, 1, 2
*BEAM SECTION, ELSET=BeamElements, SECTION=RECT, MATERIAL=Steel
0.1, 0.1
*Nset, nset=FixedEnd
1,
*Nset, nset=LoadEnd
2,
*Boundary
FixedEnd, ENCASTRE
*STEP
*FREQUENCY,eigensolver=lanczos,
10,30,5
*END STEP
*STEP
*STEADY STATE DYNAMICS, SUBSPACE PROJECTION, FREQUENCY SCALE=LINEAR
10,20,6
*SELECT EIGENMODES
5
*CLOAD, OP=NEW
LoadEnd,1,100.0
*END STEP

```

This input file setup demonstrates the initiation of a subspace-based steady-state dynamic analysis targeting a specific range of frequencies to assess the dynamic behavior under harmonic loading conditions. The main analysis step (*STEADY STATE DYNAMICS) is configured to project the dynamic equilibrium equations onto a subspace defined by selected eigenmodes. The SUBSPACE PROJECTION keyword indicates that the system's response is calculated based on a reduced model that includes only the most influential modes. The *SELECT EIGENMODES command specifies that only a subset of the calculated eigenmodes-here, the first 5-are used for the dynamic analysis. This selection is essential for ensuring that the model remains computationally manageable while still capturing the critical dynamic behavior of the system.

3.6.5 Direct-Solution Steady-State Dynamic Analysis

Direct-Solution Steady-State Dynamic Analysis is a crucial computational technique in structural dynamics, particularly for evaluating the response of systems to harmonic excitation. Unlike mode-based and subspace-based analyses, which utilize reduced models based on eigenmodes or subspaces of selected modes respectively, the direct-solution steady-state dynamic analysis method calculates the response directly in terms of the physical degrees of freedom of the system. It offers several distinct features and advantages:

- **Procedure Type:** This is a linear perturbation procedure that provides the steady-state dynamic response of a structure directly from its assembled mass, damping, and stiffness matrices.
- **Computational Detail:** The Direct-Solution Steady-State Dynamic Analysis (SSD) method calculates the steady-state response of structures directly using the physical degrees of freedom. Unlike modal analysis, which reduces the problem to modal coordinates, direct SSD confronts the full complexity of the dynamic system. This approach involves solving the frequency domain form of the equations of motion, expressed as:

$$(-\omega^2 M + i\omega C + K)\hat{u} = \hat{F}$$

where:

- M is the mass matrix,
- C is the damping matrix,
- K is the stiffness matrix,
- ω is the angular frequency of excitation,
- \hat{u} represents the complex amplitude of the displacement response,
- \hat{F} is the amplitude of the harmonic load.

The above equation, $K_{\text{eff}}\hat{u} = \hat{F}$ with $K_{\text{eff}} = -\omega^2 M + i\omega C + K$, effectively captures the dynamics of the system under harmonic excitation. This method is computationally intensive due to the need to solve large systems of complex equations directly at each frequency point of interest, making it more accurate, especially for systems with complex material behaviors like viscoelasticity or significant damping. It provides high-fidelity insights into the dynamic interactions within the system without any modal approximation, ensuring detailed and accurate prediction of dynamic responses.

- **Accuracy:** It is particularly noted for its high accuracy in cases where material properties vary with frequency or where the structure exhibits nonsymmetric stiffness-conditions where eigenvalues might not be easily extracted.
- **Applications:** Suitable for analyzing systems with nonsymmetric stiffness matrices, or when damping cannot be approximated using modal damping alone. It is also applicable in the presence of viscoelastic materials.

Frequency Specification: In defining a direct-solution steady-state dynamic step, the frequency range and the density of frequency points within this range should be specified. These points can be uniformly distributed (linear spacing) or spaced to give more focus near the start or end of the range (logarithmic spacing). The choice of spacing impacts how finely the response is calculated across the frequency spectrum, which is critical for capturing peak responses accurately.

Input File Example: The setup for a direct-solution steady-state dynamic analysis in an Abaqus input file involves specifying the type of frequency interval and the method of frequency calculation. Here are detailed examples of each configuration:

***STEADY STATE DYNAMICS, DIRECT, FREQUENCY SCALE=LOGARITHMIC**

Using logarithmic spacing is advantageous when expecting significant changes in response at lower frequencies or wanting to capture detailed behavior near resonance peaks more efficiently. This setting spaces frequency points in a logarithmic scale, increasing the resolution at lower frequencies, which is useful for systems with a broad frequency response.

***STEADY STATE DYNAMICS, DIRECT, FREQUENCY SCALE=LINEAR**

Linear frequency spacing is used when a uniform distribution of frequency points is required across the specified range. This is typical for analyses where the response is expected to vary linearly or when the interest is spread evenly across the entire frequency spectrum.

This configuration allows for detailed control over how the harmonic analysis is conducted, ensuring that engineers can tailor the simulation to reflect specific testing or operational conditions.

Damping: The presence of damping is crucial to prevent the response from becoming unbounded when the forcing frequency matches a natural frequency of the structure. Accurately modeling damping is vital for precise results, especially near natural frequencies. Damping in this context can be implemented through various methods:

- Dashpots,
- Rayleigh damping, which includes material and element-associated damping factors,
- Acoustic damping, relevant for acoustic elements and infinite elements,
- Structural damping, for handling damping forces proportional to structural stresses,
- Viscoelasticity, integrated into the material definitions for capturing frequency-dependent behaviors.

Initial Conditions: The base state for a steady-state dynamic analysis captures the state of the system at the end of the last general analysis step. If the sequence begins with a perturbation step, initial conditions set during this stage are crucial as they establish the starting point for dynamic analysis. This is especially important in analyses where the preceding steps involve non-linear behavior or other complex interactions that affect the system's state. For example, in a structural analysis involving plastic deformation, the residual stresses and deformed geometry become the initial state for subsequent dynamic analysis.

Initial conditions that directly prescribe dynamic solution variables, such as velocities, are generally not applicable in steady-state dynamic analysis. Instead, the focus is on how the structure's state is shaped by prior loading or interactions that affects its dynamic

response. This linkage ensures that any pre-existing stresses or deformations are considered, providing a more accurate and realistic simulation of the structure's behavior under dynamic loading conditions.

Boundary Conditions: Boundary conditions in steady-state dynamic analysis can be applied to both the real and imaginary parts of any degree of freedom. It is physically not possible to restrain one part and not restraint the other part. Conditions are specified for both the in-phase and out-of-phase components of the displacement or velocity.

Example of Boundary conditions for displacement or velocity:

```
*BOUNDARY, REAL, TYPE=Displacement
12001001, 1, 1, 4.447408612316e-07

*BOUNDARY, IMAGINARY, TYPE=Displacement
13571303, 2, 2, -1.110874671554e-05

*BOUNDARY, REAL, TYPE=Velocity
12001001, 1, 1, 4.447408612316e-07

*BOUNDARY, IMAGINARY, TYPE=Velocity
13571303, 2, 2, -1.110874671554e-05
```

The entries in the boundary condition commands represent:

- The first number is the node number where the condition is applied.
- The second and third numbers specify the degrees of freedom (DoF) affected, where: '1, 2, 3' correspond to linear displacements or velocities in the x, y, and z directions, respectively, '4, 5, 6' correspond to rotational movements around the x, y, and z axes, respectively.
- A range, such as '1, 1', indicates the condition applies to a single DoF, while a range like '1, 3' would apply to x, y, and z linear DoFs.
- The last number specifies the actual boundary value applied, whether for displacement or velocity, in phase or out of phase.

These specifications allow the model to handle dynamic loads realistically, modeling both the magnitude and phase of the load's effect on the structure. This nuanced approach is crucial for accurately predicting the dynamic response of the structure under operational conditions, ensuring both realism and precision in the simulation outputs.

Loads: The model can include various types of loads, all assumed to vary sinusoidally over the specified frequency range. The Available loads are:

- Concentrated nodal forces,
- Distributed pressure or body forces,

- Incident wave loads to model sound waves,

```
*CLOAD, REAL
node number, DOF, magnitude
*CLOAD, IMAGINARY
node number, DOF, magnitude
*DLOAD, REAL
element set, type, magnitude, distribution
*DLOAD, IMAGINARY
element set, type, magnitude, distribution
```

Explanation:

- *CLOAD, REAL and *CLOAD, IMAGINARY commands are used to apply concentrated nodal forces that vary sinusoidally. The real part specifies the in-phase component of the force, while the imaginary part specifies the out-of-phase component.
- *DLOAD, REAL and *DLOAD, IMAGINARY commands apply distributed loads (such as pressures) across elements. Like the concentrated loads, the real command defines the sinusoidal load's in-phase component, and the imaginary command defines the out-of-phase component. These specifications allow for precise modeling of dynamic effects under harmonic excitation, enabling the simulation to accurately reflect the complex interplay of forces within the modeled structure during dynamic loading conditions.

Material Options and Inertia Effects in SSD Analysis: In direct steady-state dynamic analysis, the primary focus is on the response of the structure under harmonic loading conditions. Typically, material properties such as density are crucial as they contribute to the mass matrix of the system, influencing the dynamic behavior. For analyses involving very low frequency excitations where inertial effects are negligible compared to stiffness effects, setting the density to a nominal value effectively removes the influence of mass. This simplification is useful when the interest lies primarily in the stiffness response of the material or structure [35].

Example Input File: Below is an example of how to set up a Direct solution steady-state dynamic analysis in an Abaqus input file:

```
*Heading
** Job Name: SubspaceBasedAnalysis
*Material, name=Steel
*Elastic
210E3, 0.3
*Density
7800
*Node, nset>AllNodes
1, 0, 0, 0
2, 1, 0, 0
```

```
*Element, type=B31, elset=BeamElements
1, 1, 2
*BEAM SECTION, ELSET=BeamElements, SECTION=RECT, MATERIAL=Steel
0.1, 0.1
*Nset, nset=FixedEnd
1,
*Nset, nset=LoadEnd
2,
*Boundary
FixedEnd, ENCASTRE
*STEP
*Steady State Dynamics, direct, frequency scale=linear
500,1500,101
*CLOAD, OP=NEW
LoadEnd,1,100.0
*END STEP
```

The provided Abaqus input file sets up a Direct Solution Steady-State Dynamic Analysis, focusing on evaluating the structure's response under harmonic excitation without resorting to a prior modal analysis. This approach directly incorporates the physical degrees of freedom, enhancing accuracy in predicting the dynamic behavior. The file defines a linear elastic material for a beam structure, applies fixed constraints at one end, and introduces a harmonic load at the other. The analysis step specifies a direct dynamic procedure across a linearly scaled frequency range from 500 Hz to 1500 Hz, calculated at 101 frequency points, aiming to capture the structure's response at each frequency without reducing the model complexity through modal decomposition. This setup is ideal for examining the direct impact of dynamic loads on the structure, providing a detailed insight into its vibrational characteristics without the simplification of modal participation factors.

3.7 Structural Elements in Coupled Acoustic Structural Analysis

Before conducting a coupled acoustic-structural analysis, it is essential to choose appropriate structural elements that accurately capture the vibrational response of the system. The type of structural elements used significantly influences the accuracy of results, computational efficiency, and the ability to simulate real-world behavior under dynamic loading conditions.

This section discusses the fundamental structural elements used in coupled acoustic-structural simulations, focusing on their formulation and practical applications.

3.7.1 Shell Elements

Shell elements are a fundamental component in finite element analysis for modeling thin structures such as vehicle bodies and aircraft fuselages. In Abaqus, these elements are classified mainly into triangular and quadrilateral shapes, commonly referred to as S3R for triangular and S4R for quadrilateral elements, where 'R' signifies reduced integration.

Element Choice: The selection between triangular (S3R) and quadrilateral (S4R) shell elements typically depends on the specific geometrical complexities of the model. Triangular shell elements are particularly advantageous in modeling areas with intricate geometries due to their ability to more easily conform to irregular shapes. Conversely, quadrilateral elements are favored for their enhanced accuracy in more regular, structured geometries.

Order of Elements:

- **First-Order Elements:** These elements (e.g., S3, S4 without suffixes) provide a linear approximation through each element. They are commonly employed in scenarios where the analysis demands are moderate and the geometrical representation does not require high precision.
- **Second-Order Elements:** Elements such as S8R include mid-side nodes that offer a quadratic approximation of the geometry, significantly enhancing the modeling accuracy, particularly in curved regions. These elements are used when the analysis requires a detailed representation of the geometry to capture complex behaviors accurately [36].

Reduced Integration: Reduced integration techniques are crucial in finite element analysis to mitigate numerical problems such as shear locking. Shear locking occurs when thin shell elements inaccurately stiffen due to constraints imposed by numerical integration, affecting elements that are slender or have a high aspect ratio. This phenomenon can lead to erroneous results, such as overly stiff responses to loads.

Reduced integration addresses this issue by decreasing the number of integration points within each element. Typically, elements are integrated using Gauss points, where full integration might use a complete set for all strain components. In reduced integration, fewer Gauss points are used, which helps in avoiding the over-constraint of displacement fields that lead to shear locking.

This reduction in integration points serves two primary purposes:

- **Reduction of Numerical Stiffness:** It lessens the computation-induced stiffness, allowing the element to deform more realistically under load, thus providing a more accurate representation of physical behavior.
- **Computational Efficiency:** It lowers the computational burden by simplifying the calculation without significantly compromising the accuracy of results. This is particularly beneficial in complex models where computational resources may be a limiting factor.

By implementing reduced integration, the elements can more accurately simulate the intended physical behaviors of thin structures without the adverse effects of numerical stiffness, making it a valuable technique in structural simulations involving thin elements [37].

3.7.2 Solid Elements

Solid elements in Abaqus such as hexahedrons (C3D8R), tetrahedrons (C3D4), and pentahedrons (C3D6) form the backbone of 3D structural modeling. These elements differ primarily in their geometric configurations, which affects their integration into various meshing strategies:

- **Hexahedral elements (C3D8R):** Known for their robustness in regular, block-like geometries, these elements are often used for their high accuracy and efficiency in structured meshing. The 'R' in C3D8R denotes reduced integration, which helps in reducing computational expense and avoiding common numerical problems such as volumetric locking.
- **Tetrahedral elements (C3D4):** These elements are particularly advantageous for meshing complex geometries that are difficult to discretize with hexahedrons. They provide flexibility but can sometimes lead to less accurate stress distributions and require more elements to achieve the same level of accuracy as hexahedrons.
- **Pentahedral elements (C3D6):** Often used for transitional meshing between hexahedral and tetrahedral meshes, providing a good balance in terms of mesh quality and computational efficiency in complex geometries [38].

Meshing and Discretization: The process of meshing in software like Hypermesh involves converting the geometric model into a finite element model by discretizing it into elements. The quality of this discretization directly influences the accuracy, efficiency, and convergence of the simulation. Effective meshing strategies consider the type of structural element used, the expected regions of high deformation, and the geometric complexity of the model.

These elements are fundamental in simulating how structures behave under various load conditions, including acoustic pressures, and are crucial for detailed analysis in fields such as automotive, aerospace, and civil engineering.

3.8 Acoustic Medium

An acoustic medium is crucial for modeling the propagation of sound within various environments in coupled acoustic-structural analyses. Typically, this medium is an elastic fluid where the stress state is hydrostatic, meaning it supports no shear stress, and pressure changes are directly proportional to the volumetric strain.

Defining an Acoustic Medium

In the realm of acoustic simulation, the medium is defined by its ability to conduct sound waves, represented by small pressure changes due to small amplitude excitations. The fundamental equations governing the motion and behavior of the acoustic medium in such simulations are derived from the conservation laws applied to a compressible, inviscid fluid. The equilibrium equation for an acoustic medium, neglecting convective effects which are minimal for velocities up to approximately Mach 0.1, is expressed as:

$$\frac{\partial p}{\partial x} + \gamma \dot{u}_f + \rho_f \ddot{u}_f = 0, \quad (3.8.8)$$

where p represents the dynamic pressure, γ is the volumetric drag, \dot{u}_f and \ddot{u}_f are the velocity and acceleration of the fluid particles, respectively, and ρ_f is the fluid density.

The relationship between pressure and volumetric strain in an inviscid and compressible acoustic medium is given by:

$$p = -K_f \varepsilon_V, \quad (3.8.9)$$

where $\varepsilon_V = \varepsilon_{11} + \varepsilon_{22} + \varepsilon_{33}$ is the volumetric strain, and K_f is the bulk modulus of the fluid, which defines the fluid's resistance to compressibility.

Input File Usage for Defining an Acoustic Medium

In computational models, the acoustic medium is defined with parameters for the bulk modulus and fluid density. The typical input commands in a Abaqus would include:

```
*ACOUSTIC MEDIUM, BULK MODULUS=<value>
DENSITY=<value>
```

Volumetric Drag and Energy Dissipation

Energy dissipation in an acoustic medium, which leads to the attenuation of acoustic waves, can be modeled using a volumetric drag coefficient, γ . This coefficient represents the loss of energy due to the medium's resistance to fluid flow and is particularly important in frequency-domain analyses where it can vary with frequency. The input for defining frequency-dependent volumetric drag in a steady-state dynamics procedure is [39]:

```
ACOUSTIC MEDIUM, VOLUMETRIC DRAG=<expression as function of frequency>
```

3.9 Acoustic Elements in Coupled Acoustic Structural Analysis

In the realm of coupled acoustic-structural analysis, the acoustic elements play a critical role in modeling how sound interacts with structures. These elements are specially designed to manage sound propagation through various media, particularly focusing on the dynamics of acoustic pressure.

Definition and Types of Acoustic Elements

Acoustic elements in finite element analysis are characterized by their capability to handle acoustic pressure as the primary degree of freedom. This allows for accurate

simulation of sound waves within a defined domain, which can be either planar, axisymmetric, or three-dimensional. These elements are typically classified based on their shape and the method of pressure interpolation:

- **Element Shapes:** The basic shapes of acoustic elements include:
 - Two-dimensional elements such as quadrilaterals and triangles, suitable for planar and axisymmetric analyses.
 - Three-dimensional elements such as hexahedrals, tetrahedrals, wedges, and pyramids, allowing for complex volumetric modeling.
 - In Abaqus, these elements are named as AC3D4 (4-node linear acoustic tetrahedron), AC3D6 (6-node linear acoustic pentahedron), AC3D8 (8-node linear acoustic hexahedron).
- **Shape and Meshing Considerations:**
 - Quadrilateral and hexahedral elements generally provide higher accuracy and are preferable for regular geometries.
 - Triangular and tetrahedral elements are favored for complex geometries due to their flexibility in meshing intricate shapes.
 - Pyramid elements serve as transitional elements to facilitate meshing between hexahedral and tetrahedral elements in a mesh.

Interpolation Orders and Integration

Acoustic elements can utilize either linear or quadratic interpolation for acoustic pressure:

- **Linear Acoustic Elements:** These elements provide a linear variation in acoustic pressure across the element and are characterized by piecewise constant pressure gradients. They are efficient for transient analyses, such as in shock simulations using explicit solvers.
- **Quadratic Acoustic Elements:** These elements offer a quadratic variation in acoustic pressure and piecewise linear gradients. They are especially effective in steady-state dynamic analyses due to their enhanced accuracy in predicting Sound Pressure Levels (SPL).
- For Acoustic elements in Abaqus/standard, integration is typically full, meaning that each node contributes to the element's stiffness matrix calculation, enhancing the accuracy at the cost of computational intensity [40].

Material Properties for Acoustic Medium

For acoustic elements to simulate the physics of acoustic medium, the definition of material properties is essential:

- **Bulk Modulus (K_p):** The bulk modulus of an acoustic medium quantifies its compressibility under pressure variations. A higher bulk modulus indicates a less compressible medium. In acoustic simulations, the bulk modulus directly affects how sound pressure waves propagate through the medium. Changes in pressure due to sound waves cause the medium to compress or expand, with the bulk modulus defining the relationship between the induced pressure and the resultant volumetric strain. This relationship is crucial when calculating sound pressure levels in environments where the medium interacts with structural boundaries, as it impacts how sound waves are transmitted or reflected at these interfaces.
- **Density (ρ_f):** The density of the acoustic medium influences the mass properties of the sound-propagating medium. It affects the inertia of the medium, which in turn influences the speed of sound within the medium. The speed of sound is calculated as $\sqrt{K_p/\rho_f}$, demonstrating that sound travels faster in media with higher bulk modulus and lower density. In coupled acoustic-structural analysis, the density impacts how sound waves carry energy through the medium, affecting their attenuation and the energy transfer to structural elements. This is important in determining the vibrational response of structures exposed to acoustic loads, as the intensity and speed of sound waves govern the dynamic pressure fluctuations impacting the structure.

Understanding and appropriately utilizing these acoustic elements and their properties enable precise simulation of how sound waves interact travel in the acoustic medium.

3.10 Modeling Infinite Domains in Abaqus for Exterior Problems

In the analysis of acoustic problems where structures interact with an expansive or infinite acoustic medium-like a submarine operating deep underwater or a building subjected to ambient environmental noise-it is crucial to simulate boundary conditions accurately. This ensures that acoustic waves propagate realistically into the far field without artificial reflections, which could distort simulation results. For instance, consider a submarine submerged in the deep ocean, where it might experience fluid loads and radiate sound into the water as if the ocean were infinitely large. The degree to which the surrounding fluid can be treated as unbounded largely depends on the number of wavelengths between the submarine and any physical boundary. At high frequencies, the fluid may effectively appear infinite, but at lower frequencies, nearby boundaries like the ocean floor or surface could significantly influence acoustic behavior. Similarly, a loudspeaker in a room might emit high-frequency sounds that seem to propagate in an infinite air medium, while lower frequencies are noticeably affected by the room's walls.

Traditional finite elements are inadequate because they cannot simulate the infinite domain effectively. To handle the infinite domains, Abaqus provides several methods: Impedance-Type Radiation boundary Conditions, Perfectly Matched Layers, and Acoustic Infinite Elements. These methods are designed to accurately simulate the propagation of acoustic waves into an infinite extent without requiring the geometric discretization

of the entire space..

Impedance-Type Radiation Boundary Conditions

In this case, acoustic elements are used to model the region between the vibrating structure and a simple geometric surface which is located away from the structure. These conditions model the boundary as a non-reflective surface, allowing waves to radiate away from the structure. Although these conditions are approximate, they provide reasonably accurate results when the boundary is placed sufficiently far from the source, typically at least half the wavelength of the lowest frequency of interest. The accuracy of this approach depends on the mesh size of the elements used to discretize the acoustic medium and the radius of the acoustic cavity surrounding the vibrating structure.

Perfectly Matched Layers

For problems requiring high accuracy in capturing wave behavior at boundaries, perfectly matched layers (PMLs) are used. PMLs absorb incoming acoustic waves regardless of their angle of incidence, effectively simulating an infinite domain. This method modifies the behavior of acoustic elements to absorb all incident waves, thus preventing reflections. It is recommended to use several layers of PML elements, typically between four to seven, to ensure effective absorption. The outer boundary of the PML region should maintain zero pressure and same material properties as those of the acoustic elements to avoid any reflective effects.

3.10.1 Acoustic Infinite Elements

Acoustic infinite elements in Abaqus are designed to simulate the behavior of acoustic waves as they propagate into an infinite medium without reflecting back, effectively extending the finite element method into unbounded domains. These elements are typically implemented at the outer boundaries of a finite element mesh of the acoustic domain surrounding the structure, seamlessly connecting the finite computational domain to the infinite expanse of the surrounding medium.

Function and Placement: Acoustic infinite elements function by allowing the computational model to transition smoothly from a discretely meshed region to an infinite domain. This transition is critical in preventing reflections back into the computational domain, which could otherwise distort analysis results. The placement of these elements is strategic: they are positioned where acoustic wave amplitudes diminish, ensuring that the simulated waves decay naturally as they propagate outward. This placement minimizes the need for larger computational domains, thereby enhancing computational efficiency while maintaining accuracy.

Technical Advantages and Computational Aspects: The formulation of acoustic infinite elements differs significantly from simpler impedance-type radiation conditions. Within Abaqus, these elements are part of a sophisticated scheme where the infinite exterior is conceptually subdivided into elements. This setup enforces a method of weighted residuals on these elements, analogous to traditional finite element methods but extended into the infinite domain. This approach introduces additional degrees of freedom, corresponding to interpolation functions that extend infinitely. While this leads to nonsymmetric infinite element matrices, making them computationally more intensive

than basic radiation conditions, the high accuracy afforded by this method allows for a significantly reduced finite element region. This reduction in the modeled domain size effectively offsets the higher computational cost, making acoustic infinite elements a potent tool for detailed acoustic analysis in scenarios where precision is important [41].

Types of Acoustic Infinite Elements:

Abaqus provides several types of acoustic infinite elements which have acoustic pressure as the only degree of freedom:

- **ACIN2D2:** A 2-node linear 2D, acoustic infinite element
- **ACIN2D3:** A 3-node quadratic 2D acoustic infinite element.
- **ACIN3D3:** A 3-node linear 3D, acoustic infinite triangular element.
- **ACIN3D4:** A 4-node linear 3D, acoustic infinite quadrilateral element.
- **ACIN3D6:** A 6-node quadratic 3D, acoustic infinite triangular element.
- **ACIN3D8:** A 8-node quadratic 3D, acoustic infinite quadrilateral element.

Mapping and Connectivity:

Since Acoustic infinite elements bridge the finite computational domain to the theoretical infinite extent of the surrounding acoustic medium, Proper integration and connectivity are essential for their effective performance:

Nodal Connectivity: The connection between the finite acoustic elements and the infinite elements must be seamless. This connectivity is crucial for ensuring that the transition from the finite element mesh to the infinite domain is smooth, avoiding any discontinuities that could disrupt the wave propagation simulation. The nodes of the acoustic finite elements are used to define the infinite elements, therefore a node to node connectivity is created between the acoustic finite and infinite elements, maintaining continuity in the mesh.

Reference Points and Normal Vectors: For acoustic infinite elements, the accurate mapping of physical space to the infinite domain is facilitated by a well-defined reference point and correctly oriented nodal normal vectors. The reference point, typically positioned at or near the geometric center of the boundary encircling the finite elements, defines a characteristic length for coordinate mapping. This setup is critical in cases like acoustic radiation from a spherical surface, where the reference point ideally lies at the sphere's center. The reference point's location determines the 'radius' and 'node ray' for each node involved in the infinite elements, as illustrated in 3.10.6. A 'node ray' is a unit vector pointing from the reference point towards the node. These vectors are crucial as they are used in the mathematical formulation of the infinite elements, ensuring that the wave propagation is modeled correctly extending into the infinite domain. The correct placement of node rays aids in calculating the 'cosine' values at the interface nodes of the acoustic infinite elements. This value is computed as the smallest dot product between the unit node ray and the unit normals of all surrounding element faces (see 3.10.7). It's critical that these cosine values remain positive; negative values trigger an error.

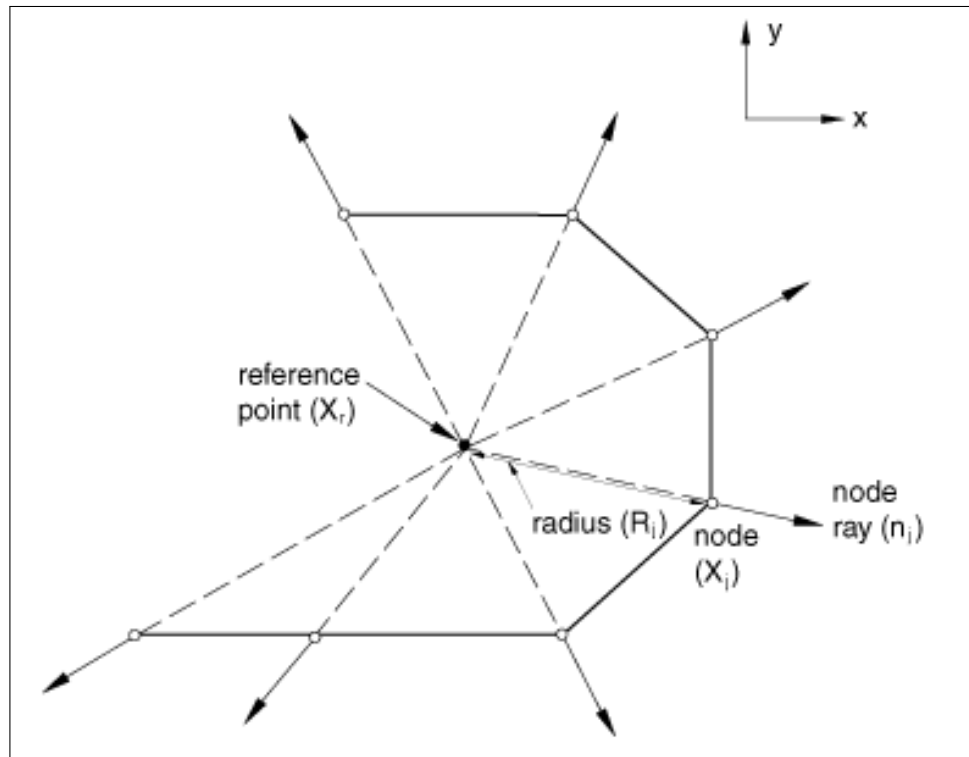


Figure 3.10.6: Reference point and node rays for acoustic infinite elements [2].

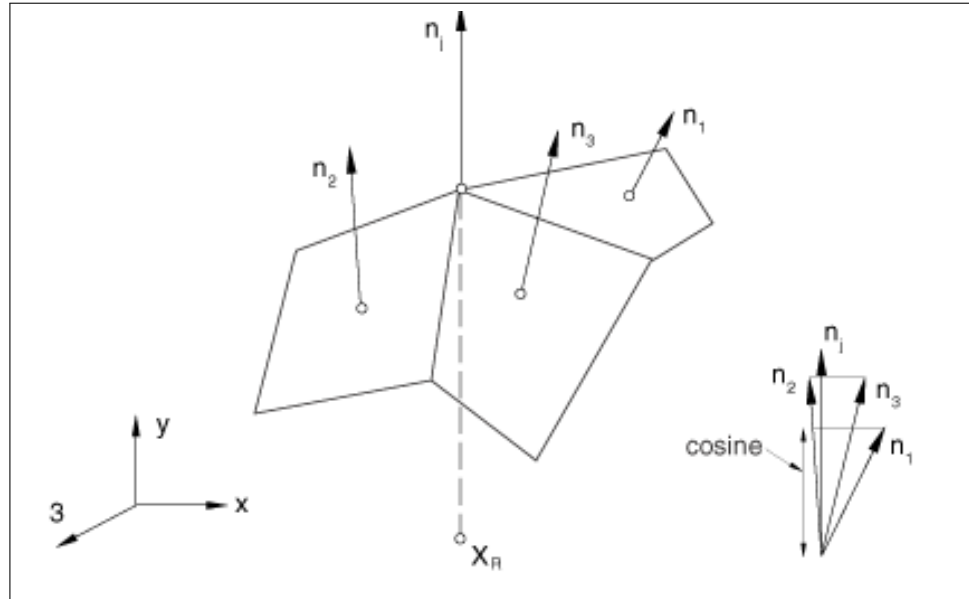


Figure 3.10.7: Defining the cosine for acoustic infinite elements [2].

In the Abaqus input file, the reference point for the acoustic infinite elements can be defined as follows, which ensures that all calculations related to the element positioning and orientation are correctly referenced:

```
*SOLID SECTION, ELSET=outer_infinite, REF NODE=5000788, MATERIAL=air
```

Here, ELSET refers to the set of acoustic infinite elements. REF NODE is the node number of a specific node, ideally located at or near the geometric center of the acoustic domain to serve as the reference point for the element's mapping. The MATERIAL specifies that the elements use the properties of the air, or whichever fluid represents the acoustic medium.

Normal Vectors: The nodal normal vectors, which must point outward into the infinite domain, are crucial for defining the spatial mapping of the infinite elements. These vectors help in ensuring that the area or volume mapped by the infinite elements increases with distance, simulating the expansion into an infinite domain. Each node attached to an infinite element must have a unique outward-pointing normal vector to cover the infinite domain effectively without overlaps.

Advantages of Acoustic Infinite Elements: Compared to other methods, acoustic infinite elements offer a higher level of accuracy in modeling far-field behaviors and complex wave interactions. They allow for a significant reduction in the computational domain size without sacrificing the accuracy of the results, providing a balance between computational efficiency and solution fidelity.

3.11 Comparative Overview of Fully and Sequentially Coupled Analysis

In acoustic-structural analysis, the choice between fully and sequentially coupled methodologies hinges on the specific requirements and constraints of the simulation scenario.

Fully Coupled Analysis: This method integrates the acoustic and structural domains into a single system of equations, ensuring that the interaction between the acoustic medium and the structural response is captured simultaneously. This approach is beneficial when the acoustic load significantly influences the structural behavior. For instance, in scenarios where the acoustic pressure from the surrounding air impacts the vibration of a system, such as a muffler in operation, the fully coupled model accounts for these effects comprehensively. However, this method can be computationally intensive due to the larger system of equations that must be solved.

Sequentially Coupled Analysis: Alternatively, sequentially coupled analysis divides the problem into two separate but sequentially dependent stages. This method treats one part of the system (typically the one less affected by interaction) as the “global” model, while the other part (significantly influenced by the interaction) is handled as a “submodel”. This division can significantly reduce computational demands, as each sub-problem is smaller and simpler than the fully coupled system. Sequential coupling is advantageous in scenarios where structural vibrations generate sound pressure waves in the surrounding medium, but the resulting pressure changes in the medium have a negligible effect on the structural vibrations. If preliminary tests show minimal difference in results between the fully and sequentially coupled approaches within the relevant frequency range, the latter, more cost-effective method is often preferred.

Both approaches have their merits, and the choice depends on the specific acoustic and

structural dynamics of the problem at hand. While fully coupled analysis offers higher fidelity, sequentially coupled analysis provides efficiency, making it suitable for larger scale or less interaction-intensive scenarios [42].

3.12 Fully Coupled Acoustic-Structural Analysis

Fully coupled acoustic-structural analysis represents the most comprehensive and general approach to solving structural-acoustic problems. This method accounts for the bidirectional interaction between structural vibrations and the surrounding acoustic medium, ensuring that all relevant effects are captured in a single system of equations. In this approach, not only do the structural vibrations influence the acoustic pressure, but the changes in the acoustic pressure in turn affect the structural vibrations, creating a complex, interdependent system. While highly accurate, this approach can also be computationally expensive, particularly for large-scale problems where the acoustic pressure has minimal impact on the structure.

The governing equations for harmonic response analysis in the context of pure acoustic and coupled acoustic-structural problems are as follows:

Pure Acoustic Problems

For problems involving only the acoustic domain, the following equation is solved:

$$(-\omega^2[M_a] + i\omega[C_a] + [K_a]) \{p\} = \{f_F\}$$

Here:

- $[M_a]$ is the acoustic mass matrix,
- $[C_a]$ is the acoustic damping matrix,
- $[K_a]$ is the acoustic stiffness matrix,
- $\{p\}$ is the acoustic pressure vector, and
- $\{f_F\}$ is the external acoustic force vector.

This equation models the propagation of sound waves in the acoustic domain, assuming no interaction with structural elements.

Fluid-Structure Interaction Problems

For fully coupled acoustic-structural problems, the acoustic and structural matrices are combined into a single system of equations[43]:

$$-\omega^2 \begin{bmatrix} [M_s] & 0 \\ \rho_0 R^T & [M_f] \end{bmatrix} \begin{bmatrix} \{u\} \\ \{p\} \end{bmatrix} + i\omega \begin{bmatrix} [C_s] & 0 \\ 0 & [C_f] \end{bmatrix} \begin{bmatrix} \{u\} \\ \{p\} \end{bmatrix} + \begin{bmatrix} [K_s] & -[R] \\ -[R^T] & [K_f] \end{bmatrix} \begin{bmatrix} \{u\} \\ \{p\} \end{bmatrix} = \begin{bmatrix} \{f_s\} \\ \{f_f\} \end{bmatrix}$$

Here:

- $[M_s]$ and $[M_f]$ are the structural and acoustic mass matrices, respectively,

- $[C_s]$ and $[C_f]$ are the structural and acoustic damping matrices, respectively,
- $[K_s]$ and $[K_f]$ are the structural and acoustic stiffness matrices, respectively,
- $[R]$ and $[R^T]$ represent coupling matrices that define the interaction between the structure and the acoustic medium,
- $\{u\}$ is the structural displacement vector,
- $\{p\}$ is the acoustic pressure vector, and
- $\{f_s\}$ and $\{f_f\}$ are the external force vectors acting on the structure and acoustic medium, respectively.

The first row of the equation represents the structural dynamics, accounting for the influence of acoustic pressure through the coupling term $[R]$. The second row models the acoustic behavior, incorporating the effects of structural vibrations via the coupling matrix $[R^T]$. The fully coupled formulation captures the mutual interaction between the structure and the surrounding acoustic medium. Structurally, vibrations generate pressure waves in the medium, while the resulting acoustic pressure modifies the structural response. The coupling terms $[R]$ and $[R^T]$ ensure that these interactions are accurately modeled. This bidirectional feedback loop is essential for applications like vibration control, sound radiation analysis, and acoustic optimization in lightweight structures.

By solving the fully coupled equations, engineers can achieve a detailed understanding of the interplay between structural and acoustic phenomena, enabling precise predictions and optimized designs.

When to Use Fully Coupled Analysis

Fully coupled analysis is particularly appropriate in scenarios where the interaction between the structure and the acoustic medium is strong and cannot be ignored. Examples include:

- Lightweight structures in contact with dense fluids, where acoustic pressure significantly affects structural vibrations.
- Cases involving resonance phenomena, where the bidirectional interaction amplifies the response.
- Situations where the accuracy of sequential or uncoupled methods is insufficient due to complex interactions.

3.12.1 Structural Acoustic Coupling in Fully Coupled Analysis using surface-based tie constraint

When an acoustic medium is in contact with a structure, momentum and energy transfer occur across the boundary between the two media. The acoustic pressure field, represented using acoustic elements, generates normal surface traction on the structure, while the acceleration field, modeled with structural elements, introduces a natural forcing term at the fluid boundary. A surface-based approach can be employed to enforce

this coupling. This method involves using separate nodes for the structural and acoustic meshes. The interaction is defined by creating surfaces on both the structural and fluid meshes and applying a surface-based tie constraint to establish the connection between the two.

3.12.2 Implementation of Surface-Based Tie Constraints in Simulation

Surface-based tie constraints are a versatile method for coupling acoustic and structural domains in simulations. The following steps outline the implementation process and considerations for using this approach effectively in Abaqus.

Creating Surfaces for Coupling

The first step in defining a surface-based tie constraint is the creation of primary (main) and secondary surfaces in Abaqus:

- The main surface can be created either by selecting nodes or elements.
- The secondary surface, however, must always be element-based.

Either the structural or acoustic surface can be designated as the primary or secondary surface, but the choice affects the solution's accuracy. The following guidelines can help determine the appropriate assignment:

- The surface with the coarser mesh should typically be designated as the main surface.
- The mesh refinement depends on the wave speeds of the materials at the interface. The material with the lower wave speed generally requires finer meshing and is better suited as the secondary surface.
- If solution details near the interface are critical, the meshes on both sides of the interface should be refined equally, based on the requirements of the material with the lower wave speed.

Defining the Tie Constraint

The tie constraint between the two surfaces is defined in the Abaqus input file using the following syntax:

```
*TIE, NAME=the_interaction_name  
secondary_surface, main_surface
```

This automatically couples the degrees of freedom (DoFs) at the interface:

- **Acoustic Pressure:** Acoustic pressure boundary conditions (DOF 8) is applied to nodes on the surface of the acoustic mesh.

- **Translation:** The translational boundary conditions (DOFs 1, 2, 3) are applied to the surface of the structural mesh.

Behavior of Surface-Based Tie Constraints

The behavior of surface-based tie constraints can be understood as follows:

- When a tie constraint is applied, Acoustic-Structural Interface (ASI) elements are internally created on the secondary surface. These elements introduce new degrees of freedom (DoFs) that facilitate coupling between the structural and acoustic domains.
- The added DoFs on the secondary surface are then tied to the main surface, ensuring consistent interaction between the two domains.
- If the acoustic surface is chosen as the secondary surface:
 - Translational DoFs (u_x, u_y, u_z) are added to the acoustic mesh to account for displacements.
 - These translational DoFs are then coupled with the structural mesh through the tie constraint, allowing the structural displacements to influence the acoustic behavior.
 - These DoFs can also be processed as output, providing insights into the acoustic response.
- If the structural surface is chosen as the secondary surface:
 - Pressure DoFs (POR) are added to the structural mesh to represent the acoustic pressures.
 - These pressure DoFs are tied to the acoustic mesh through the tie constraint, allowing the acoustic pressures to influence the structural response.
 - Like the translational DoFs, these pressure DoFs can also be processed as output for further analysis.

This mechanism ensures seamless interaction between the structural and acoustic domains, with the tie constraint effectively coupling the relevant degrees of freedom. The method is flexible, allowing either the structural or acoustic surface to act as the secondary surface, depending on the specific requirements of the simulation.

Automatic Computation of Regions of Influence

Abaqus automatically computes the region of influence for each internally generated acoustic-structural interface element. This ensures accurate coupling between the two domains. However, care must be taken when defining the secondary surface:

- If the secondary surface significantly overhangs the main surface, the regions of influence may extend to parts of the overhang.
- Overhanging portions of the secondary surface may exhibit nonphysical coupled DoFs:

- Displacements, if the secondary surface is acoustic.
 - Acoustic pressures, if the secondary surface is structural.
- These nonphysical results on the overhang do not affect the remainder of the solution but should be understood as non-meaningful artifacts.

Interface Alignment

Proper alignment of the structural and acoustic surfaces at the interface is critical for achieving accurate results:

- The surfaces must overlap precisely to avoid gaps or misalignment.
- The normal vectors of the structural and acoustic elements at the interface should point towards each other to ensure correct coupling.

Practical Implications

The flexibility of surface-based tie constraints allows for non-matching meshes between the structural and acoustic domains. This feature is particularly useful in scenarios where:

- The structural domain has a more complex geometry and requires finer meshing, while the acoustic domain can remain coarser.
- Separate surfaces are necessary due to differences in meshing strategies or modeling requirements.

Conclusion: Surface-based tie constraints offer an efficient and accurate method for simulating acoustic-structural interactions. By ensuring proper mesh refinement, surface alignment, and understanding the limitations of overhanging secondary surfaces, this approach enables engineers to model complex interactions effectively, even when the structural and acoustic meshes differ significantly.

3.12.3 Output and Postprocessing in Fully Coupled Acoustic Structural Analyses

This section provides an overview of the various output options available in Abaqus for fully coupled acoustic-structural analyses, including details on how these outputs are calculated and how they can be requested. It also discusses the use of infinite elements for far-field acoustic simulations and introduces the concept of Equivalent Radiated Power (ERP).

Field Output vs. History Output in Abaqus

Abaqus generates two primary categories of output data: **Field Output** and **History Output**. While both allow users to extract and review simulation results, each type serves a distinct purpose and requires different setup parameters.

Field Output

- Captures spatially distributed data over the entire model or a specified region (e.g., a set of elements or nodes).
- Typically used to analyze results at specific time or frequency increments. Examples include acoustic pressure distributions, sound pressure level (SPL), or velocity fields in the fluid or structural domain.
- Supports contour plots and other visualizations. For instance, the acoustic pressure distribution on a cutting plane in the acoustic cavity at a given frequency can be visualized.

History Output

- Records time-dependent or frequency-dependent data at specific points. Typical usage involves monitoring key quantities (e.g., sound pressure at a single node, displacement at a key location, or harmonic response of selected nodes).
- Generates time-series or frequency-response plots, enabling a more detailed investigation of how certain variables evolve over the analysis.
- Useful for extracting results at specific receiver or microphone locations in an acoustic domain.

3.12.3.1 Sound Pressure Output

In an acoustic medium, the **POR** variable in Abaqus denotes the acoustic pressure at the nodes of acoustic elements. In steady-state dynamic analyses, **POR** becomes a complex-valued quantity representing magnitude and phase of the acoustic pressure.

Sound Pressure Level (SPL)

Abaqus can compute additional quantities related to acoustic pressure. The *sound pressure level* (SPL) is defined as

$$\text{SPL} = 20 \log_{10} \left(\frac{p}{p_{\text{REF}}} \right),$$

where p_{REF} is a reference pressure. The reference pressure (p_{REF}) serves as a baseline for comparing sound pressures and is used as a standard in calculating the Sound Pressure Level (SPL). It defines the intensity or loudness of a sound relative to this baseline. For air, in the context of human hearing, $p_{\text{REF}} = 20 \mu\text{Pa}$ (micro-pascals), which represents the threshold of hearing for a pure tone at 1 kHz under standard conditions. This is the faintest sound that an average, healthy human ear can perceive [6, Chapter 2, p. 68]. In the consistent unit system of tonne, millimeter, and second used here, this value corresponds to 2×10^{-11} . Common reference points include:

- $p = 20 \mu\text{Pa} \implies \text{SPL} = 0 \text{ dB}$ (threshold of human hearing).
- If p is ten times p_{REF} , $\text{SPL} = 20 \text{ dB}$.

3.12.3.2 Total Energy Output Quantities

For exterior acoustic analyses, Abaqus offers energy-related output variables. One such variable is **RADPOW**, representing the radiated power across a specified boundary.

- **RADPOW** quantifies the acoustic power passing through a given acoustic boundary (such as a surface of infinite elements in a far-field analysis).
- Useful for assessing the amount of energy radiated into the surrounding medium.

3.12.3.3 Equivalent Radiated Power (ERP)

Equivalent Radiated Power (ERP) is a measure that estimates the maximum acoustic power a vibrating structure could radiate if each portion of its surface were perfectly efficient (i.e., no fluid feedback or partial reflections). To compute ERP, a uniform acoustic impedance of $\rho_0 c_0$ is assumed at every point on the structure (the characteristic impedance of an ideal fluid), effectively assigning a radiation efficiency of 1. This idealization is typically referred to as applying *plane wave conditions* because it treats each surface patch with uniform acoustic impedance and 100% radiation efficiency, ignoring geometry or scattering complexities so that the velocity of each patch is directly converted into radiated power.

Significance of ERP

- Provides a simplified measure of sound radiation potential.
- Helps locate high-radiation zones on the structure's surface to guide noise reduction efforts.
- Widely used in automotive, aerospace, and consumer electronics for preliminary design evaluations.

Mathematical Formulations

In plane waves, the amplitude remains constant with the wave propagation and therefore the ratio of acoustic pressure to particle velocity remains constant and is directly proportional to the medium's intrinsic properties [44, Chapter 1, p. 9]. Under plane wave assumptions, the acoustic impedance Z_0 is defined as $Z_0 = \rho c$, where ρ is the density of the medium, and c is the speed of sound.

In the case of plane waves, sound propagates in a single direction with uniform pressure and velocity fields. Acoustic impedance represents the opposition to sound flow, analogous to electrical impedance in circuits. It is defined as the ratio of acoustic pressure p to particle velocity v at any point:

$$Z_0 = \frac{p}{v}$$

For plane waves, the acoustic pressure p and particle velocity v are related by the governing equations of wave propagation. In a uniform medium:

$$p(x, t) = p_0 e^{i(kx - \omega t)},$$

$$v(x, t) = v_0 e^{i(kx - \omega t)},$$

where:

- p_0 : Amplitude of the acoustic pressure,
- v_0 : Amplitude of the particle velocity,
- k : Wavenumber ($k = \frac{\omega}{c}$),
- ω : Angular frequency ($\omega = 2\pi f$),
- x : Position, and
- t : Time.

From the linearized momentum equation [44, Chapter 1, p. 5]:

$$\frac{\partial v}{\partial t} = -\frac{1}{\rho} \frac{\partial p}{\partial x}.$$

For a harmonic plane wave, substituting $p = p_0 e^{i(kx - \omega t)}$ and solving for v :

$$v = \frac{p}{\rho c}.$$

Thus, the impedance Z_0 becomes:

$$Z_0 = \frac{p}{v} = \rho c.$$

This shows that the acoustic impedance in plane wave conditions depends only on the medium's density ρ and the speed of sound c .

Formula for ERP

The Equivalent Radiated Power (ERP) is defined as the total acoustic power radiated by the structure per unit area of its surface. Under idealized plane wave conditions, the acoustic power (P) is the product of acoustic pressure (p) and normal velocity (v_n), integrated over the radiating surface:

$$\text{ERP} = \int_S p v_n dS.$$

Under the plane wave assumption, substituting $p = \rho c v_n$, the ERP simplifies to:

$$\text{ERP} = \rho c \int_S |v_n|^2 dS,$$

where:

- v_n : Normal component of the structural velocity,
- S : Radiating surface area,

- ρ : Density of the medium, and
- c : Speed of sound in the medium.

This formula quantifies the acoustic power radiated by a structure, assuming plane wave conditions, making it a practical measure for evaluating the sound radiation potential of vibrating surfaces.

Comparision between ERP and RADPOW

- In Abaqus, the RADPOW is the result of the actual acoustic pressure distribution and accounts for realistic propagation effects, including losses due to wave cancellations on complex surfaces and non-radiating modes (portions of vibration that do not produce effective acoustic waves).
- In realistic scenarios, not all the vibrational energy contributes to acoustic radiation because of suboptimal radiation efficiency, which is defined as the ratio of actual power radiated by a surface to the power that would be radiated by an ideal piston [45]. By contrast, the Equivalent Radiated Power (ERP) assumes ideal plane wave conditions. This assumption simplifies the calculation but can lead to an overestimation of the radiated power.

As a result, ERP often predicts a higher maximum power than RADPOW. Intuitively, ERP can be thought of as a "theoretical upper bound" on the radiated power, while RADPOW represents the practical, realistic value.

Validation Check:

As a validation check in simulations, it is expected that:

$$\text{ERP} \geq \text{RADPOW}.$$

If ERP is found to be less than RADPOW, it may signal inconsistencies in:

- Material properties (e.g., incorrect density or speed of sound),
- Boundary conditions (e.g., improper definition of infinite elements),
- Simulation setup (e.g., mesh resolution or solver parameters).

This relationship highlights the importance of ERP as an idealized benchmark and RADPOW as a practical output for realistic acoustic analysis.

3.12.3.4 Using Infinite Elements to project the results to a Far-Field

When performing a steady-state dynamic analysis with three-dimensional acoustic infinite elements (ACIN3D3, ACIN3D4, ACIN3D6, or ACIN3D8), Abaqus provides additional nodal variables that aid in evaluating the far-field pressure:

- INFN: The acoustic infinite element normal vector.

- INFR: The acoustic infinite element radius used in the coordinate mapping of infinite elements.
- PINF: The acoustic infinite element pressure coefficients.

Far-Field Pressure Computation

Abaqus offers a Python script to project results onto a specified spherical surface and compute the far-field pressure at any required distance from the vibrating source. The far-field acoustic pressure is approximated as [46]:

$$\lim_{r \rightarrow \infty} p(r) = \lim_{r \rightarrow \infty} \left(\frac{1}{kr} e^{-ikr} p_{\text{FAR}} \right),$$

where k is the wavenumber, and p_{FAR} is the acoustic far-field pressure. By running:

```
abaqus fetch job=acousticVisualization
```

and executing the script in the *Visualization* module, a projected mesh on a user-defined spherical surface can be created and write out new output variables:

- POR, PORdB: Acoustic pressure (linear and in dB).
- PFAR, PFARDB: Far-field pressure (linear and in dB).
- INTEN_FAR: Far-field acoustic intensity.

This procedure simplifies the evaluation and visualization of far-field sound pressure levels at large distances from the vibrating structure.

3.13 Sequentially Coupled Acoustic Structural Analysis

Sequentially coupled analysis is suitable for situations where the normal surface traction exerted by the acoustic fluid on the structure is negligible compared to other forces acting on the structure. An example of such a scenario is a vibrating machine radiating sound into the surrounding air. In this case, the reaction pressure of the air on the machine is insignificant to the structural response and can be safely neglected.

In sequentially coupled analysis, the structural analysis is performed first, independently of the fluid domain. The acoustic analysis follows and is driven by the structural response at the interface. By solving the problem in two separate steps, the solution is effectively decoupled, resulting in reduced computational cost, especially for large-scale problems.

The governing equations for sequentially coupled analysis are as follows:

Structural Analysis

The structural displacement or velocity is computed first using:

$$(-\omega^2[M_s] + i\omega[C_s] + [K_s])\{u\} = \{f_s\}.$$

Here:

- $[M_s]$, $[C_s]$, and $[K_s]$ are the structural mass, damping, and stiffness matrices, respectively.
- $\{u\}$ is the structural displacement vector.
- $\{f_s\}$ is the external force vector acting on the structure.

Acoustic Analysis

The structural response ($\{u\}$) is then used as a boundary condition for the acoustic analysis:

$$(-\omega^2[M_f] + i\omega[C_f] + [K_f])\{p\} = \{f_f\} + [R^T]\{u\}.$$

Here:

- $[M_f]$, $[C_f]$, and $[K_f]$ are the acoustic mass, damping, and stiffness matrices, respectively.
- $\{p\}$ is the acoustic pressure vector.
- $\{f_f\}$ is the external force vector acting on the acoustic domain.
- $[R^T]$ represents the coupling between the structural displacement and the acoustic pressure at the interface.
- **Fully Coupled Analysis:** In fully coupled analysis, the structural and acoustic domains interact bidirectionally. This interaction is captured by the off-diagonal coupling terms $[R]$ and $[R^T]$ in the governing equations. Feedback from the acoustic domain to the structure is explicitly considered, making the analysis more accurate but computationally expensive.
- **Sequentially Coupled Analysis:** In sequentially coupled analysis, the interaction is one-way. The structural response ($\{u\}$) is computed first and passed as input to the acoustic analysis. The coupling term $[R^T]$ is included only in the acoustic equation, while feedback from the acoustic domain to the structure is neglected ($[R] = 0$ in the structural equations). This approach is computationally efficient and sufficient for problems where the fluid's effect on the structure is negligible.

3.13.1 Submodeling in Sequential Coupling

Sequential coupling in Abaqus is implemented using the submodeling technique. Submodeling allows the results of a coarse global model to drive a refined local analysis. In the context of acoustic-structural coupling, this technique involves two distinct analyses:

- **Global Model:** The first analysis includes the structure. For instance, in the case of a vibrating machine, the global model contains the machine and its response under external forces. The structural response ($\{u\}$) is computed and used as input for the subsequent analysis.

- **Submodel:** The second analysis includes the acoustic fluid and its interaction with the structure. Abaqus interpolates the displacement fields between the global and submodels. It involves:
 - An acoustic mesh representing the fluid domain.
 - ASI elements defined at the structural-acoustic interface.
 - Displacement boundary conditions driven by the structural response obtained from the global model.

3.13.2 Structural Acoustic Coupling in Sequentially Coupled Analysis using Acoustic Structural Interface Elements

In the submodeling process, separate meshes are created for the structure and the acoustic cavity. The structural-acoustic interface is lined with ASI elements, which act as intermediaries to transfer the displacements from the global structural model to the acoustic submodel. The displacement results at the structural-acoustic interface from the global analysis, saved in the output database (.odb) or results file (.fil), are used as inputs to the submodel analysis.

The syntax for initiating the submodel analysis using the global model results in Abaqus is as follows:

```
abaqus job=<submodel_job_name> globalmodel=<global_job_name>.odb
```

Modeling ASI Elements

The mesh of the acoustic fluid in the submodel does not need to match the structural mesh from the global analysis. Abaqus automatically interpolates the structural displacements saved from the global analysis and applies them to the driven nodes of the acoustic submodel. This feature ensures that the coupling between the global structural model and the acoustic submodel is seamless.

It is critical to ensure that the normals of the ASI (Acoustic Structural Interface) elements point into the acoustic fluid. This orientation guarantees accurate application of the structural displacements as boundary conditions for the acoustic submodel. The accuracy of the submodel analysis relies on the proper orientation of these elements and the correct transfer of boundary conditions from the global structural model.

The figures below 3.13.8 and 3.13.9 illustrate the relationship between the global model and the submodel:

ASI Elements in 3D Models

In Abaqus, the following ASI elements are available for use in 3D models:

- ASI3D3: 3-node linear elements
- ASI3D4: 4-node linear elements
- ASI3D6: 6-node quadratic elements

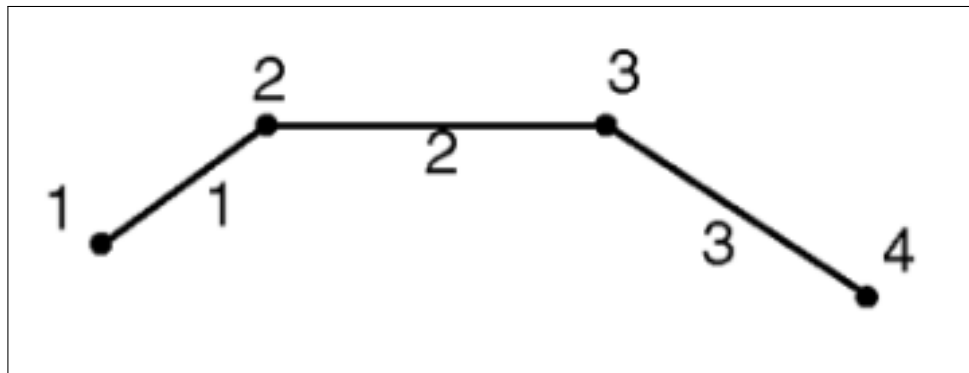


Figure 3.13.8: Global Model. The structural model with elements and nodes is used to compute the displacement field. The boundary of the structure, shown as a line interface, will drive the acoustic submodel by transferring the computed structural displacements. The global model provides the input for the submodel, ensuring that the boundary conditions at the interface are accurately captured.

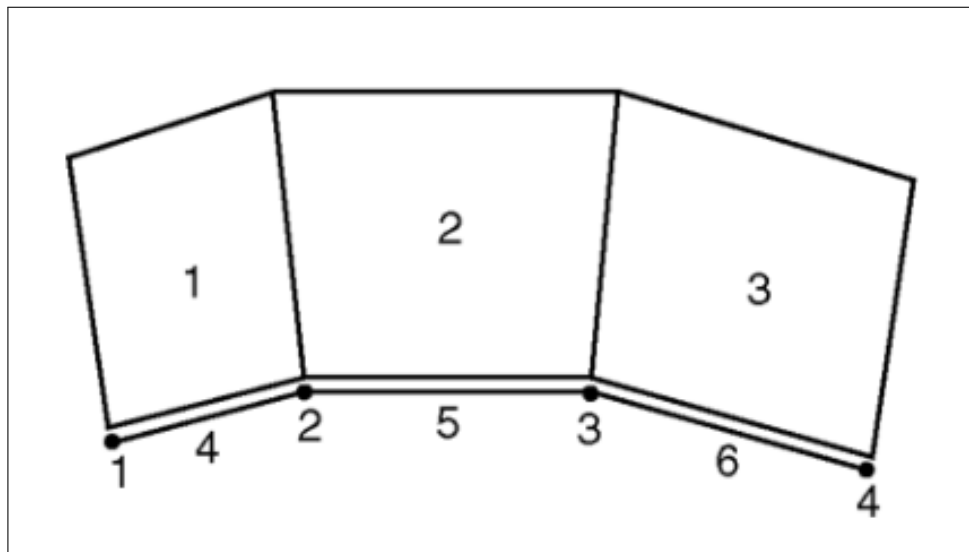


Figure 3.13.9: Submodel. The acoustic mesh with ASI elements along the structural interface is shown. The nodes along the ASI interface are driven by interpolated structural displacements from the global model. This allows the acoustic submodel to calculate the acoustic pressure field in response to the structure's vibrations. The correct orientation of the ASI element normals into the acoustic domain ensures the physical accuracy of the simulation.

- ASI3D8: 8-node quadratic elements

The active degrees of freedom (DoFs) for these elements are:

- DoFs 1, 2, and 3: Translational displacements in the x , y , and z directions, respectively.
- DoF 8: Acoustic pressure.

Syntax for Coupling Global and Submodel Using ASI Elements

The coupling between the global model and submodel using ASI elements is defined as follows in the input file:

```
*INTERFACE, ELSET=asi
*NSET, NSET=asi, ELSET=asi
*SUBMODEL, ABSOLUTE=1.e-3, GLOBAL ELSET=global_mesh
global_boundary_elements,
```

- The ***INTERFACE** command defines the section properties for the ASI elements.
- A node set (**NSET**) is created from the ASI elements, as these nodes are driven by the displacements from the global structural model.
- The ***SUBMODEL** command activates the submodeling procedure. The **GLOBAL ELSET** specifies the boundary elements of the global model whose displacements will drive the submodel. If the nodes of the submodel lie within the **ABSOLUTE** tolerance from the nodes of the global model, the coupling is achieved.

This implementation enables accurate modeling of the structural-acoustic coupling, providing a seamless transfer of boundary conditions between the global structural model and the acoustic submodel.

3.13.3 Outputs in Sequentially Coupled Acoustic-Structural Analyses

All the outputs available for fully coupled analyses, as discussed in the previous section, are also accessible in sequentially coupled analyses, with the exception of the acoustic power variable **RADPOW**. In sequentially coupled analyses, an alternative history output variable, **ALLQB**, is provided. This variable represents the energy dissipated through quiet boundaries (infinite elements) [47].

The acoustic power can be derived from **ALLQB** by multiplying it with the frequency of the acoustic wave (see Appendix A). This relationship enables a comparison between **RADPOW** from fully coupled analyses and the product of **ALLQB** and frequency from sequentially coupled analyses. The equation for acoustic power can be expressed as:

$$\text{Acoustic Power} = \text{ALLQB} \cdot f,$$

where f is the frequency of the acoustic wave.

3.14 Boundary Element Method

The Boundary Element Method (BEM) is a numerical technique for solving partial differential equations (PDEs) by discretizing only the boundary of the domain rather than the entire volume. This approach significantly reduces the computational complexity,

making it advantageous for problems involving infinite or semi-infinite domains, where traditional Finite Element Method (FEM) approaches may require an impractically large number of elements.

Unlike FEM, which approximates the solution u throughout the entire domain, BEM directly approximates both the solution u and its normal derivative q on the boundary, leading to more accurate boundary representation. However, BEM requires knowledge of a fundamental solution to the governing PDE, whereas FEM does not have this requirement. The governing equations in BEM result in a dense, fully populated system matrix, typically of the form $Hu = Gq$, as opposed to the sparse matrices encountered in FEM, which take the form $Ku = F$ [48].

Table 3.14.1: Comparison between Finite Element Method (FEM) and Boundary Element Method (BEM)

Aspect	Finite Element Method (FEM)	Boundary Element Method (BEM)
Domain Discretization	Entire domain is discretized into finite elements	Only the boundary is discretized into boundary elements
Applicability	Suitable for finite domains	Suitable for infinite or semi-infinite domains
Accuracy of Approximation	Approximates the solution u , and its derivative q must be computed separately	Directly approximates both u and its derivative q
System Matrix	Results in a large, sparse matrix of the form $Ku = F$	Leads to a small, dense matrix of the form $Hu = Gq$
Prior Knowledge of Solution	No prior knowledge of the fundamental solution is required	Requires a fundamental solution to the PDE for formulation
Computational Cost	Computational effort depends on the number of elements, which increases for large domains	More efficient for problems involving infinite domains but results in dense system matrices
Handling of Nonlinearities	Easily handles nonlinear and inhomogeneous problems	More challenging to apply to nonlinear or inhomogeneous problems
Common Applications	Structural mechanics, heat transfer, fluid dynamics	Acoustics, elastodynamics, electrostatics, and problems involving infinite domains

BEM is particularly well-suited for acoustic, elastodynamic, and fluid flow problems, where infinite domains naturally arise. However, its application to inhomogeneous or nonlinear problems can be more challenging compared to FEM. Despite this, its ability

to efficiently handle large-scale problems while reducing computational cost makes it a valuable method in various engineering and scientific applications.

3.14.1 Derivation of the Boundary Element Method for the Helmholtz Equation

The Boundary Element Method (BEM) reformulates the Helmholtz equation as a boundary integral equation, reducing the problem dimensionality by solving only on the boundary. This section details the derivation, emphasizing the role of Green's functions and layer potentials.

Weighted Residual Formulation

Consider the Helmholtz equation in a domain $\Omega \subset \mathbb{R}^3$ with wavenumber k :

$$(\nabla^2 + k^2)u(\mathbf{x}) = 0, \quad \mathbf{x} \in \Omega, \quad (3.14.10)$$

where $u(\mathbf{x})$ represents the acoustic pressure. To derive the boundary integral equation, **fundamental solution** $G(\mathbf{x}, \mathbf{y})$ is used. The fundamental solution of a partial differential equation is the response of the system to a point source, which satisfies:

$$(\nabla^2 + k^2)G(\mathbf{x}, \mathbf{y}) = -\delta(\mathbf{x} - \mathbf{y}), \quad (3.14.11)$$

where δ is the Dirac delta function. Physically, $G(\mathbf{x}, \mathbf{y})$ represents the field at \mathbf{x} due to a point source at \mathbf{y} . For 3D problems, G is explicitly [49]:

$$G(\mathbf{x}, \mathbf{y}) = \frac{e^{ikr}}{4\pi r}, \quad r = \|\mathbf{x} - \mathbf{y}\|. \quad (3.14.12)$$

Role of the Delta Distribution

The delta distribution $\delta(\mathbf{x} - \mathbf{y})$ satisfies [50]

$$\int_{\mathbb{R}^n} \delta(\mathbf{x} - \mathbf{y}) \varphi(\mathbf{x}) d\mathbf{x} = \varphi(\mathbf{y}),$$

for any sufficiently smooth (test) function φ . This property makes it a powerful tool to isolate the response of the PDE to a localized source at \mathbf{y} . In BEM formulations, one often uses the delta function to test the underlying PDE at a point, or equivalently, one exploits its role in deriving Green's identities via integrals over domains/boundaries. The fundamental solution $G(\mathbf{x}, \mathbf{y})$ (also called Green's function in free space) emerges naturally as the solution to (3.14.11).

Integral Equation Derivation

Multiply Eq. (3.14.10) by $G(\mathbf{x}, \mathbf{y})$ and integrate over Ω :

$$\int_{\Omega} [(\nabla^2 + k^2)u(\mathbf{x})] G(\mathbf{x}, \mathbf{y}) d\Omega = 0. \quad (3.14.13)$$

Using Green's second identity and Eq. (3.14.11), this simplifies to [51]:

$$u(\mathbf{y}) = \int_{\partial\Omega} \left[G(\mathbf{x}, \mathbf{y}) \frac{\partial u(\mathbf{x})}{\partial n} - u(\mathbf{x}) \frac{\partial G(\mathbf{x}, \mathbf{y})}{\partial n} \right] dS(\mathbf{x}), \quad (3.14.14)$$

where $\partial/\partial n$ denotes the normal derivative directed outward from Ω . Equation (3.14.14) expresses $u(\mathbf{y})$ in the domain using boundary values of u and $\partial u/\partial n$ [49].

Boundary Integral Equation

For $\mathbf{y} \in \partial\Omega$, the integral becomes singular, requiring careful evaluation. Applying the **jump conditions** leads to [51]:

$$c(\mathbf{y})u(\mathbf{y}) = \int_{\partial\Omega} \left[G(\mathbf{x}, \mathbf{y}) \frac{\partial u(\mathbf{x})}{\partial n} - u(\mathbf{x}) \frac{\partial G(\mathbf{x}, \mathbf{y})}{\partial n} \right] dS(\mathbf{x}), \quad (3.14.15)$$

where $c(\mathbf{y})$ is a geometric coefficient ($c = 1/2$ for smooth boundaries). This is the **direct boundary integral equation** (BIE), relating boundary values of u and $\partial u/\partial n$.

Single and Double Layer Potentials

The boundary integral equation (BIE) employs layer potentials to represent acoustic fields. Below are the definitions aligned with BEMPP's notation and Green's representation theorem:

- **Single Layer Potential (\mathcal{V})**: Represents fields generated by a distribution of monopole sources (normal derivative/flux):

$$\mathcal{V}[\phi](\mathbf{x}) = \int_{\partial\Omega} G(\mathbf{x}, \mathbf{y})\phi(\mathbf{y}) dS(\mathbf{y}), \quad \phi = \frac{\partial u}{\partial n}, \quad (3.14.16)$$

where $\phi = \partial u/\partial n$ is the normal velocity on $\partial\Omega$, and $G(\mathbf{x}, \mathbf{y})$ is the Green's function.

- **Double Layer Potential (\mathcal{K})**: Represents fields generated by dipole distributions (boundary pressure):

$$\mathcal{K}[\psi](\mathbf{x}) = \int_{\partial\Omega} \frac{\partial G(\mathbf{x}, \mathbf{y})}{\partial n(\mathbf{y})}\psi(\mathbf{y}) dS(\mathbf{y}), \quad \psi = u, \quad (3.14.17)$$

where $\psi = u$ is the acoustic pressure on $\partial\Omega$, and the normal derivative $\partial/\partial n(\mathbf{y})$ is taken *with respect to the source point \mathbf{y}* .

Final Representation Theorem

Combining these, Green's theorem becomes [49]:

$$u(\mathbf{x}) = \mathcal{V} \left[\frac{\partial u}{\partial n} \right] (\mathbf{x}) - \mathcal{K}[u](\mathbf{x}), \quad \mathbf{x} \in \Omega, \quad (3.14.18)$$

Solution Strategy

1. **Boundary Discretization:** The boundary $\partial\Omega$ is meshed into elements. Using collocation or Galerkin methods, the boundary integral equation(Eq. (3.14.15)) is discretized into a linear system. This equation directly relates boundary values of u and $\partial u/\partial n$ through the single-layer (\mathcal{V}) and double-layer (\mathcal{K}) operators.
2. **Boundary Condition Application:** Known values of u or $\partial u/\partial n$ are substituted. For acoustics, common conditions include:
 - Dirichlet: $u = \bar{u}$ (prescribed pressure),
 - Neumann: $\partial u/\partial n = \bar{v}$ (prescribed normal velocity).
3. **Solve for Unknowns:** The linear system is solved to obtain unknown boundary quantities.
4. **Domain Solution:** With u and $\partial u/\partial n$ known on $\partial\Omega$, Eq. (3.14.18) computes u anywhere in Ω .

Physical Interpretation

BEM naturally satisfies the Sommerfeld radiation condition for exterior problems, as $G(\mathbf{x}, \mathbf{y})$ inherently models outgoing waves. The layer potentials \mathcal{V} and \mathcal{K} encode the contribution of boundary sources to the far field, avoiding volumetric meshing. This makes BEM ideal for infinite-domain acoustics.

3.15 The BEMPP Python Library: Architecture and Workflow

The Boundary Element Method Python Package (BEMPP)² is an open-source boundary element method (BEM) library designed for solving acoustic, electromagnetic, and wave propagation problems. Its Python interface combines flexibility with high-performance C++ kernels, making it ideal for exterior acoustics simulations. The version used in this thesis is BEMPP-Cl.

BEMPP offers a range of features that facilitate efficient BEM computations. Some of its key capabilities include:

- Provides an intuitive Python-based interface for easy implementation of BEM formulations.
- Supports only triangular surface meshes and allows seamless import/export in multiple formats, including Gmsh and VTK.
- Enables efficient formulation and solution of acoustic and electromagnetic transmission problems.

²<https://bempp.com/>

- Supports both CPU and GPU parallelization, improving computational efficiency for large-scale problems.
- Facilitates the formulation of complex product operators, including preconditioning techniques.
- Provides integration with FEniCS³, enabling hybrid finite element and boundary element computations.

Function Spaces and Grid Functions

Function spaces define the discretization of boundary quantities (pressure u , velocity $\partial u / \partial n$) [52]:

- **Continuous Spaces (\mathcal{P}_1):** Piecewise linear functions (Lagrange elements), suitable for smooth pressure fields.
- **Discontinuous Spaces (\mathcal{P}_0):** Piecewise constant functions, often used for normal velocities with jump discontinuities.
- **Grid Functions:** Discrete representations of functions in these spaces. A grid function \mathbf{f}_h stores coefficients of the basis functions [53]:

$$f_h(\mathbf{x}) = \sum_{i=1}^N f_i \phi_i(\mathbf{x}),$$

where ϕ_i are basis functions (e.g., constants per element for \mathcal{P}_0).

Boundary Operators

Boundary operators are used to discretize Boundary integral equation (3.14.15) into matrices for linear system assembly. Key operators for the Helmholtz equation $(\nabla^2 + k^2)u = 0$ include [54]:

Solvers

BEMPP provides dense and fast multipole (FMM)-accelerated solvers:

- **Direct Solvers:** LU decomposition for small systems.
- **Iterative Solvers:** Generalized minimal residual method (GMRES), Conjugate gradient (CG), with block diagonal preconditioning.
- **Fast Multipole (FMM):** Reduces time-complexity from $\mathcal{O}(N^2)$ to $\mathcal{O}(N \log N)$ for large-scale problems but requires huge memory compared to GMRES.

³<https://fenicsproject.org/>

Table 3.15.2: Boundary Operators for the Helmholtz Equation

Operator	Symbol	Matrix Entries
Single-layer	\mathbf{V}	$m_{ij} = \int_{\Gamma} \int_{\Gamma} G_k(\mathbf{x}, \mathbf{y}) \phi_j(\mathbf{y}) \psi_i(\mathbf{x}) dy dx$
Double-layer	\mathbf{K}	$m_{ij} = \int_{\Gamma} \int_{\Gamma} \frac{\partial G_k(\mathbf{x}, \mathbf{y})}{\partial n_y} \phi_j(\mathbf{y}) \psi_i(\mathbf{x}) dy dx$

Variables and notation:

- Γ : The boundary (surface) where the integral is defined.
- $G_k(\mathbf{x}, \mathbf{y})$: The Green's function (fundamental solution) of the Helmholtz equation with wavenumber k .
- $\partial/\partial n_y$: Normal derivative at \mathbf{y} , along the outward normal to Γ .
- $\phi_j(\mathbf{y}), \psi_i(\mathbf{x})$: Basis/test functions used in the discretization (e.g., in a Galerkin approach).
- m_{ij} : The (i, j) -th entry of the corresponding system matrix.

The Generalized Minimal Residual (GMRES) method is an iterative solver employed in BEMPP to solve large, sparse linear systems arising from discretized boundary integral equations. As a Krylov subspace method, GMRES iteratively minimizes the residual norm $\|\mathbf{Ax} - \mathbf{b}\|$ without requiring the system matrix \mathbf{A} to be symmetric [55], making it ideal for acoustics problems with complex-valued operators. Its convergence is accelerated using preconditioners, such as block diagonal approximations, to mitigate ill-conditioning inherent in high-frequency Helmholtz systems. In BEMPP, GMRES is configured with user-defined tolerances and restart intervals to balance computational efficiency and memory usage, ensuring robust solutions for large-scale exterior acoustic simulations.

Potential Operators

Potential operators compute the acoustic field $u(\mathbf{x})$ in the domain Ω after solving the BIE:

Summary of Acoustic Calculation in BEMPP

The BEMPP workflow for exterior acoustics begins by importing a surface mesh representing the vibrating structure. Function spaces are defined to discretize boundary quantities: continuous piecewise linear elements (\mathcal{P}_1) for acoustic pressure (u) and discontinuous piecewise constants (\mathcal{P}_0) for normal velocity ($\partial u / \partial n$). Boundary operators—single-layer (\mathcal{V}) and double-layer (\mathcal{K}) are assembled to encode the Helmholtz integral equation (3.14.15). These operators are discretized into a linear system. Prescribed velocities (Neumann conditions) are applied, and the system is solved iteratively (e.g., GMRES) to obtain unknown boundary pressures. With boundary data resolved, Pontial operators 3.15.3, computes the acoustic field at any point \mathbf{x} in the domain. This workflow

Table 3.15.3: Potential Operators for the Helmholtz Equation

Operator	Definition	Interpretation
<i>Single-layer potential</i>	$(\mathcal{V}\mu)(\mathbf{x}) = \int_{\Gamma} G_k(\mathbf{x}, \mathbf{y}) \mu(\mathbf{y}) d\mathbf{y}$	Sums “monopole” sources over Γ
<i>Double-layer potential</i>	$(\mathcal{K}v)(\mathbf{x}) = \int_{\Gamma} \frac{\partial G_k(\mathbf{x}, \mathbf{y})}{\partial n_y} v(\mathbf{y}) d\mathbf{y}$	Sums “dipole” sources over Γ

Variables and notation:

- Γ : The boundary where the densities $\mu(\mathbf{y})$ or $v(\mathbf{y})$ are defined.
- $G_k(\mathbf{x}, \mathbf{y})$: Green’s function (fundamental solution) of the Helmholtz equation with wavenumber k .
- $\frac{\partial}{\partial n_y}$: Outward normal derivative with respect to \mathbf{y} .
- $\mu(\mathbf{y}), v(\mathbf{y})$: Continuous density functions representing physical quantities (e.g., monopole or dipole sources).

combines computational efficiency with rigorous physics, avoiding volumetric meshing while ensuring accuracy in acoustic calculations.

3.15.1 Null Field Approach and Representation Formulas in BEMPP

This section describes how the *null field approach* is employed in BEMPP to model acoustic radiation around a vibrating structure (e.g., a cube) under free-field conditions. In essence, the *null field approach* assumes that no acoustic field (i.e. a “null field”) exists within the interior of a closed boundary, thereby simplifying the boundary integral formulation for exterior radiation problems. The formulation leverages single- and double-layer potential operators to represent the total acoustic pressure on both the structure’s surface and at external points (e.g. on a far-field sphere).

The following subsections detail how this assumption leads to the boundary integral equations used in BEMPP, allowing one to compute the acoustic field without requiring a volumetric mesh of the domain.

Representation Formula

Consider a boundary Γ enclosing a region Ω^- (interior domain). For exterior acoustic radiation problems, the total acoustic pressure P_{total} in the region outside Γ (i.e., $\mathbb{R}^3 \setminus \Omega$) can be written as

$$P_{\text{total}}(\mathbf{x}) = \mathcal{D} P_{\text{total}}(\mathbf{x}) - i\omega \rho_0 \mathcal{S} U_{\text{total}}(\mathbf{x}), \quad \mathbf{x} \notin \Gamma, \quad (3.15.19)$$

where:

- \mathcal{D} is the *double-layer potential* operator, representing dipole-like contributions on Γ .

- \mathcal{S} is the *single-layer potential* operator, representing monopole-like contributions on Γ .
- U_{total} is the (known) normal velocity distribution on Γ .
- ω is the angular frequency, and ρ_0 is the fluid density.

This *representation formula* indicates that the total field in the exterior can be reconstructed from boundary integrals alone, avoiding the need for volumetric meshing of the acoustic domain (a key advantage of boundary element methods).

Physical Intuition:

- SU_{total} captures how vibrating surface elements act as distributed monopole sources, radiating outward.
- $\mathcal{D}P_{\text{total}}$ encodes dipole effects, reflecting the fact that the *normal derivative* of pressure on the boundary effectively acts like pairs of equal and opposite monopoles. By integrating these localized “dipoles” over the boundary, the wave radiation pattern acquires directional features determined by how quickly pressure changes across the interface.

Boundary Integral Equation via the Null Field Approach

To solve for P_{total} on Γ , *null field condition* is imposed inside the closed surface Γ . Specifically, for interior points $\mathbf{x} \in \Gamma^- \subset \Omega^-$:

$$P_{\text{total}}(\mathbf{x}) = 0 \quad \text{for } \mathbf{x} \in \Omega^-.$$

Thus, Γ^- is a surface lying infinitesimally inside Γ .

When evaluating the double-layer potential \mathcal{D} at an interior point close to Γ , a well-known *jump condition* arises:

$$\lim_{\mathbf{x} \rightarrow \Gamma^-} \mathcal{D} P_{\text{total}}(\mathbf{x}) = (\mathbf{D} - \frac{1}{2}\mathbf{I}) P_{\text{total}},$$

where \mathbf{D} is the *double-layer boundary operator* (a discretized version of \mathcal{D}), and \mathbf{I} is the identity operator. Since we set $P_{\text{total}} \equiv 0$ just inside Γ , the representation formula (3.15.19) becomes:

$$(\mathbf{D} - \frac{1}{2}\mathbf{I}) P_{\text{total}} = i\omega\rho_0 \mathbf{S} U_{\text{total}}. \quad (3.15.20)$$

This is the *boundary integral equation* (BIE) that must be solved to obtain the unknown pressure field on the boundary. Here, \mathbf{S} is the *single-layer boundary operator*, discretizing the operator \mathcal{S} in (3.15.19).

Interpretation:

- The $-\frac{1}{2}\mathbf{I}$ term arises from the classical jump relation for the double-layer potential as one crosses Γ from inside to outside.

- Imposing $P_{\text{total}} = 0$ just inside Γ models a scenario where the region Ω^- (the “interior”) does not sustain any acoustic field. This is consistent with the structure displacing outward into the surrounding fluid without reflecting sound back inside.
- The right-hand side, $i\omega\rho_0 \mathbf{S} U_{\text{total}}$, indicates that known *normal velocities* (from a structural solver) drive the acoustic field on the boundary.

Matrix Representation in a Discretized Form

Once the boundary Γ is meshed and basis functions are selected (e.g., continuous linear polynomials), the operators \mathcal{S} and \mathcal{D} become concrete system matrices \mathbf{S} and \mathbf{D} . Similarly, the pressure and velocity fields on Γ become vectors $\mathbf{p}_{\text{total}}$ and $\mathbf{u}_{\text{total}}$. The boundary integral equation (3.15.20) thus transforms to:

$$[\mathbf{D} - \frac{1}{2}\mathbf{I}] \mathbf{p}_{\text{total}} = i\omega\rho_0 \mathbf{S} \mathbf{u}_{\text{total}}. \quad (3.15.21)$$

Solving this linear system (e.g., via GMRES) yields $\mathbf{p}_{\text{total}}$, the vector of nodal acoustic pressures on Γ .

Computing Pressure in the Exterior Domain

Once $\mathbf{p}_{\text{total}}$ is known on the boundary, *any* point \mathbf{x} in the exterior domain (e.g. on a far-field sphere) can have its pressure evaluated using:

$$P_{\text{total}}(\mathbf{x}) = \mathbf{D} \mathbf{p}_{\text{total}} - i\omega\rho_0 \mathbf{S} \mathbf{u}_{\text{total}}, \quad \mathbf{x} \notin \Gamma. \quad (3.15.22)$$

This reconstruction formula leverages the single- and double-layer potentials to “project” the boundary solution into the infinite exterior. Hence, one easily obtains acoustic pressure at any observation point.

Summary

In BEMPP, one adopts a null field approach by imposing zero interior pressure on Γ^- . The boundary integral equation

$$\left(\mathbf{D} - \frac{1}{2}\mathbf{I}\right) P_{\text{total}} = i\omega\rho_0 \mathbf{S} U_{\text{total}},$$

is solved numerically to find $\mathbf{p}_{\text{total}}$ on Γ . Equation (3.15.22) then recovers the field at external points in the unbounded domain. This elegant formulation exemplifies the core advantage of boundary element methods: *only the boundary must be discretized*, and once boundary unknowns are computed, the pressure can be evaluated anywhere in the exterior with no added volumetric modeling.

Chapter 4

Methodology

This chapter details the methodologies employed to conduct acoustic simulations using Finite Element Method (FEM) in Abaqus and Boundary Element Method (BEM) in BEMPP. The objective is to evaluate different acoustic simulation approaches, compare their computational efficiency, and validate their accuracy in predicting sound pressure levels (SPL).

The first section focuses on comparing fully coupled and sequentially coupled acoustic-structural simulations of a prototype cube model in Abaqus. This comparison aims to assess whether the computationally efficient sequentially coupled approach can provide results comparable to the fully coupled method.

The second section presents a sequentially coupled acoustic analysis of a wind turbine gearbox, where structural displacement data obtained from Simpack multibody simulations is transferred to Abaqus for acoustic calculations. This methodology is crucial for as it creates a integrated workflow for acoustic analysis using Simpack and Abaqus.

The third section extends the analysis by implementing Boundary Element Method (BEM) using BEMPP. The sound pressure levels computed for the prototype cube model in BEMPP are compared with the results obtained from Abaqus. This comparison highlights the applicability of BEM for exterior acoustic problems.

Through these methodologies, this study aims to identify the most computationally efficient and accurate approach for exterior acoustic analysis under free-field conditions.

4.1 Comparative Analysis of Fully Coupled and Sequentially Coupled Acoustic Simulations in Abaqus

This section outlines the model setup, meshing strategies, acoustic-structural interface definitions, frequency response analysis, and output variables for both approaches, providing a foundation for the subsequent results and discussion.

4.1.1 Objective

As discussed in the theoretical background chapter, the fully coupled analysis accounts for the bidirectional interaction between the structural and acoustic domains. Specifically, it considers:

- The effect of structural vibrations on the surrounding acoustic medium.
- The feedback effect of acoustic pressure variations in the fluid on the structural vibrations.

In contrast, the sequentially coupled approach simplifies this interaction by treating it as unidirectional. The structural response is computed first, and its effects on the acoustic medium are then analyzed, without considering the reciprocal influence of the acoustic domain on the structure.

This section presents a comparative study using both methods to calculate the sound pressure around a prototype cube model subjected to harmonic vibrations. The prototype cube model is chosen because it has a simple geometry that is easier to model. The cube is surrounded by atmospheric air, serving as the acoustic medium for sound propagation. The comparison is based on:

- The accuracy of sound pressure levels (SPL) obtained from both methods.
- The computational efficiency of each approach.

The analysis conducted here is a coupled acoustic structural analysis with far-field boundary conditions, where the sound waves emitted from the vibrating structure propagate outward without reflection. To simulate the far-field behavior, acoustic infinite elements are utilized, which effectively model the dissipation of sound energy as the waves extend indefinitely into the surrounding acoustic domain.

The goal is to assess whether the sequentially coupled method can serve as a viable alternative to the fully coupled analysis in scenarios where computational resources are constrained. If the sequentially coupled results closely align with those of the fully coupled analysis, it would confirm its suitability for such applications, offering a significant reduction in computational cost without compromising accuracy.

4.1.2 Model Setup for Fully Coupled Acoustic-Structural Analysis of the Prototype Cube

Structural Mesh

The first step in the analysis involves creating the structural mesh for a hollow steel cube with an outer edge length of 100 mm and a wall thickness of 1 mm. This prototype cube is meshed using Altair HyperMesh¹, and the mesh is then exported to Abaqus. The structural elements chosen are S4R (*Quadrilateral shell elements with four nodes*),

¹Hypermesh: <https://altair.com/hypermesh>

which provide six degrees of freedom (DOF) at each node (three translational and three rotational). For the purposes of acoustic coupling, only the translational DOFs are relevant, as they drive the vibrations that generate sound waves in the surrounding medium.

A uniform mesh size of 10 mm is applied to the cube as shown in the 4.1.1. The cube has 602 nodes and 600 quadrilateral shell elements. A concentrated harmonic load of 100 N in the positive x -direction is applied at the center of one face (the face normal to the x -axis) as shown in 4.1.2. The material properties of steel are defined in a consistent unit system of tonne, millimeter, and second, as Abaqus does not enforce a specific system of units. The relevant material properties are:

- Density: 7.8500×10^{-9} tonne/mm³
- Young's modulus: 2.1×10^5 MPa
- Poisson's ratio: 0.3
- Structural damping: 0.01

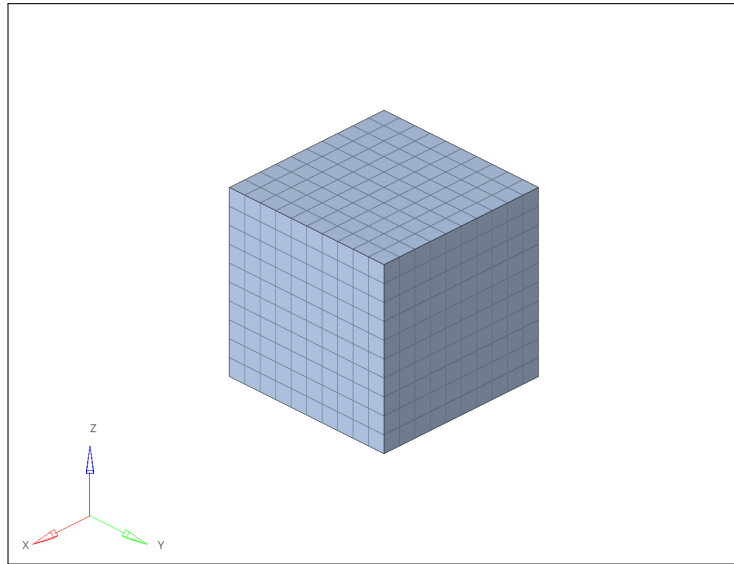


Figure 4.1.1: Mesh of the prototype cube model used in both fully coupled and sequentially coupled analysis.

Acoustic Cavity Mesh

The objective is to evaluate the sound pressure level (SPL) at a distance of 200 mm from the center of the cube. To achieve this, an acoustic cavity needs to be modeled around the structure, extending from the outer surface of the cube to a spherical boundary with a radius of 200 mm. A spherical geometry is chosen for the acoustic domain because of its simplicity in representing outward radiation in all directions. The material properties assigned to the elements of the acoustic cavity correspond to atmospheric air with the following values:

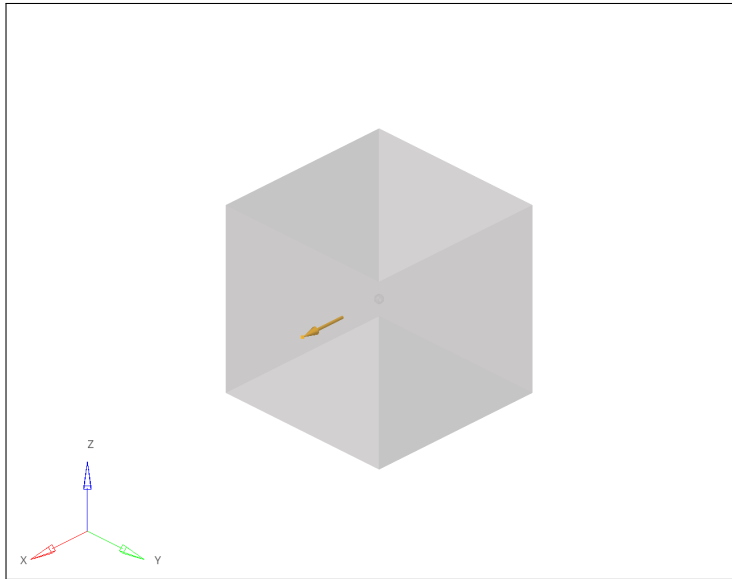


Figure 4.1.2: Illustration of the harmonic load of 100N applied to the prototype cube model.

- Density: 1.2200×10^{-12} tonne/mm³
- Bulk Modulus: 0.144 tonne/mm-sec²
- No damping is assigned to the acoustic cavity, as the damping effects of sound waves in air are considered negligible for this analysis. Additionally, since the objective is to compare the results between fully coupled and sequentially coupled methodologies, damping is uniformly ignored in both methodologies to ensure consistency in the comparison.

Hexahedral meshes are known for their superior accuracy compared to tetrahedral meshes. However, achieving a hexahedral mesh is challenging in regions with irregular geometries, such as the gap between the cube and the sphere. To balance accuracy and practicality, the cavity is divided into two regions as shown in the figure 4.1.3:

1. **Inner Region (from cube surface up to 150 mm radius):** Meshed primarily with tetrahedral (AC3D4 in Abaqus) elements. Tetra elements are better suited for complex or irregular boundaries—here, the transition from the cube to the sphere.
2. **Outer Region (from 150 mm to 200 mm radius):** Meshed using a structured hexahedral (AC3D8 in Abaqus) elements. In this region, the volume between two concentric spheres is regular, making it suitable for hexahedral meshing. Pentahedral (AC3D5) elements appear in transition zones.

Tetrahedral Meshing Process

1. *Surface Meshing of the Inner Sphere (150 mm radius):*
A spherical shell of radius 150 mm is generated and meshed with a mix of quadrilateral(quad) and some triangular(tria) shell elements. While quadrilaterals are

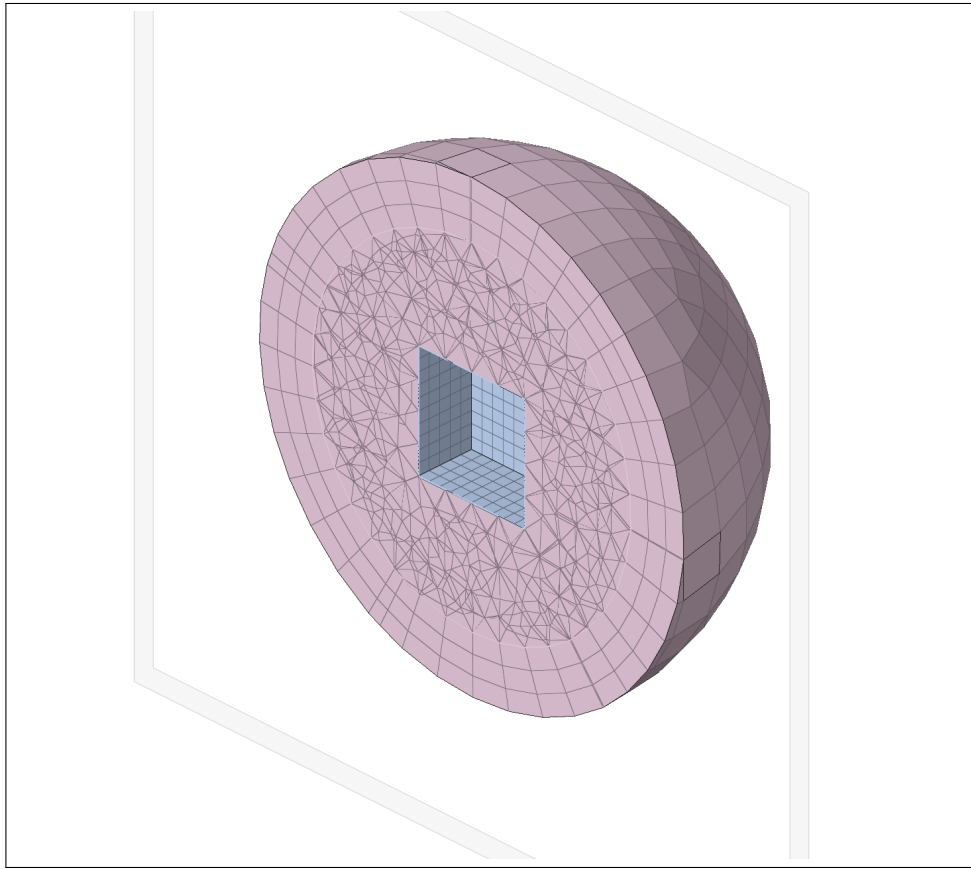


Figure 4.1.3: XZ-plane section cut view of the acoustic cavity mesh surrounding the prototype cube model, showing the inner region meshed with tetrahedral elements and the outer region meshed with hexahedral elements.

generally preferred for better accuracy, a few triangular elements are included to maintain good flow of the mesh where the geometry is converging.

2. Volume Meshing of the Inner Region:

Once a watertight surface mesh is created (ensuring there are no free edges between the cube and the spherical surface), the volume enclosed is meshed with tetrahedral elements (AC3D4). A key quality metric used is the *tet collapse* parameter, which ranges from 0 (completely degenerate tetrahedron) to 1 (perfectly equilateral tetrahedron). Here, a threshold of > 0.2 is used to maintain adequate element quality [56].

Hexahedral Meshing of the Outer Region

For the remaining 50 mm of radial distance (from 150 mm to 200 mm radius), a second spherical shell is created at 200 mm. The shell elements from the 150 mm sphere are projected onto this outer surface so that corresponding nodes align, facilitating a structured mesh approach (the *Solid Map* feature in HyperMesh).

- **Hexa-to-Hexa Mapping:** When quadrilateral faces on the inner sphere map to quadrilateral faces on the outer sphere, the volume between them is filled with hexahedral elements (AC3D8).

- **Tri-to-Tri Mapping:** Where triangular faces exist, pentahedral elements (AC3D5) are generated in the transition zones.

Table 4.1.1: Element and Node Count in the Acoustic Cavity Mesh of the Prototype Cube Model

Mesh Component	Count
Total Nodes	4,700
Tetrahedral Elements (AC3D4)	15,800
Hexahedral Elements (AC3D8)	1,400
Pentahedral Elements (AC3D5)	90
Triangular Infinite Element (ACIN3D3)	30
Quadrilateral Infinite Element (ACIN3D4)	494

Infinite Elements

The outermost shell of elements (at the 200 mm radius) is designated as the far-field boundary using acoustic infinite elements (ACIN3D3 or ACIN3D4 for tria and quad elements respectively). These elements model an unbounded acoustic domain by simulating the dissipation of acoustic waves as they travel to infinity, preventing non-physical reflections at the boundary.

The infinite elements are extracted from the faces of the 3D elements in the outermost layer of the acoustic cavity mesh. Each face of the 3D elements becomes a shell element, sharing its nodes with the 3D elements of the cavity. These shell elements are then assigned infinite-element properties to act as the far-field boundary.

A reference point for these infinite elements is defined at the center of the sphere (coincident with the center of the cube) as shown in the figure 4.1.4. The vector from this reference point to each node on the infinite-element boundary establishes the radial direction of wave propagation, ensuring that the acoustic waves travel outward seamlessly into the unbounded domain.

Summary

In this fully coupled acoustic-structural analysis:

- The steel cube is modeled using shell elements (S4R) to capture structural vibrations.
- The surrounding acoustic cavity is discretized with tetrahedral (AC3D4), pentahedral (AC3D5), and hexahedral (AC3D8) elements from 0 to 200 mm radius.
- The outer boundary at 200 mm is treated with acoustic infinite elements (ACIN3D3, ACIN3D4) to emulate free-field conditions.

This detailed modeling approach ensures that structural vibrations are accurately coupled with the surrounding acoustic field, allowing for precise calculation of the sound pressure at the specified distances. The complete model is shown in the figure 4.1.5

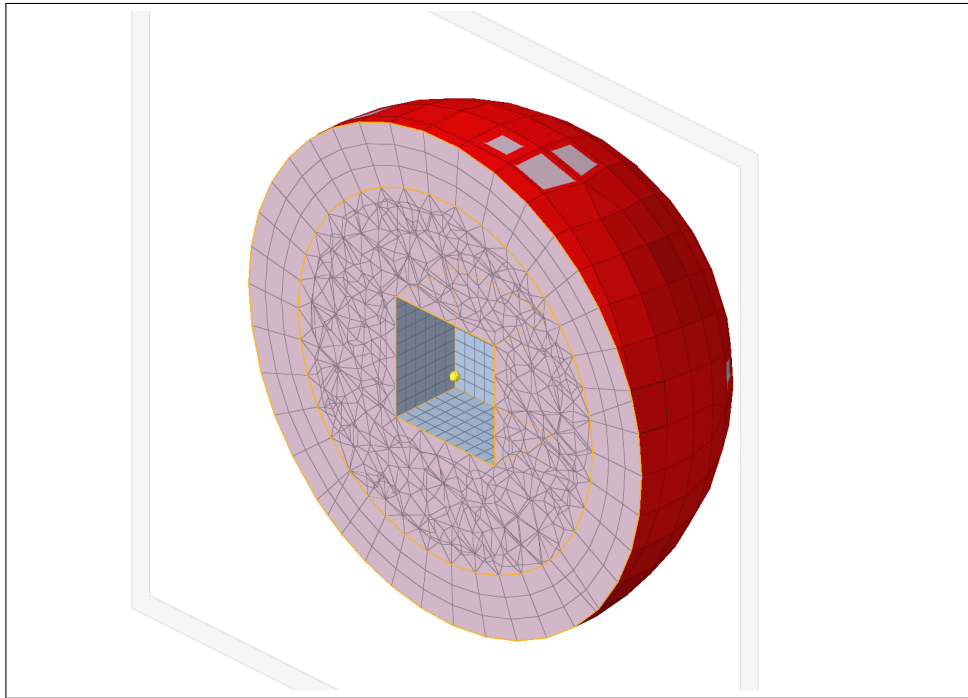


Figure 4.1.4: XZ-plane section cut view of the acoustic cavity mesh showing the outermost layer of infinite elements (in red) and the reference point for these elements (yellow node) defined at the center of the sphere.

4.1.3 Mesh Resolution and Acoustic Cavity Dimensions

Accurate modeling of acoustic phenomena in finite element analysis requires careful consideration of both the mesh resolution and the extent of the acoustic domain. Inadequate mesh refinement is a common source of error in acoustic and vibration analyses. Abaqus recommends that at least six (and preferably ten or more) internodal intervals of the acoustic mesh should fit into the shortest acoustic wavelength present in the analysis. In steady-state dynamic analyses, this shortest wavelength typically corresponds to the highest frequency of interest and the medium with the lowest speed of sound.

Mesh Refinement Criteria

An "internodal interval" is the distance between two adjacent nodes in an element. For a linear element, this distance essentially represents the element size. Let L_{\max} denote the largest internodal interval in the mesh, n_{\min} the minimum number of intervals per wavelength (with a recommended lower bound of 6), f_{\max} the maximum excitation frequency, and

$$c = \sqrt{\frac{K_f}{\rho_f}}$$

the speed of sound in the acoustic medium, where K_f is the bulk modulus and ρ_f is the density of the fluid. Abaqus provides the following guidelines for the maximum allowable element size [57]:

$$L_{\max} < \frac{c}{n_{\min} f_{\max}} \quad \text{or equivalently} \quad f_{\max} < \frac{c}{n_{\min} L_{\max}}.$$

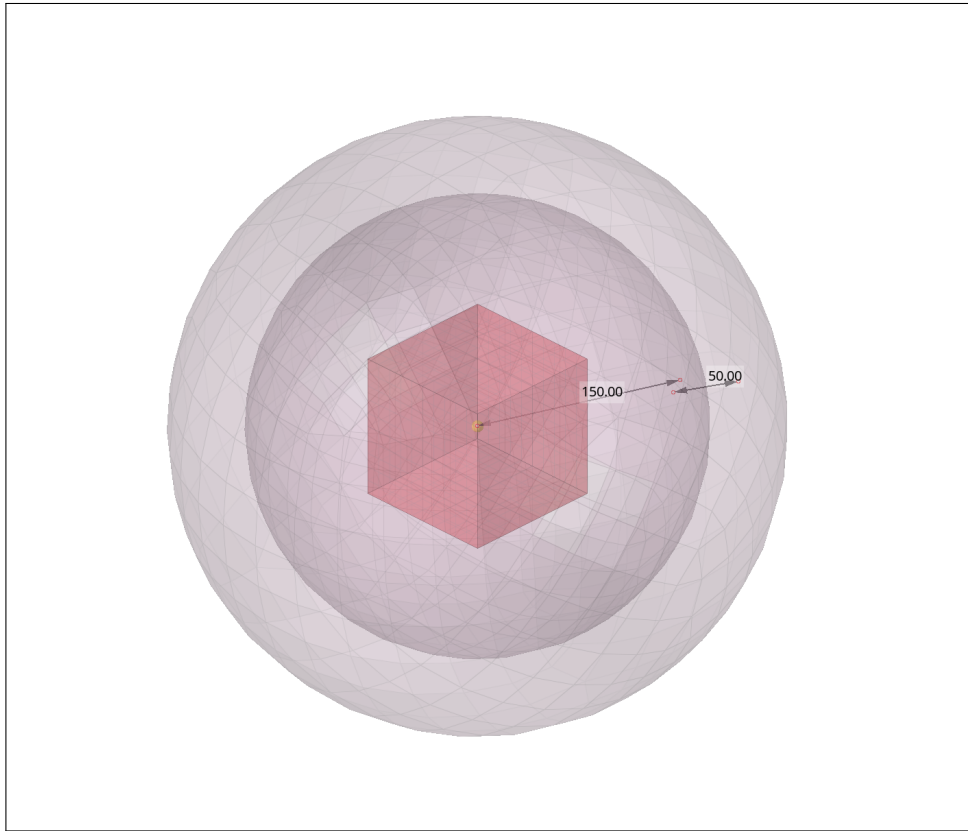


Figure 4.1.5: Translucent view of the complete model for the fully coupled acoustic-structural simulation setup, showing the cube structure at the center, surrounded by the inner and outer acoustic cavity.

If the target frequency range is known, these expressions can be used to estimate the largest acceptable element dimension. Conversely, if the mesh size is prescribed, one can estimate the highest valid frequency for that mesh.

Application to the Cube Model

In the fully and sequentially coupled analyses of the steel cube, the steady-state dynamic frequency range extends from 500 Hz to 1000 Hz. The shortest acoustic wavelength λ_{\min} occurs at 1000 Hz. If the speed of sound is taken as $c = 343550 \text{ mm/s}$, the corresponding wavelength is:

$$\lambda_{\min} = \frac{c}{f_{\max}} = \frac{343550 \text{ mm/s}}{1000 \text{ Hz}} = 343.55 \text{ mm.}$$

Choosing $n_{\min} = 10$ elements per wavelength (a more stringent requirement than the recommended minimum of 6) implies:

$$L_{\max} = \frac{\lambda_{\min}}{n_{\min}} = \frac{343.55 \text{ mm}}{10} \approx 34 \text{ mm.}$$

In this study, an average element size of 25 mm was used, with no element exceeding 34 mm in internodal distance. Thus, the mesh is sufficiently refined to capture acoustic wave propagation up to 1000 Hz.

Determination of Acoustic Cavity Radius

For exterior acoustic problems, the accuracy also depends on the treatment of the far-field boundary. In Abaqus, the boundary can be applied via infinite elements, but these need a certain standoff distance r_1 of finite acoustic elements from the vibrating source. The recommended standoff thickness r_1 is often expressed in wavelengths at the minimum frequency of interest, f_{\min} :

$$r_1 > \frac{c m_{\min}}{f_{\min}} \quad \text{or} \quad f_{\min} > \frac{c m_{\min}}{r_1},$$

where m_{\min} is the desired fraction of a wavelength. The recommended value of m_{\min} in Abaqus manual is: $m_{\min} = \frac{1}{4}$ [57]. In this analysis, the minimum frequency is 500 Hz, corresponding to a wavelength

$$\lambda_{\max} = \frac{c}{f_{\min}} = \frac{343550 \text{ mm/s}}{500 \text{ Hz}} = 687.1 \text{ mm.}$$

Substituting $m_{\min} = \frac{1}{4}$ yields

$$r_1 = \lambda_{\max} m_{\min} = 687.1 \times \frac{1}{4} \approx 171.77 \text{ mm.}$$

To ensure even better accuracy, the spherical acoustic cavity in this study has a radius of 200 mm, which comfortably satisfies the minimum standoff requirement.

Computational Considerations

Finally, the total number of nodes, N , in an exterior acoustic-structural model depends on both the volume enclosed by the standoff region (r_1) and the mesh density (L_{\max}). In a d -dimensional problem, N can be approximated by:

$$N \sim \left(\frac{r_1}{L_{\max}} \right)^d \sim \left(\frac{f_{\max}}{f_{\min}} m_{\min} n_{\min} \right)^d.$$

As r_1 and n_{\min} increase, the number of elements grows, leading to higher computational costs. Balancing accuracy requirements with available computational resources is thus a critical part of designing an efficient and reliable acoustic simulation. In this study, the chosen mesh size and cavity satisfy the requirement.

4.1.4 Acoustic-Structural Interface Using Structural Ties in Fully Coupled Analysis

As described in the theoretical background chapter (Section 3.12.2), structural ties are used to couple the acoustic and structural domains in fully coupled analyses. In Abaqus, structural ties are defined by creating element-based surfaces on the interface between the structure and the acoustic domain. For the prototype cube model, the surfaces are defined as follows:

- An element-based surface is created on the outer surface of the cube.

- Another element-based surface is created on the innermost layer of the acoustic cavity.

These surfaces are shown in Figure 4.1.6 and 4.1.7. The surface created on the innermost layer of the acoustic cavity, named `acou_str`, is designated as the primary surface. The surface created on the cube, named `str_acou`, is designated as the secondary surface. This designation ensures accurate coupling, as the primary surface is generally the one with the coarser mesh, which in this case is the acoustic cavity surface.

The surfaces are created in HyperMesh using the *Set Segment* option, where the user selects the elements on which the surface is to be created.

Normal Vector Orientation

To ensure correct coupling between the structural and acoustic domains, the normal vectors of the structural and acoustic elements at the interface must point towards each other. This orientation guarantees proper mapping of degrees of freedom between the two domains.

As illustrated in Figure 4.1.8:

- The normals of the `str_acou` surface point outward from the cube, towards the acoustic cavity.
- The normals of the `acou_str` surface point inward, towards the cube.

This configuration establishes a bidirectional interaction between the structural and acoustic domains, allowing for the accurate exchange of displacements at the interface.

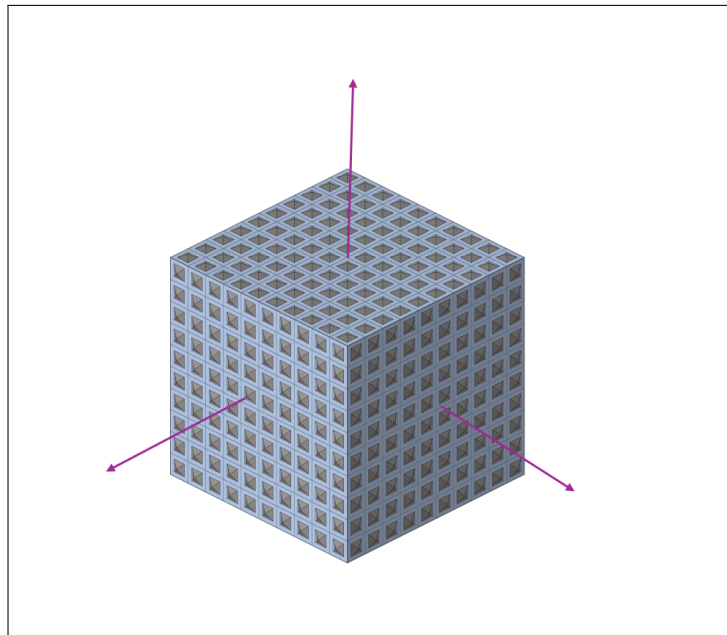


Figure 4.1.6: `str_acou` surface pointing outward from the cube towards the acoustic cavity.

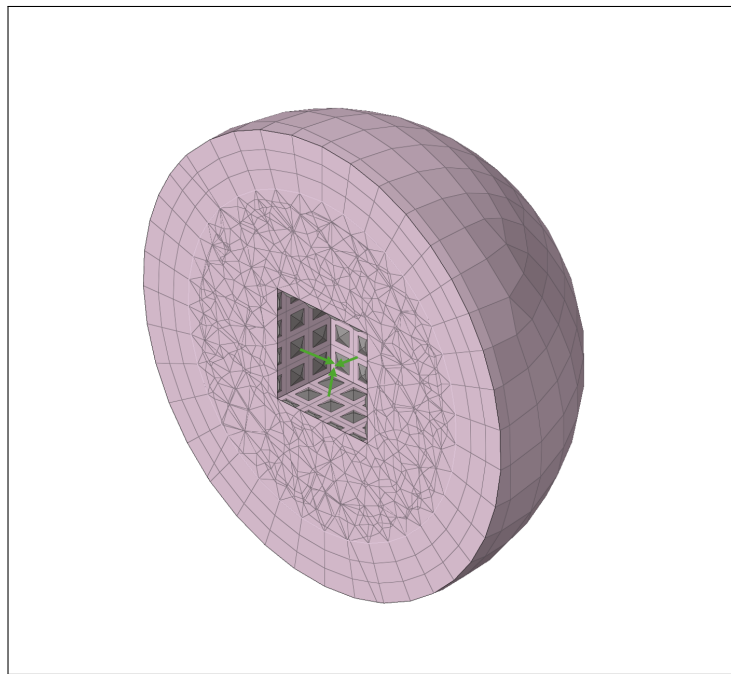


Figure 4.1.7: `acou_str` surface at the interface pointing inward towards the cube.

4.1.5 Frequency Response Analysis in Fully Coupled Simulation

The primary analysis step for the fully coupled simulation is a direct-solution steady-state dynamic analysis. This method directly computes the system's response in terms of its physical degrees of freedom. The analysis involves performing a frequency sweep from 500 Hz to 1000 Hz with a step size of 10 Hz, resulting in a total of 51 frequencies.

Loading Conditions

In this analysis, a harmonic load of 100 N is applied on a single node located on the surface of the cube as shown in the Figure 4.1.2. The node set containing this node is defined as `accn` in the input file. For each frequency in the sweep, the magnitude of the concentrated load oscillates sinusoidally at the corresponding frequency. This excitation causes the cube to vibrate, and these vibrations are transmitted into the surrounding acoustic medium via the structural ties.

Acoustic Wave Propagation

As the cube vibrates, pressure variations are induced in the acoustic cavity, generating sound waves that propagate outward. The acoustic infinite elements placed at the far-field boundary ensure that these waves travel outward without reflection, simulating free-field conditions.

The corresponding Abaqus input file syntax for this analysis step is shown below:

```
*Step
  Step-1: Frequency Response
*Steady State Dynamics, direct, frequency scale=linear
```

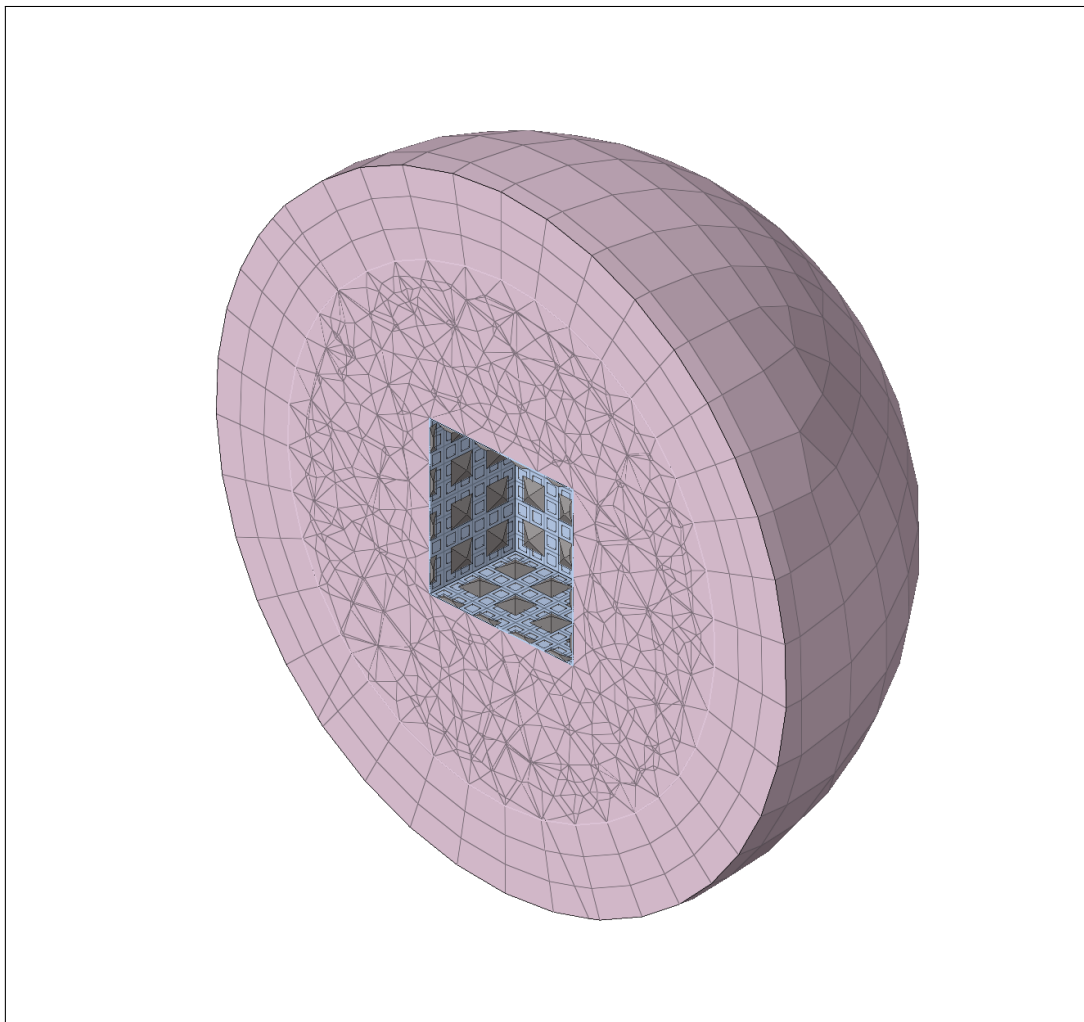


Figure 4.1.8: Structural Ties are used to tie the displacements between `str_acou` and `acou_str` surfaces.

```
500,1000,51  
*CLOAD, OP=NEW  
accn,1,100.0  
*End step
```

4.1.6 Output Definition

The complex sound pressure is computed for the nodes on the infinite-element boundary. This output is used to evaluate the sound pressure levels (SPL) and serves as the basis for comparison with the sequentially coupled analysis. Additionally RADPOW and ERP is also used to validate the model as mentioned in the (Section 3.12.3.3)

Syntax for field output POR in Abaqus Input File

The following syntax is used in the Abaqus input file to define the output of sound pressure at specific nodes:

```
*OUTPUT, FIELD, FREQUENCY=1
*NODE OUTPUT, NSET=por
POR
```

The node set `por` consists of the nodes of the acoustic infinite elements that are located at a distance of 200 mm from the center of the cube. These nodes are used to calculate the sound pressure at the specified location.

In this example:

- `*OUTPUT, FIELD, FREQUENCY=1` specifies that field output should be recorded at every frequency increment of the step, corresponding to each frequency in a frequency-domain analysis.
- `*NODE OUTPUT, NSET=por` defines the node set `por` for which the output is requested.
- `POR` is the output variable representing the sound pressure at the specified nodes.

Syntax for RADPOW output in Abaqus Input File

`RADPOW` represents the radiated power across a specified boundary. In this analysis, `outer_infinite` is an element set containing the infinite elements which represents the boundary:

```
*OUTPUT, HISTORY
*ENERGY OUTPUT, ELSET=outer_infinite
RADPOW
```

Alternatively, the radiated energy can be output using `RADEN` instead of `RADPOW`.

ERP calculation in Abaqus

Equivalent Radiated Power (ERP) estimates the acoustic power radiated by a vibrating cube under idealized plane wave conditions. The steady-state dynamic (SSD) step provides the normal velocity field at the nodes of the cube. Abaqus offers an output variable, `AVNSQ` (area-weighted surface normal velocity squared), which is utilized for calculating the Equivalent Radiated Power (ERP). To request `AVNSQ`, a self-contact interaction must be defined on the cube's surface that radiates sound (e.g., `str_acou`), as illustrated below:

```
** Define a surface interaction to calculate AVNSQ (ERP)
*SURFACE INTERACTION, NAME=dummy_One
*CONTACT PAIR, INTERACTION=dummy_One
str_acou

*OUTPUT, FIELD, FREQUENCY=1
*CONTACT OUTPUT
AVNSQ
```

In this example, `str_acou` represents an element-based surface on the cube structure emitting sound. By summing the `AVNSQ` values over the entire surface and multiplying by ρc , it is possible calculate the total ERP. A python script is utilized to calculate ERP after conducting the SSD.

4.1.7 Model Setup for the Sequentially Coupled Acoustic–Structural Analysis of the Prototype Cube

The overall geometry and mesh configuration for the sequentially coupled analysis of the prototype cube are the same as those described for the fully coupled model (Section 4.1.2). The same steel cube, acoustic cavity, infinite elements, and mesh resolution criteria are used. A harmonic load is applied to the cube in an identical manner.

However, unlike the fully coupled approach—which uses structural ties to link the cube and acoustic medium—this sequentially coupled method employs *acoustic–structural interface (ASI) elements* to couple displacements from the structural domain to the acoustic domain. This change in how displacements are transferred forms the core distinction between the two approaches.

4.1.8 Acoustic–Structural Interface with ASI Elements in Sequentially Coupled Analysis

In the fully coupled simulation, the entire assembly (cube and acoustic cavity) is solved within a single analysis step. By contrast, the sequentially coupled approach uses a submodeling technique that involves two separate runs:

1. **Global model analysis:** This run includes *only* the structural cube mesh. The nodes on the cube that drive displacement into the acoustic domain are grouped into a node set named `cube_asi`.
2. **Submodel analysis:** This run contains the acoustic cavity mesh, including the infinite elements. The innermost layer of the cavity mesh, adjacent to the cube, consists of ASI elements (see Figure 4.1.9 for an illustration). These ASI elements share node sets (`asi`) that receive displacement boundary conditions from the global model.

A snippet from the Abaqus input file for the submodel is shown below, highlighting key commands that define ASI elements and the submodel relationship:

```
*Interface, elset=asi  
*Nset, nset=asi, elset=asi  
*Submodel, absolute=1.e-3, global elset=cube_asi  
    asi,
```

The commands serve the following purposes:

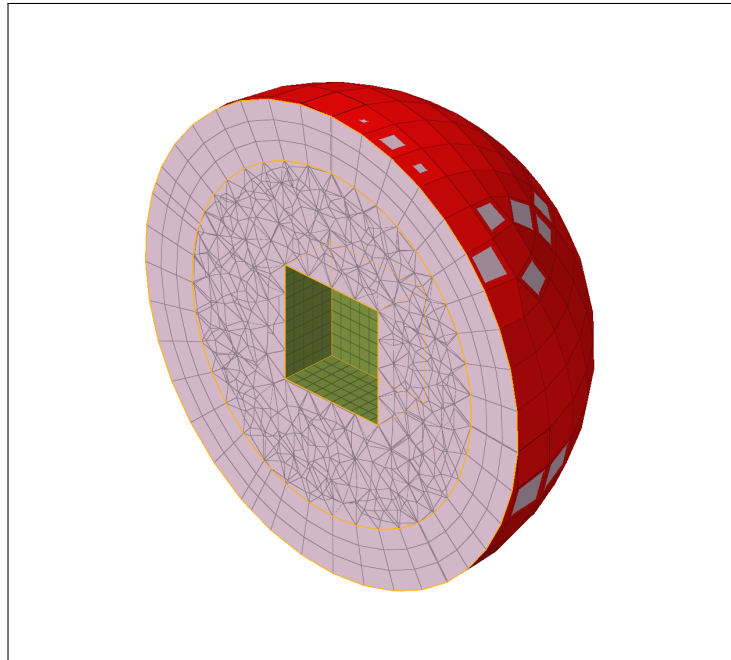


Figure 4.1.9: XZ-plane section cut view of the submodel consisting of acoustic cavity mesh, infinite elements (in red) and the ASI elements (in green)

- ***Interface, elset=asi:** USed to define section properties to ASI elements.
- ***Nset, nset=asi, elset=asi:** Defines a node set named **asi** based on the same element set. These nodes can be driven by the global model.
- ***Submodel, absolute=1.e-3, global elset=cube_asi:** Activates submodeling by referencing the global element set **cube_asi**, which holds the displacement results. The **asi** node set then inherits these displacements in the submodel analysis.

4.1.9 Frequency Response Analysis in the Sequentially Coupled Simulation

Similar to the fully coupled approach, a *direct-solution steady-state dynamics* (SSD) analysis is carried out to capture the frequency response of the system. However, in the sequential approach, this SSD procedure is split across two runs:

Global Model Run (Structure Only)

The first run analyzes the structural cube subjected to the harmonic load. The step definition in the Abaqus input file:

```
*Step
Step-1: Frequency Response
*Steady State Dynamics, direct, frequency scale=linear
  500, 1000, 51
*CLOAD, OP=NEW
```

```

accn, 1, 100.0
*Output, field, frequency=1
*Node output
UT
*End Step

```

In this run:

- The frequency range is from 500 Hz to 1000 Hz, with 51 increments.
- The **accn** node receives a harmonic load of ± 100 N in the specified direction.
- **UT** (translational displacement) is requested as field output at each frequency step.

When this run completes, the output database (.odb file) contains the displacement field **UT** necessary for driving the submodel.

4.1.9.1 Submodel Run (Acoustic Cavity + ASI Elements + Infinite Elements)

In the second run, the acoustic submodel references the global solution. The Abaqus input file includes commands to read the displacements at the interface nodes:

```

*Steady State Dynamics, direct, frequency scale=linear
500, 1000, 51
*Boundary, submodel, step=1
asi, 1, 3
*Output, field, frequency=1
*Node output
POR
*Output, history, frequency=1
*Energy output
ALLQB
*End Step

```

Key points:

- ***Boundary, submodel**: Applies the global model displacements (**UT**) to the nodes in the set **asi**, effectively coupling the structure (from the previous run) to the acoustic domain.
- **POR**: Requests acoustic pressure output at each frequency increment.
- **ALLQB**: Since **RADPOW** is not available in a purely acoustic submodel, **ALLQB** (a total energy measure) is requested instead. By multiplying **ALLQB** by the frequency, the acoustic radiated power for comparison with the fully coupled results can be calculated. Alternatively, **RADEN** from fully coupled analysis can be directly compared to **ALLQB** from sequentially coupled analysis.

4.2 Sequentially Coupled Acoustic Analysis of a Wind Turbine Gearbox Using Simpack and Abaqus

This section outlines the essential steps for performing a sequentially coupled acoustic analysis of a wind turbine gearbox. Initially, the fundamental structure of a wind turbine is examined, along with the motivation for focusing on the gearbox's acoustic response. Subsequently, the methodology for integrating time-domain displacement data from Simpack into Abaqus for far-field sound pressure predictions is introduced, highlighting key challenges and benefits of this approach.

Multibody Simulation (MBS) is a computational technique used to analyze the dynamic behavior of interconnected rigid or flexible bodies under various loading conditions. It is widely employed in mechanical and automotive engineering, biomechanics, and structural dynamics to study system motion, forces, and interactions between components. Simpack² is a commercially available MBS software designed for simulating nonlinear, transient dynamics in mechanical systems.

4.2.1 Wind Turbine Overview and Motivation for Gearbox Acoustic Analysis

Modern wind turbines are complex electromechanical systems designed to convert the kinetic energy of moving air into electrical power. A typical horizontal-axis wind turbine consists of several major components (see Figure 4.2.10 for an illustration):

- **Rotor Blades:** Capture the wind's kinetic energy through aerodynamic lift. The rotating blades are attached to a central hub.
- **Nacelle:** Houses the primary machinery, such as the gearbox and generator, on top of the tower. The nacelle protects sensitive components from environmental factors and facilitates maintenance access.
- **Gearbox:** Steps up the relatively low rotational speed of the rotor to the higher speed required by the generator. It is typically a multi-stage assembly (e.g., two planetary stages followed by a parallel-axis gear stage) to achieve the needed speed ratio.
- **Generator:** Converts the mechanical rotation into electrical energy. The gearbox and the generator operate in tandem to ensure the rotor's motion is efficiently converted into electricity at a suitable frequency and voltage.
- **Tower and Foundation:** Provide structural support and elevate the rotor-nacelle assembly to heights where wind speeds are generally higher and more consistent.

²Simpack: <https://www.3ds.com/products/simulia/simpack>

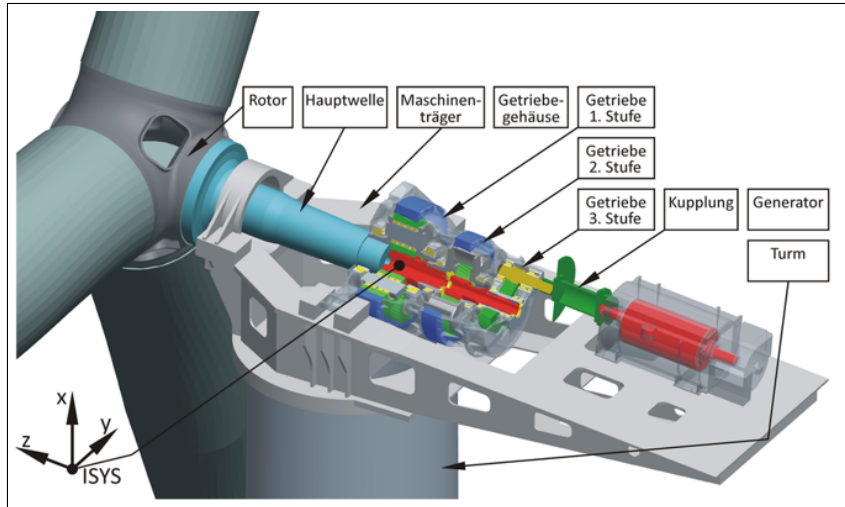


Figure 4.2.10: Schematic of a typical horizontal-axis wind turbine (Source: Chair of Machine Elements, TU Dresden, 2022) [3].

The gearbox is a critical and complex component of a wind turbine's drivetrain, subjected to substantial mechanical loads during operation. The noise from the gearbox is one of the major sources of noise from the wind turbine. Gearbox-induced vibrations propagate through bearing connections to the housing structure, which subsequently radiates acoustic energy into the surrounding atmosphere. This noise emission exhibits distinct tonal components across the frequency spectrum: high-frequency harmonics manifest as characteristic whining tones (500-2000 Hz), while low-frequency excitation (80-500 Hz) generates rumbling noise. The persistent tonal nature of these acoustic emissions, combined with stringent environmental noise regulations, necessitates rigorous coupled acoustic structural analysis to ensure compliance with international standards such as IEC 61400-11[58] and optimal turbine design.

Integration of Simpack and Abaqus

Vibration and noise from the gearbox cannot be fully captured by static or simplified dynamic models. Instead, a *multibody dynamics approach* in Simpack is often employed to simulate realistic operating conditions:

- **Time-Domain Simulation:** Simpack performs a detailed time-domain run, accounting for gear contacts, bearing dynamics, and torque fluctuations over a range of operating speeds.
- **Frequency Extraction:** From a portion of this time-domain data (usually once the generator has reached a *steady operating state*), frequency-specific displacements of the nodes of gearbox casing are extracted. These values represent the gearbox casing's vibrational signature at its working speed.

In this thesis, these frequency-domain displacements from Simpack serve as boundary conditions in a steady-state dynamic analysis in Abaqus. By doing so:

- The vibrational behavior of the gearbox under state conditions is used for the acoustic analysis.

- It is used to simulate the acoustic field around the gearbox casing using far-field boundary conditions, enabling the prediction of sound pressure levels (SPL) at various distances.

Methodology Scope

A pre-existing shell mesh (thickness 1mm) of the gearbox casing and node-specific displacement data (magnitude and phase) from Simpack's frequency-domain analysis across the 90-200 Hz range serve as the starting point for the acoustic simulations. The gearbox casing's shell mesh is processed and converted into a watertight geometry without free edges suitable for acoustic modeling. This step ensures compatibility with volumetric meshing techniques required for the acoustic analysis.

The following sections detail the modeling approach and simulation workflow for transferring displacement data from Simpack into Abaqus for the exterior acoustic analysis of the wind turbine gearbox casing. The methodology covers the following key aspects:

- **Acoustic Cavity Creation:** A volumetric mesh consisting of tetrahedral acoustic elements is generated around the gearbox casing. Infinite elements are incorporated at the outer boundary to accurately simulate far-field radiation and prevent non-physical reflections.
- **Boundary Condition Integration:** The frequency-domain displacement data from Simpack is applied to the gearbox casing within Abaqus' steady-state dynamic analysis. Python scripts are utilized to convert the Simpack output into the appropriate format required for defining boundary conditions in Abaqus.
- **Coupling Approaches:** A comparative study is conducted to evaluate the effectiveness of two different coupling techniques-**structural ties** and **acoustic-structural interface (ASI) elements**-in predicting the acoustic response. The influence of each method on the resulting sound pressure distribution is analyzed.

This methodology establishes a structured approach for integrating multibody simulation results with finite element-based acoustic analysis, ensuring an accurate and computationally efficient framework for evaluating gearbox noise emissions.

4.2.2 Acoustic Cavity Modeling around the Gearbox Casing

The initial shell mesh of the gearbox casing was provided as input. Before generating the volumetric acoustic mesh around it, the casing mesh required cleaning to ensure a fully *watertight* geometry. Specifically:

- All holes and gaps were closed.
- Irrelevant or redundant features, such as bolt holes, small fillets, minor surface irregularities, and fine geometric details that do not significantly impact the acoustic response, were removed to simplify the geometry while preserving overall structural integrity.

- Any remaining free edges were eliminated to avoid discontinuities that would prevent proper volumetric meshing.

After these steps, the gearbox casing was suitable for acoustic meshing without any free edges.

Creation of the Acoustic Cavity and Infinite Elements

Following the guidelines in Abaqus (detailed in Section 4.1.3), an acoustic cavity was constructed around the gearbox by:

1. Generating an outer spherical surface centered at the gearbox. This surface was assigned as the location for *infinite elements* (ACIN3D3 to capture far-field sound radiation (see Section 3.10.1). Only triangular elements are used in the outer sphere because the open-source Boundary Element Method library BEMPP supports only triangular elements. Additionally, as part of the future work, a comparative analysis of acoustic simulation results between Abaqus and BEMPP is planned.
2. Filling the volume between the spherical surface and the gearbox casing with tetrahedral acoustic elements (AC3D4), as illustrated in Figure 4.2.11.

First-order tetrahedral elements were used in this study. However, a detailed mesh convergence study, as well as a comparison with second-order and hexahedral elements, remains as future work. The present study serves as a qualitative comparison of two simulation methodologies rather than a final validation. Further investigation will assess whether higher-order elements offer a significant accuracy improvement that justifies the additional computational cost.

The reference point for the infinite elements was defined at the center of the gearbox so that the outward radial direction for wave propagation could be established. This setup allows acoustic waves to travel outward seamlessly into the unbounded domain.

Determination of Sphere Radius

Based on Abaqus recommendations, the radius r_1 of the outer sphere must satisfy

$$r_1 > \frac{c m_{\min}}{f_{\min}} \quad \text{or} \quad f_{\min} > \frac{c m_{\min}}{r_1},$$

where $c = 343,550 \text{ mm/s}$ (in the tonne–millimeter–second unit system) is the speed of sound, and m_{\min} is the desired fraction of a wavelength. While the minimum frequency of interest in this analysis is 90 Hz, the mesh was conservatively designed to accommodate down to 40 Hz, yielding:

$$\lambda_{\max} = \frac{c}{f_{\min}} = \frac{343,550 \text{ mm/s}}{40 \text{ Hz}} \approx 8588.75 \text{ mm}.$$

Using $m_{\min} = \frac{1}{4}$ [57]:

$$r_1 = \lambda_{\max} \times m_{\min} = 8588.75 \times 0.25 \approx 2147 \text{ mm}.$$

A slightly larger radius of 2300 mm was selected to incorporate a safety margin.



Figure 4.2.11: A sectional view of the acoustic cavity mesh around the gearbox.

Mesh Size for the Frequency Range

The shortest acoustic wavelength λ_{\min} appears at the highest frequency of interest, 200 Hz:

$$\lambda_{\min} = \frac{c}{f_{\max}} = \frac{343,550 \text{ mm/s}}{200 \text{ Hz}} = 1717.75 \text{ mm.}$$

To capture wave propagation accurately, at least eight *internodal intervals* (elements) per wavelength were targeted:

$$L_{\max} = \frac{\lambda_{\min}}{n_{\min}} = \frac{1717.75 \text{ mm}}{8} \approx 215 \text{ mm.}$$

Hence, an average tetra element size of 215 mm was used in the acoustic cavity. The mesh was generated using Altair HyperMesh³, ensuring a *tet collapse* metric above 0.2 [56]. Figure 4.2.12 shows the final cavity mesh, including the outer shell designated as infinite elements.

Material Properties of the Acoustic Domain: The acoustic cavity elements were assigned the properties of air under standard atmospheric conditions:

³Hypermesh: <https://altair.com/hypermesh>

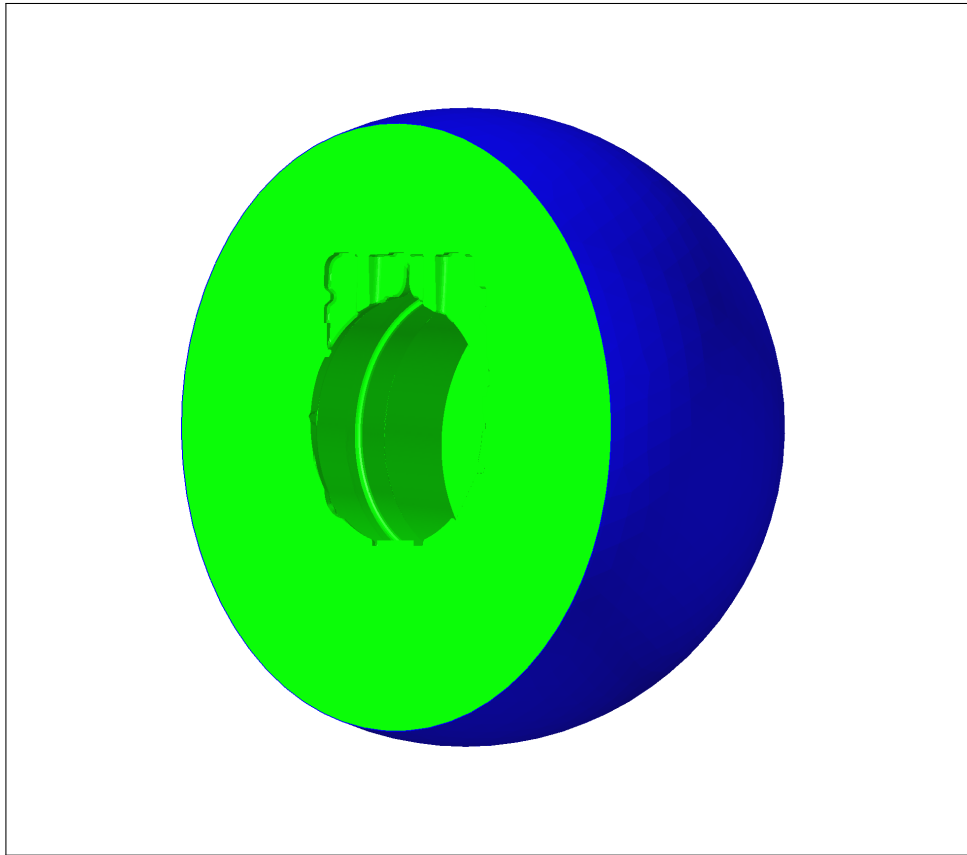


Figure 4.2.12: A sectional view of the acoustic cavity mesh, highlighting the infinite elements (blue) at the outermost boundary.

- Density: $\rho = 1.2200 \times 10^{-12}$ tonne/mm³
- Bulk Modulus: $K_f = 0.144$ tonne/(mm · s²)
- Damping: Neglected in this analysis, as air's attenuation effects are minimal.

This configuration supports frequencies from 90 Hz up to 200 Hz and permits sound waves to propagate outward without nonphysical reflections at the boundary, ensuring a realistic free-field representation.

4.2.3 Methods for Coupling Harmonic Displacements to Acoustic Cavity

The prescribed harmonic displacements from Simpack were integrated with the acoustic cavity mesh through two distinct methodologies developed in this work:

4.2.3.1 Structural Tie Coupling Method

The structural tie approach implements sequential coupling through constrained kinematic relationships between structural and acoustic domains. To optimize computational

efficiency while preserving geometric fidelity, a controlled mesh coarsening strategy was implemented prior to acoustic domain construction. This coarsening process reduces the structural node count by through remeshing, significantly decreasing:

- System matrix sizes in the acoustic solver
- Steady-state dynamic analysis memory requirements

The coarsened mesh serves as a geometric wrapper that:

- Maintains original casing topology
- Provides compatible surface for tie constraints
- Enables acoustic element sizing independent of structural mesh

The implementation workflow consists of three primary phases:

1. Structural Mesh Coarsening:

- Original gearbox mesh: Average element size 10 mm
- Remeshed wrapper: Uniform element size 50 mm
- Coarsening ratio: 5 : 1 (reduces node count by 72%)

2. Acoustic Domain Construction:

- Coarse wrapper mesh used as inner boundary
- Outer spherical boundary at 2300 mm radius
- Tetrahedral acoustic elements (215 mm average size)

3. Interface Coupling:

- Once the acoustic cavity is generated using the gearbox wrapper mesh, the wrapper mesh itself is no longer required. The acoustic cavity is then coupled to the original gearbox casing mesh using structural tie constraints. Element-based surfaces are defined at the interface on both the gearbox casing and the acoustic cavity, ensuring that the normal vectors are correctly oriented toward each other, as described in the prototype cube model (Section 4.1.4).
- Tie constraints are created between the two surfaces enforcing displacement continuity:

$$\mathbf{u}_{\text{acoustic}} = \mathbf{T} \cdot \mathbf{u}_{\text{structural}}$$

where \mathbf{T} is the tie constraint operator matrix

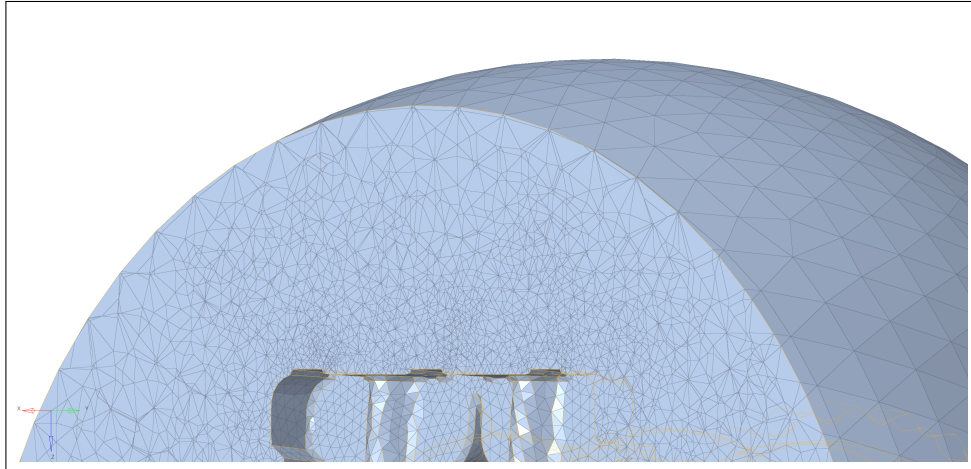


Figure 4.2.13: Cross-sectional view of coarse acoustic cavity mesh assembly

Table 4.2.2: Coarse Acoustic Cavity Mesh Statistics

Component	Count
Total Nodes	276,820
Tetrahedral Elements (AC3D4)	1,569,428
Triangular Infinite Elements (ACIN3D3)	3,840

Material Property Considerations

In the implemented sequentially coupled approach, the structural material properties do not influence the acoustic results when displacements are explicitly prescribed. This behavior stems from the fundamental formulation of boundary conditions in finite element analysis. When nodal displacements $\hat{\mathbf{u}}(x, f)$ are directly specified as boundary conditions in the frequency domain, they override the material-dependent dynamic equilibrium equations:

$$\mathbf{K}(\mathbf{E}, \nu) - \omega^2 \mathbf{M}(\rho) = \mathbf{0} \quad (4.2.1)$$

where \mathbf{K} is the stiffness matrix (dependent on Young's modulus E and Poisson's ratio ν) and \mathbf{M} is the mass matrix (dependent on density ρ). The prescribed displacement approach effectively decouples the material properties from the kinematic solution, as the solver does not compute displacements through Equation 4.2.1 but instead enforces:

$$\mathbf{u}(x, f) = \hat{\mathbf{u}}_{\text{Simpack}}(x, f) \quad \forall x \in \Gamma_{\text{gbx}} \quad (4.2.2)$$

where $\hat{\mathbf{u}}_{\text{Simpack}}$ contains frequency-domain displacements from multibody simulations and Γ_{gbx} denotes the gearbox casing surface. This creates a one-way (sequential) coupling where:

- Structural displacements drive acoustic excitation

- Acoustic feedback to structural response is neglected
- Material properties only affect unconstrained degrees of freedom

This sequential coupling approach was validated through comparative simulations using steel ($E = 210$ GPa) and dummy rubber ($E = 3000$ GPa) material properties, which produced identical sound pressure level (SPL) results as discussed in the results and discussion chapter (5.2)

4.2.3.2 Acoustic-Structural Interface (ASI) Element Method

The ASI approach sequentially couples structural vibrations to acoustic pressures through specialized interface elements as discussed in (Section 3.13.2):

1. Mesh Preparation:

- Retained original fine mesh (10 mm elements)
- Converted shell elements to ASI type (ASI3D3)

2. Acoustic Domain Generation:

- Maintained nodal continuity at interface
- Identical outer sphere configuration at a distance of (2300 mm)
- Fine tetrahedral mesh (215 mm elements)

Interpolation Accuracy Considerations: ASI (Acoustic-Structural Interface) elements allow for non-matching meshes between the gearbox structure and the acoustic cavity at the interface. This is because ASI elements can interpolate displacements from the gearbox mesh and apply them to the corresponding nodes in the acoustic cavity, eliminating the strict requirement for a node-to-node match.

However, in this study, node matching at the interface is intentionally maintained to ensure consistency in the transfer of displacements from the structural domain to the acoustic domain, thereby reducing potential sources of numerical errors.

A key concern when using interpolation is the accuracy of displacement transfer at the interface. This issue arises in the structural ties method, as explained in the previous section, where a coarse wrap mesh of the gearbox is used to generate a corresponding coarse acoustic cavity mesh. The original fine gearbox mesh is then tied to this coarse acoustic cavity mesh, leading to fewer nodes available for interpolation. Since a coarser mesh provides lower resolution displacement data, this may introduce inaccuracies in the acoustic simulation.

To assess the impact of interpolation accuracy, an alternative approach is implemented in this case where the original fine gearbox mesh is directly used to generate a fine acoustic cavity mesh. In this setup, the fine structural mesh is coupled with the fine acoustic cavity mesh, ensuring that interpolation accuracy is not limited by insufficient resolution

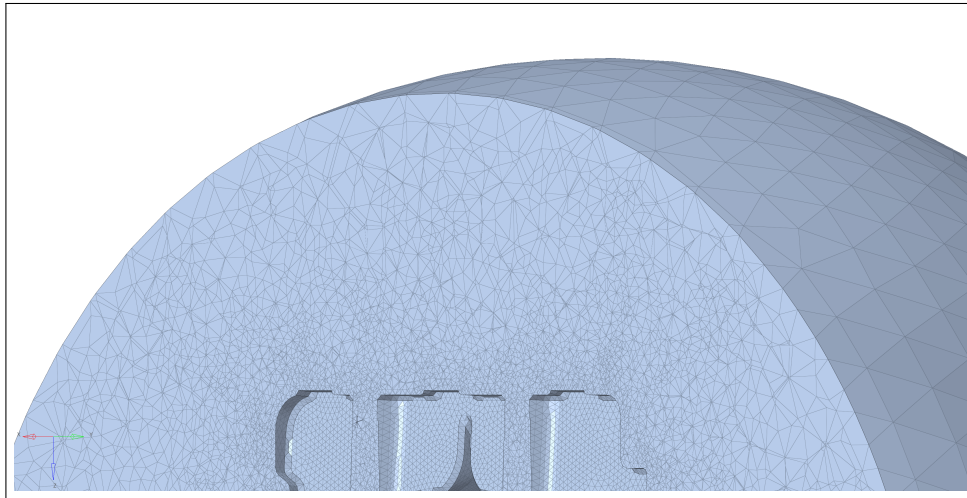


Figure 4.2.14: Fine-resolution acoustic cavity mesh for ASI coupling

in the structural mesh. The corresponding fine acoustic cavity mesh is illustrated in Figure 4.2.14.

Table 4.2.3: Fine Acoustic Cavity Mesh Statistics

Component	Count
Total Nodes	1,001,528
Tetrahedral Elements (AC3D4)	6,318,529
Triangular Infinite Elements (ACIN3D3)	3,840

Both methodologies facilitate sequential coupling but fundamentally differ in terms of:

- Computational resource requirements
- Implementation complexity

The comparative performance evaluation is presented in (Section 5.2).

4.2.4 Converting Simpack Data into Abaqus Format

Data Source and Challenges

The displacement data obtained from Simpack's time-domain multibody simulation consists of nodal vibration amplitudes and phases across operational frequencies. Key characteristics of the raw data include:

- CSV-formatted data file (.drf) structure

- Frequency-domain outputs for steady-state conditions
- Columns: Node ID, Amplitude/Phase pairs for X/Y/Z displacements

A significant challenge arises due to mesh modifications required during the preparation of the acoustic cavity in the context of applying displacement boundary conditions from Simpack. These modifications introduce complexities that must be addressed to ensure accurate simulation results:

- **Patch Elements and Remeshing:** The holes in the original gearbox mesh are filled using patch elements, and certain areas are remeshed to eliminate free edges. However, these remeshing operations alter the original node numbering, preventing the direct application of Simpack-derived displacements to the affected nodes.
- **Zero Displacement Boundary Condition:** A zero displacement boundary condition is imposed on the nodes of the patch and remeshed elements. Applying zero velocity to the patch elements is justified, as these elements do not correspond to physical components of the gearbox but are introduced solely for modeling purposes. Without enforcing zero displacements on these nodes, their unintended movements during the steady-state dynamic (SSD) analysis would contribute to the computed sound pressure, leading to inaccurate results.
- **Impact of Patch and Remeshed Nodes:** The number of nodes in patch elements is 12,532, while 3,973 nodes are remeshed. The remeshed nodes constitute only 1.43% of the total nodes in the coarse mesh, where structural ties are used. Given this small proportion, their impact on the overall simulation results is negligible.
- **Considerations for Structural Ties and ASI Elements:** In the fine mesh, which employs Acoustic-Structural Interface (ASI) elements, these remeshed and patch elements do not need to be included in the analysis. However, in the structural ties method, element-based surfaces must be continuous. As a result, these elements cannot be excluded from the analysis. The effect of applying zero displacements to these elements is analyzed in the Results and Discussion chapter.

Main Steps of the Python Script

The Python script processes displacement data obtained from Simpack and converts it into a format suitable for application as boundary conditions in Abaqus. The key steps involved in this script are:

- **Reading Input Data:** The script reads the displacement data files from a specified input directory. It also loads a file containing valid node numbers that should be retained for boundary condition application. The invalid nodes are the nodes affected by remeshing.
- **Filtering Nodes:** The script extracts only the nodes present in the provided cleaned mesh file, ensuring that the boundary conditions are applied to the correct nodes.

- **Converting Displacement Data:** The displacement amplitudes and phase values from Simpack are converted into complex numbers using:

$$u_i(f) = A_i(f)e^{j\phi_i(f)} \quad (4.2.3)$$

where $A_i(f)$ is the amplitude, $\phi_i(f)$ is the phase, and j is the imaginary unit.

- **Reformatting for Abaqus:** The script organizes the displacement data for Abaqus by creating a structured DataFrame, ensuring compatibility with Abaqus input format.
- **Generating Boundary Condition Files:** The processed displacement data is written into formatted text files, which contain:
 - Real component of displacement.
 - Imaginary component of displacement.

The script ensures that these values are properly formatted for direct use in Abaqus simulations as explained in (Section 3.6.5).

- **Output Storage:** The final formatted files are saved in a designated output directory, which are included in the Abaqus input file.

This workflow automates the conversion of frequency-domain displacement data from Simpack into Abaqus-compatible boundary conditions, enabling seamless integration between the two software tools. The full script is documented in Appendix B.

Analysis Execution

The processed displacement data drives the sequentially coupled acoustic-structural analysis:

- Steady-state dynamic (SSD) procedure
- Frequency range: 80-200 Hz
- Output: Sound pressure levels (SPL) at infinite elements

This workflow enables efficient transfer of multibody simulation results into acoustic finite element analysis while maintaining phase coherence and amplitude fidelity.

4.3 Acoustic Calculations for the Prototype Cube Model in the Boundary Element Method Python Package (BEMPP)

In this section, the sound pressure level (SPL, in dB) around a hollow steel cube (length 100 mm, thickness 1 mm) is computed using the Boundary Element Method Python

Package (BEMPP). This procedure is analogous to the sequentially coupled acoustic analysis in Abaqus (see Section 4.1.7), where the steady-state dynamic (SSD) analysis of the cube is performed first, and the resulting nodal velocities are then applied as boundary conditions in a subsequent acoustic simulation. Here, the boundary integral equation is discretized and solved in BEMPP to obtain the pressure field around the cube. The following subsections detail the steps undertaken for the structural analysis in Abaqus and the subsequent acoustic calculation in BEMPP.

4.3.1 Steady-State Dynamic Analysis of the Cube

Since BEMPP supports only triangular (tria) surface elements, the cube's shell geometry is meshed with triangular elements, as shown in Figure 4.1.2. A concentrated harmonic load of 100 N is applied on the cube, in line with the setup described in Section 4.1.2.

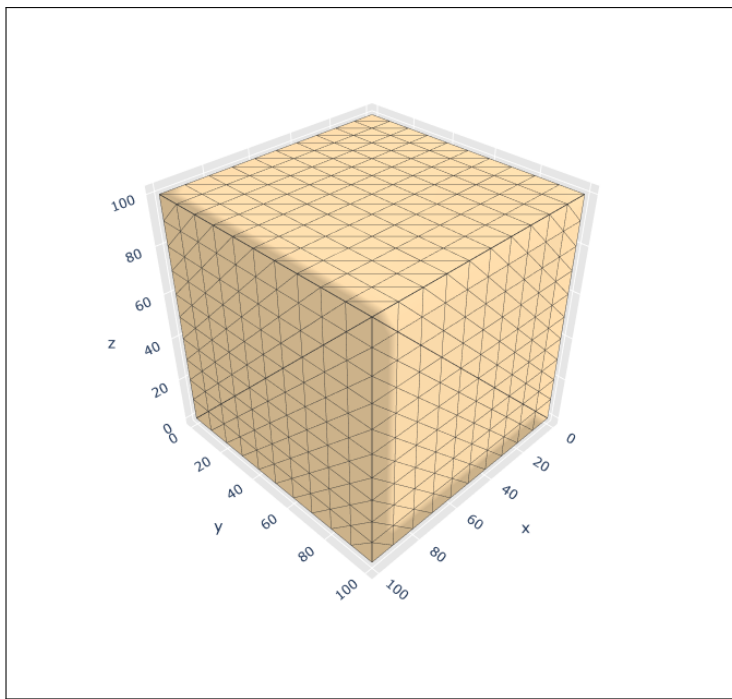


Figure 4.3.15: Prototype cube meshed with triangular elements for BEMPP.

A direct-solution steady-state dynamic analysis is then performed in Abaqus over the frequency range from 500 Hz to 1000 Hz, following the workflow described in Section 4.1.9. For each frequency increment, Abaqus outputs nodal velocities (containing both real and imaginary parts) to a dat file. A Python script is written to organize these velocity components by frequency and store them in NumPy arrays in the form `real_part + i * imag_part`.

These frequency-dependent nodal velocities serve as the boundary condition for the cube surface in BEMPP, reflecting a Neumann-type condition in the acoustic domain. The BEMPP-based acoustic solution is elaborated in the next subsection.

4.3.2 SPL Calculation in BEMPP

Unlike Abaqus, which requires a volumetric acoustic cavity mesh to capture far-field effects via finite elements, BEMPP relies solely on boundary meshes. Consequently, only the *surface* of the sphere (and not the interior volume) is needed to compute the acoustic response at a desired distance from the source. In this study, a spherical surface of radius 200 mm is generated around the cube to evaluate the sound pressure level (SPL) in the far field conditions. Figure 4.1.8 shows the cube and the outer sphere meshed with triangular elements.

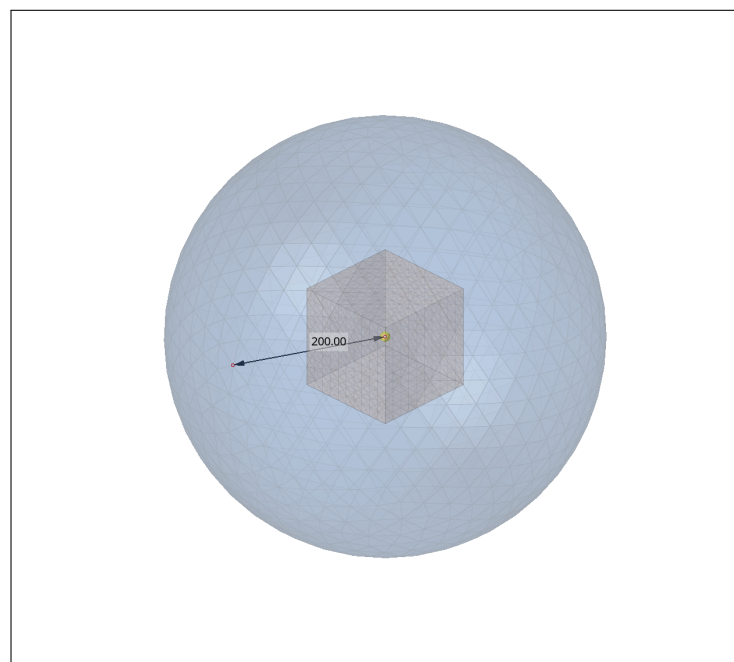


Figure 4.3.16: BEMPP model: A 200 mm radius sphere around the cube. Both surfaces are discretized with triangular elements.

Table 4.3.4: Mesh Statistics for the BEMPP Model of the Cube and Outer Sphere

Mesh Component	Count
Cube Nodes	602
Cube Elements (<code>tria</code>)	1200
Outer Sphere Nodes	830
Outer Sphere Elements (<code>tria</code>)	1656

The major steps in BEMPP to calculate sound pressure can be summarized as follows:

1) Importing the Meshes: The first step is importing the triangular surface meshes for both the cube and the outer sphere:

```
grid = bempp.api.import_grid('cube_file_path')
plotting_grid = bempp.api.import_grid('outer_sphere_file_path')
grid.plot()
```

This creates `grid` (for the cube) and `plotting_grid` (for the sphere). Although the `plot` command is optional, it can be used to verify the mesh visually in BEMPP's Python environment.

2) Defining Function Spaces: In BEMPP, *function spaces* describe how boundary variables (e.g., velocity, pressure) are interpolated. Here, continuous linear polynomial spaces (\mathcal{P}_1) are used for both the cube (`spaceP`, `spaceU`) and the outer sphere (`plotting_space`). The choice \mathcal{P}_1 indicates that each element's nodes carry piecewise linear shape functions. Including boundary dofs is crucial to ensure a one-to-one mapping with mesh nodes:

```
spaceP = bempp.api.function_space(grid, "P", 1, include_boundary_dofs=True)
spaceU = bempp.api.function_space(grid, "P", 1, include_boundary_dofs=True)
plotting_space = bempp.api.function_space(plotting_grid,
                                         "P", 1, include_boundary_dofs=True)
```

Here:

- `spaceP`: Used for pressure on the cube's surface.
- `spaceU`: Used for velocity boundary data on the cube.
- `plotting_space`: Allows pressure evaluation at each node of the outer sphere.

3) Assigning Harmonic Velocities to the Cube: After performing the structural SSD analysis in Abaqus (Section 4.1.9), the nodal velocities are written to NumPy arrays (real + $i \cdot$ imaginary). These velocities are then assigned to the cube's nodes as a Neumann-type boundary condition:

```
complex_velocity = np.load(velocity_file)
u_total = bempp.api.GridFunction(spaceU, coefficients=complex_velocity)
```

`u_total` now encapsulates the harmonic velocity field over the cube's surface for a specific frequency.

4) Building Boundary Operators for the Helmholtz Problem: Boundary operators are used to discretize Boundary integral equation and get it in the matrix form. BEMPP's boundary integral formulation of the Helmholtz equation depends on standard operators:

- `single_layer`: The single-layer operator \mathcal{S} , which integrates monopole-type sources (see Section 3.15).
- `double_layer`: The double-layer operator \mathcal{D} , which integrates dipole-type sources.
- `identity`: The identity operator \mathcal{I} , used to represent the jump behavior of the double-layer potential.

Each operator requires a domain, range, and dual space. In this example, `spaceP` (pressure) is used for all three:

```
identity = sparse.identity(spaceP, spaceP, spaceP)
double_layer = helmholtz.double_layer(spaceP, spaceP, spaceP, k)
single_layer = helmholtz.single_layer(spaceU, spaceP, spaceP, k)
```

k is the wavenumber, defined as $k = \omega/c$, where ω is the angular frequency and c the speed of sound. The `double_layer` operator will be central in solving for the acoustic pressure on the cube; the `single_layer` operator couples the velocity boundary data $\mathbf{u}_{\text{total}}$ into the acoustic field via a $i\omega\rho_0$ factor (representing fluid mass density and harmonic time dependence).

5) Solving for Pressure on the Cube: The acoustic field $\mathbf{p}_{\text{total}}$ on the cube surface is obtained by solving the linear system:

$$\left(\mathcal{D} - \frac{1}{2}\mathcal{I} \right) \mathbf{p}_{\text{total}} = i\omega\rho_0 \mathcal{S} \mathbf{u}_{\text{total}},$$

which in BEMPP can be implemented via a GMRES solver:

```
p_total, info = gmres(
    double_layer - 0.5 * identity,
    1j * omega * rho_0 * single_layer * u_total,
    tol=1E-5
)
```

Here:

- \mathcal{D} corresponds to `double_layer`.
- \mathcal{I} corresponds to `identity`.
- \mathcal{S} corresponds to `single_layer`.
- $i\omega\rho_0$ accounts for the complex wave propagation and air density.

Upon convergence, `p_total` stores the complex acoustic pressure over the cube's boundary nodes.

6) Evaluating Pressure on the Outer Sphere: Finally, The pressure on the outer sphere to approximate far-field SPL is calculated using these commands:

```
double_layer_plotting = helmholtz.double_layer(
    spaceP, plotting_space, plotting_space, k)
single_layer_plotting = helmholtz.single_layer(
    spaceU, plotting_space, plotting_space, k)

p_plotting = double_layer_plotting * p_total \
    - 1j * omega * rho_0 * single_layer_plotting * u_total
```

Corresponding to the formula:

$$\mathbf{p}_{\text{plot}}(\mathbf{x}) = \mathcal{D} \mathbf{p}_{\text{total}}(\mathbf{x}) - i \omega \rho_0 \mathcal{S} \mathbf{u}_{\text{total}}(\mathbf{x}),$$

the above code calculates the pressure at each node \mathbf{x} on the sphere. From \mathbf{p}_{plot} , the sound pressure level (SPL) in decibels is calculated using:

$$\text{SPL}(\mathbf{x}) = 20 \log_{10}(|\mathbf{p}_{\text{plot}}(\mathbf{x})|/p_{\text{ref}}),$$

where p_{ref} is the reference pressure (e.g., 2×10^{-5} Pa in SI units or 2×10^{-11} in tonne-mm-s unit system, as relevant to the chosen scaling).

Summary of BEMPP Workflow

- **Eliminates Volumetric Mesh:** Only the boundary (vibrating cube surface) plus desired evaluation surfaces (outer sphere) need discretization.
- **Direct Coupling to Structural Data:** The velocity $\mathbf{u}_{\text{total}}$ can be read from a structural solver (e.g., Abaqus) and plugged directly into the integral equation. This streamlines multiphysics coupling for acoustic radiation problems.
- **Automatic Satisfaction of Radiation Condition:** Because \mathcal{S} and \mathcal{D} are built on fundamental solutions of the Helmholtz equation that inherently satisfy the Sommerfeld radiation condition, no special boundary truncation is needed.

Chapter 5

Results and Discussion

This chapter presents the results of the numerical experiments conducted in the methodology chapter. The analysis is structured into three sections:

The first section discusses the results of the prototype cube model, comparing the fully coupled and sequentially coupled approaches.

The second section evaluates two sequentially coupled methods: one employing surface-based tie constraints and the other utilizing the Acoustic-Structural Interface (ASI) elements for coupling.

The third section presents a comparative analysis of sound pressure level (SPL) calculations using Abaqus and the Boundary Element Method Python Package (BEMPP) for the prototype cube model.

5.1 Comparison of Fully Coupled and Sequentially Coupled Acoustic Simulation Results for the Prototype Cube

This section presents a comparison between fully coupled and sequentially coupled analyses. The comparison focuses on two key metrics: the sound pressure level (SPL) and the radiated energy. Additionally, a plot of Equivalent Radiated Power (ERP) versus Radiated Power (RADPOW) is presented to verify if ERP exceeds RADPOW.

5.1.1 Sound Pressure Level (SPL) Comparison

The sound pressure levels (SPL) are calculated at a node located on an infinite element surface, positioned 200 mm away from the harmonically loaded cube in both the fully coupled and sequentially coupled analyses. The plot of SPL-dB results for both methodologies is shown in Figure 5.1.1. The x-axis represents the frequency (Hz), and the y-axis represents the sound pressure level (dB).

The observations from the SPL plot are as follows:

Sound Pressure Level at a Node Located 200 mm from the Cube Across Different Frequencies

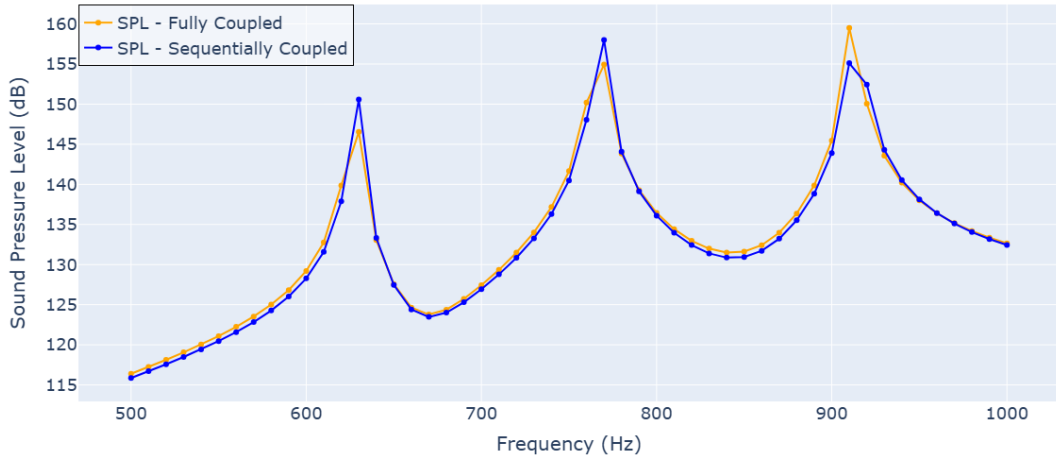


Figure 5.1.1: Comparison of SPL-dB obtained from fully coupled and sequentially coupled analyses for the prototype cube.

- The SPL results obtained from the fully coupled and sequentially coupled analyses are in excellent agreement, as evidenced by their overlapping trends across the entire frequency range.
- Both methods accurately capture the resonance peaks around 620 Hz, 780 Hz and 900 Hz. Additionally, the gradual rise and drop in SPL values across the frequency sweep are consistent between the two approaches.
- This close agreement demonstrates that the sequentially coupled method can reliably approximate the results of the fully coupled analysis.

5.1.2 Comparison of Computational Times

The computational times for both fully coupled and sequentially coupled analyses are presented in Table 5.1.1. The sequentially coupled analysis includes separate computational times for the global model and the submodel.

Table 5.1.1: Comparison of computational time for fully coupled and sequentially coupled analyses

Model	Wall-clock Time (sec)
Fully coupled	41
Global model (sequential)	7
Submodel (sequential)	30
Total (sequential coupled)	37

From Table 5.1.1, the following observations can be made:

- The total computational time for the sequentially coupled analysis is 37 sec, which is lower than the 41 sec required for the fully coupled analysis.
- In smaller models, such as the prototype cube, the fully coupled analysis does not impose a significant computational penalty due to the efficiency of Abaqus sparse solver, which leverages the sparsity of the fluid-structure coupling terms. Sparse solvers optimize computations by reducing the operations needed for zero entries in the coupling matrix, minimizing processing time. However, as the model size increases, the number of coupled nodes grows, leading to a denser coupling matrix with more non-zero entries. This reduces the effectiveness of the sparse solver and significantly increases computational demands. In such cases, the sequentially coupled approach becomes more advantageous, as it decouples the problem into two smaller systems—one for the structure and another for the fluid—avoiding the need to solve a single large coupled system [42].
- The computational efficiency of the sequentially coupled approach becomes advantageous when multiple submodels need to be analyzed, driven by a single set of global results. This feature is especially useful for industrial applications where iterative submodel analyses are required.

The results confirm that the sequentially coupled approach offers a computational advantage without compromising accuracy, making it a practical choice for scenarios involving large models or iterative submodel analyses.

5.1.3 Acoustic Radiated Energy Comparison

This section compares the sound energy radiated by the cube as calculated by fully coupled and sequentially coupled analyses. In the fully coupled analysis, the radiated energy is represented by the parameter **RADEN**, while in the sequentially coupled analysis, it is represented by the parameter **ALLQB**. Both quantities are expressed in decibels (dB) for direct comparison.

The plot shown in Figure 5.1.2 illustrates the acoustic radiated energy across a frequency range of 500 Hz to 1000 Hz. The x-axis represents the frequency (Hz), and the y-axis represents the radiated sound energy (dB).

Observations and Discussion:

- The results obtained from fully coupled and sequentially coupled analyses are in a good agreement, as evidenced by the overlapping trends across the entire frequency range. This demonstrates the reliability of the sequentially coupled approach in accurately approximating the radiated acoustic energy.
- Both methods accurately capture the resonance peaks at approximately 620 Hz, 760 Hz, and 900 Hz. These peaks represent the frequencies at which the system exhibits maximum radiated energy due to harmonic vibrations.

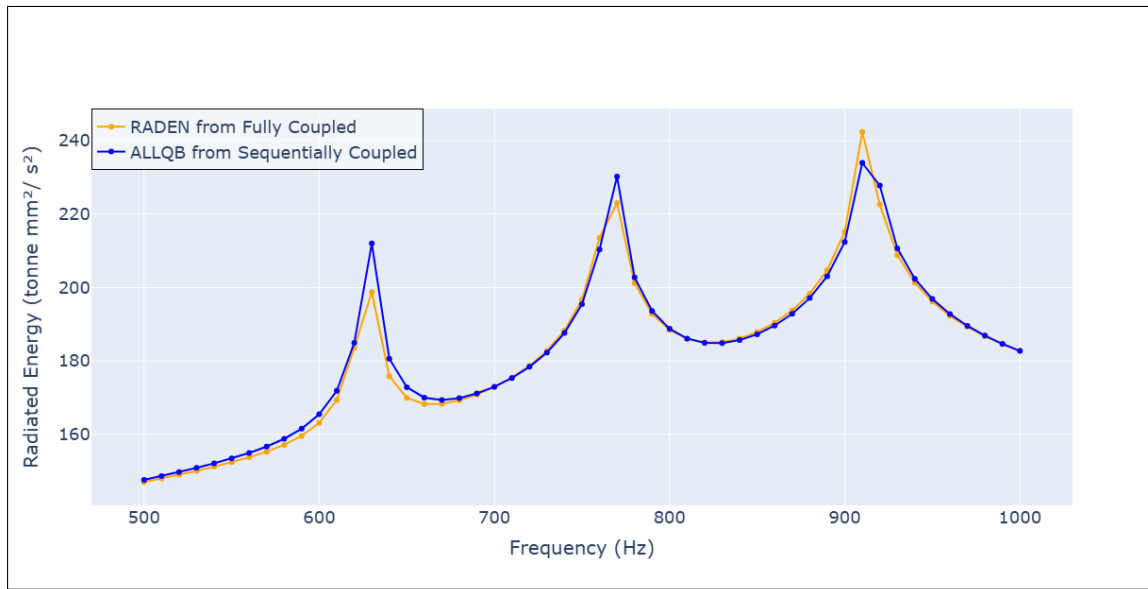


Figure 5.1.2: Comparison of acoustic radiated energy between fully coupled and sequentially coupled analyses.

5.1.4 Validation Using Equivalent Radiated Power (ERP)

One approach to validate the acoustic analysis results is by comparing the Radiated Power (RADPOW) from the cube, calculated in Abaqus, with the Equivalent Radiated Power (ERP). The ERP provides a theoretical upper limit for radiated power, assuming ideal plane wave radiation and 100% radiation efficiency across all radiating surfaces. This comparison helps evaluate the realism and accuracy of the computed acoustic radiation.

Observations:

- The ERP values are consistently higher than the RADPOW values across the frequency range, as expected. This is because ERP assumes:
 1. All surfaces of the structure are actively radiating sound.
 2. The radiation efficiency is 100%, which rarely holds true in real-world conditions.
- The significant gap between ERP and RADPOW can be attributed to the fact that the vibration source in this analysis is a point load applied to one face of the cube. Consequently, not all faces of the cube radiate sound effectively during all modes. In contrast, the ERP calculation assumes that all surfaces radiate sound equally.

Significance of ERP in Validation:

- ERP serves as a valuable tool for validating the realism of simulation results. The difference between RADPOW and ERP provides insight into the radiation efficiency of the structure.

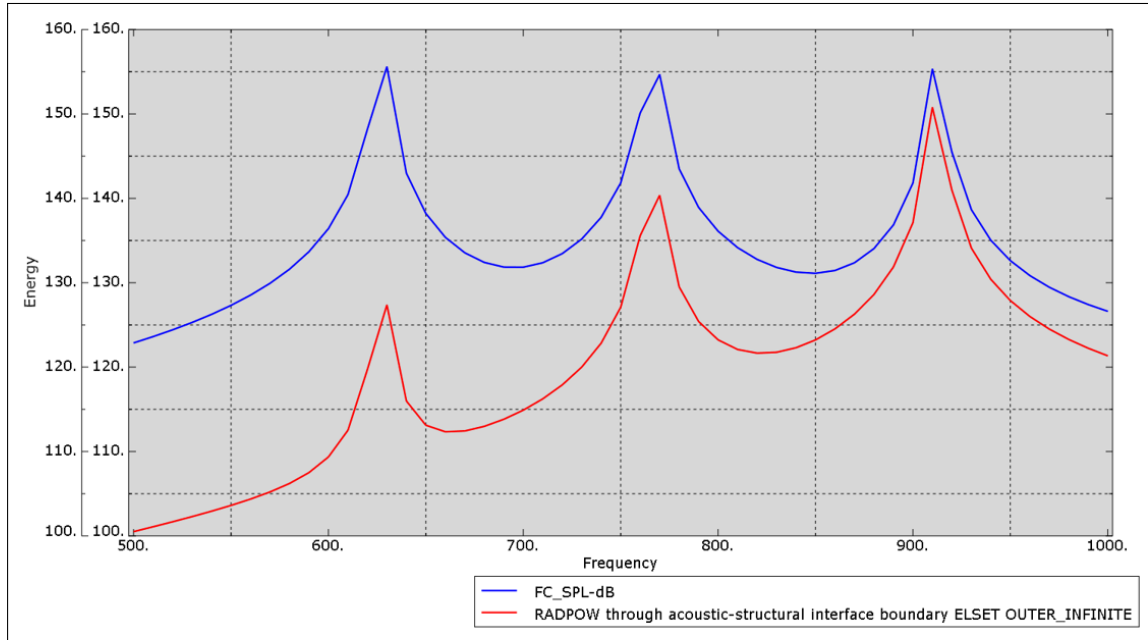


Figure 5.1.3: Comparison of Radiated Power (RADPOW) and Equivalent Radiated Power (ERP) in Fully Coupled Analysis. The red curve represents RADPOW, and the blue curve represents ERP.

- In this study, the significant gap between ERP and RADPOW highlights the localized radiation effect caused by the point load. This validates that the RADPOW results align with the physical expectations of the simulation setup.
- By comparing RADPOW and ERP, engineers can assess whether the structure's radiated sound is being captured accurately and identify regions or modes that contribute to inefficient radiation.

This comparison reinforces the importance of understanding the assumptions behind ERP calculations and their implications for interpreting simulation results in realistic scenarios.

5.1.5 Visualization of Far-Field Results at User-Defined Distances

Once the sound pressure is computed using acoustic infinite elements, which simulate free-field conditions, it is possible to calculate the far-field sound pressure at any desired distance from the vibrating cube. The far-field pressure can then be visualized on spherical surfaces as a projection of the spherical boundary defined by the acoustic infinite elements. This visualization provides valuable insights into the sound pressure distribution at different distances.

In Figure 5.1.4, the grey inner sphere represents the acoustic infinite elements, positioned at a distance of 200 mm from the cube. The sound pressure levels at 500 Hz are visualized as contour plots on two concentric spheres located at distances of 2000 mm and 2500 mm

from the cube. These spheres illustrate the propagation and distribution of the sound pressure in decibels as it radiates outward.

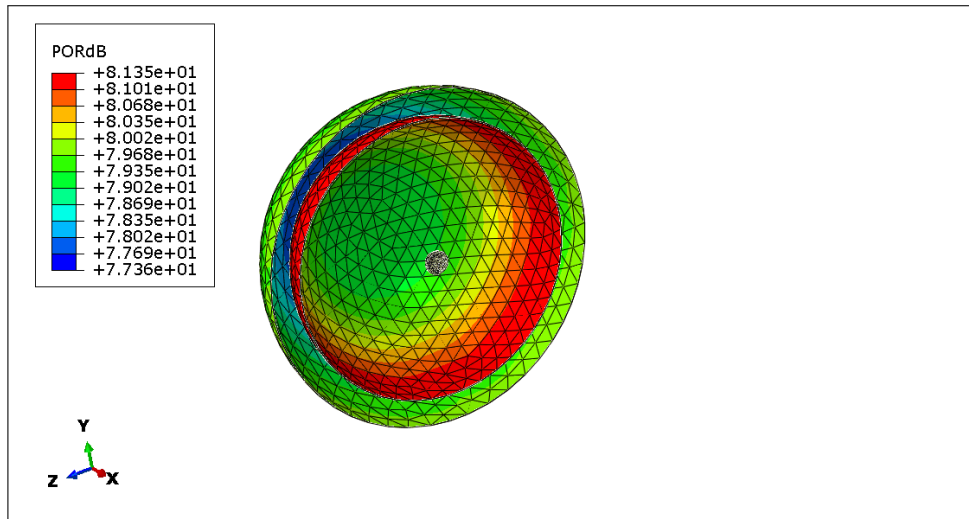


Figure 5.1.4: Visualization of sound pressure levels at 500 Hz in the far field at distances of 2000 mm and 2500 mm from the cube.

Similarly, Figure 5.1.5 presents the contour plot of the sound pressure levels at 1000 Hz, demonstrating the far-field sound pressure distribution on concentric spheres at 2000 mm and 2500 mm.

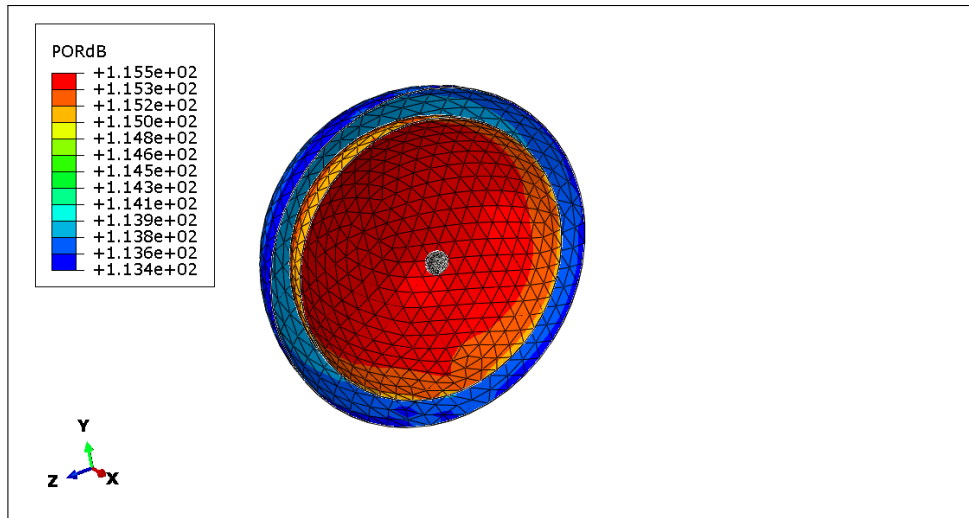


Figure 5.1.5: Visualization of sound pressure levels at 1000 Hz in the far field at distances of 2000 mm and 2500 mm from the cube.

Observations:

- It can be seen in the contour plots, that the inner sphere has a higher SPL than

the outer sphere, which indicates that as the distance from the cube increases, the sound pressure level decreases, which aligns with real-life expectations of sound propagation behavior.

- The use of acoustic infinite elements proves highly efficient. By running the simulation once with these elements, it becomes possible to calculate sound pressure levels at any far-field distance through a Python script. This eliminates the need for re-running the simulation, making the methodology computationally efficient.

5.2 Sound Pressure Analysis of Sequentially Coupled Wind Turbine Gearbox

This section presents the sound pressure level results from the sequentially coupled analysis, evaluating three critical aspects:

- Coupling method performance (Tie vs. ASI)
- Spatial sound pressure distribution around gearbox
- Structural material property sensitivity, Remeshing-induced null displacement effects and Comparision of ERP with RADPOW

5.2.1 Acoustic Coupling Method Comparison

The sound pressure level (SPL) results compare structural tie coupling (coarse mesh: 276,820 nodes) with acoustic-structural interface (ASI) coupling (fine mesh: 1,001,528 nodes). Measurement nodes on the infinite element sphere (2300 mm radius) were analyzed at front (Node 1859) and rear (Node 930) positions of the gearbox. The distance of 2300mm from the gearbox is in the far-field. The front position of the gearbox is towards the generator and the rear is towards the turbine blades. In the structural tie coupling method, a coarse wrapper mesh of the gearbox casing was used to create the acoustic mesh and hence it resulted in the coarse acoustic mesh. In the asi coupling method, the original fine gearbox casing was used to create the acoustic mesh and hence it resulted in the fine acoustic mesh.

Table 5.2.2: Comparison of Computational Resources for SSD Analysis Over the Frequency Range of 90 Hz to 200 Hz

Model	Wall-clock Time (s)	Peak Memory (GB)
Coarse Mesh	14,431	61
Fine Mesh	29,461	98

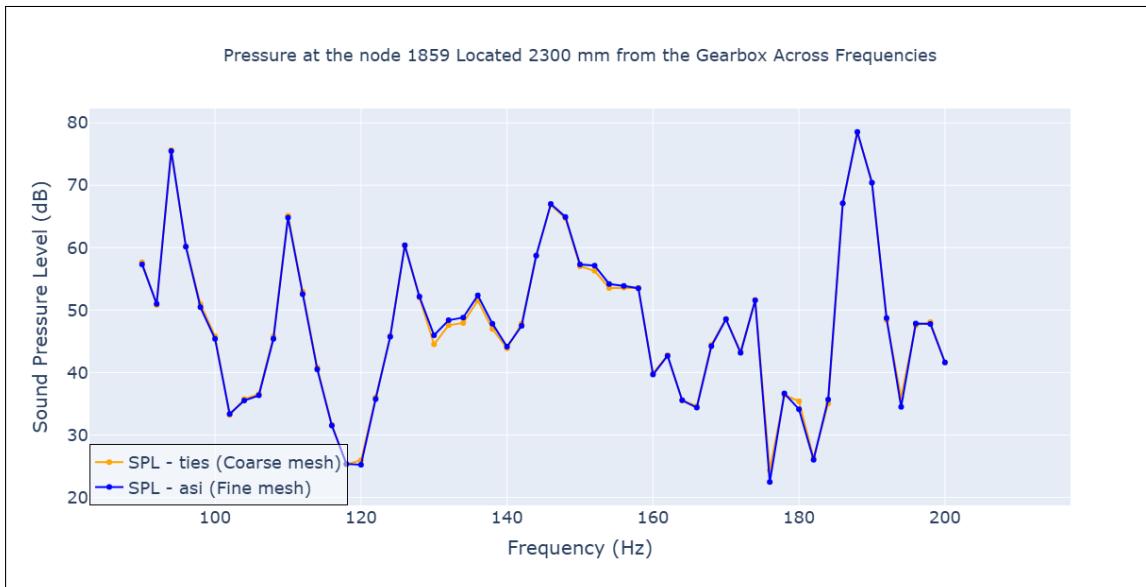


Figure 5.2.6: SPL comparison at front position (Node 1859) showing < 1 dB deviation between methods

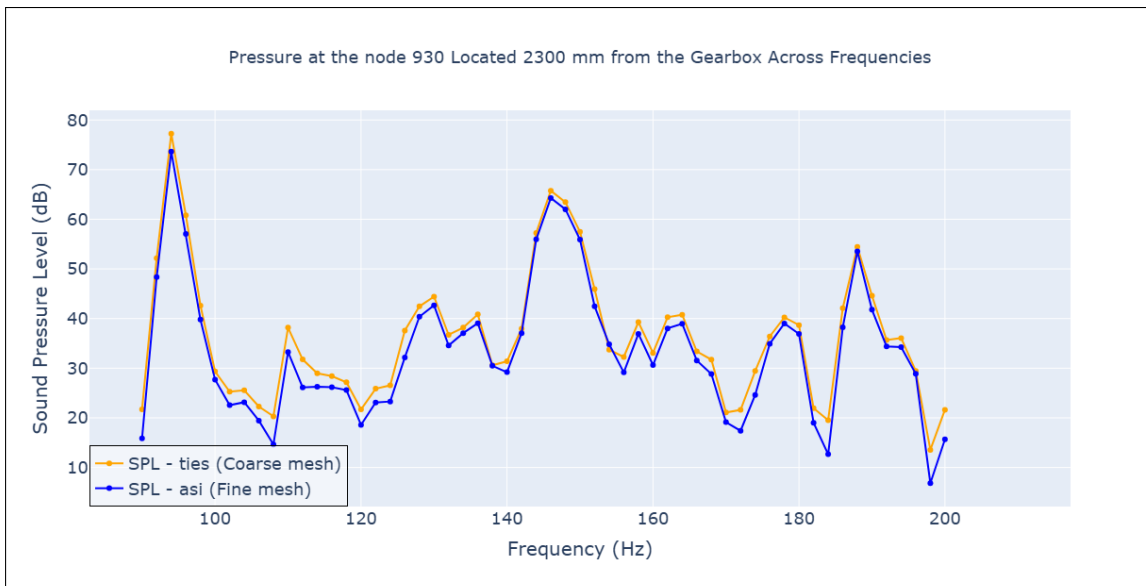


Figure 5.2.7: SPL comparison at Rear position (Node 930) with 2 dB maximum deviation

Key Observations

- **Method Agreement:** 2 dB SPL difference confirms both methods produce equivalent acoustic predictions. The difference can be attributed to numerical approximations (Figure 5.2.6) (Figure 5.2.7).
- **Resonance Peaks:** Consistent identification at 95 Hz, 148 Hz, and 190 Hz across methods.
- **Computational Efficiency:** Coarse mesh reduces solve time by 51% 5.2.2.

Mesh Strategy Recommendation: Despite achieving comparable accuracy, the coarse wrapper mesh approach—where the fine gearbox mesh is tied to the coarse acoustic cavity mesh, as described in Section 4.2.3.1—and Section 4.2.3.2 offers superior computational efficiency while ensuring:

- Element size compliance with Abaqus guidelines
- <2% solution deviation from fine mesh baseline
- Robust resonance peak identification

5.2.2 Spatial Sound Pressure Distribution Around the Gearbox

In this subsection, the Sound Pressure Level (SPL) is analyzed at six distinct nodes located on the acoustic infinite elements. These nodes are positioned at a far-field distance of 2300 mm from the gearbox, ensuring a spatially distributed measurement of radiated sound pressure. The selected nodes correspond to the front, rear, top, bottom, left, and right sides of the gearbox. This analysis helps in identifying the dominant noise-emitting surfaces, thereby enabling targeted noise reduction strategies such as additional damping treatments or structural modifications.

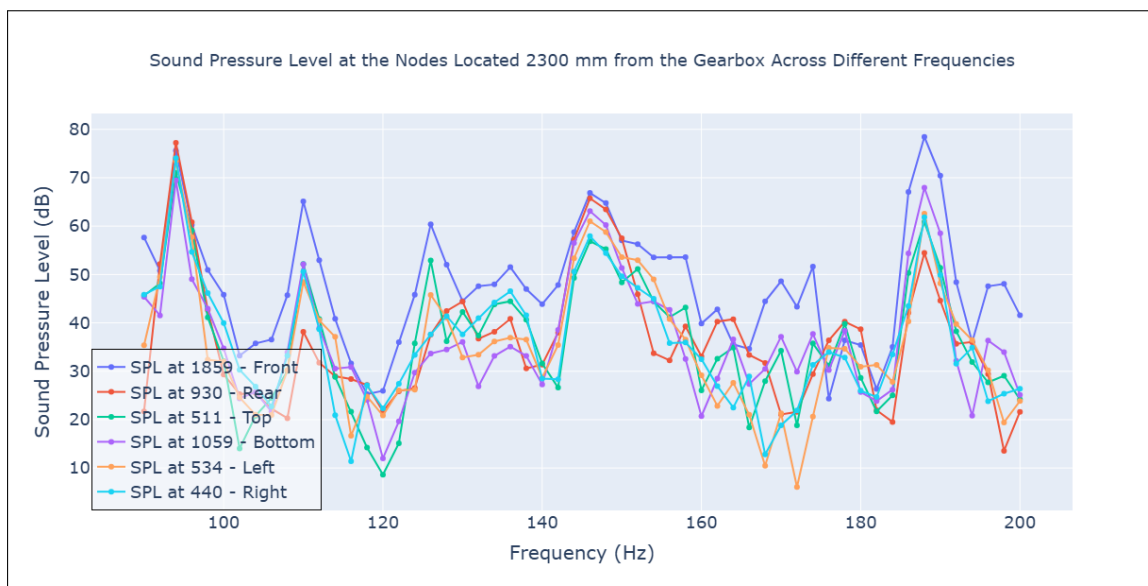


Figure 5.2.8: Spatial distribution of SPL at six far-field locations (2300 mm from the gearbox) over the frequency range of 90–200 Hz.

Observations and Analysis

From Figure 5.2.8 and Figure 5.2.9, the following key observations can be made regarding the SPL at 190Hz which has the highest peak:

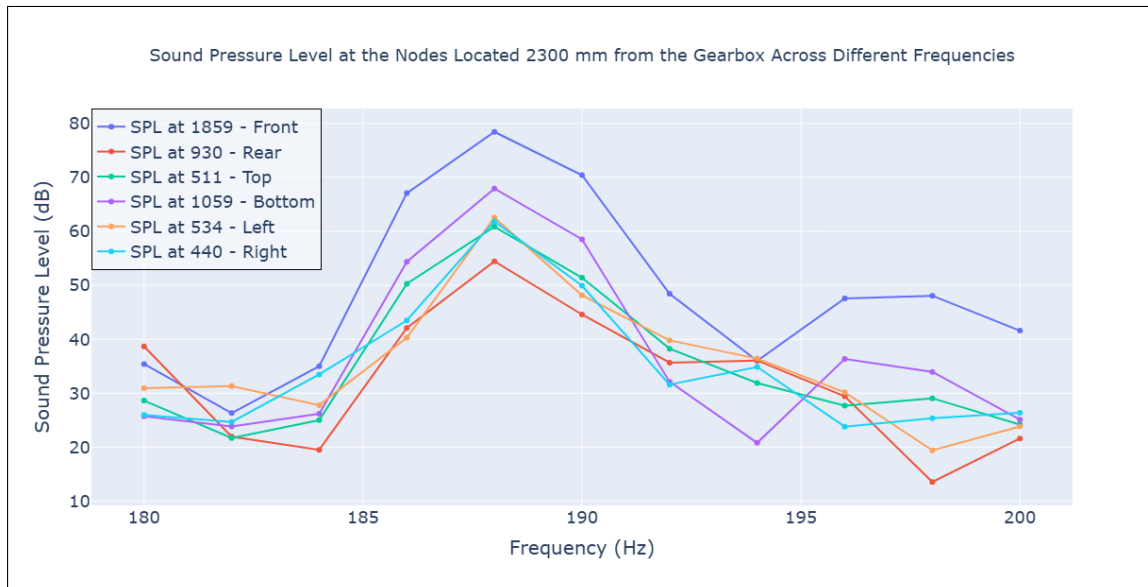


Figure 5.2.9: Magnified view of SPL distribution at six far-field locations in the frequency range of 180–200 Hz.

- The front side of the gearbox, which faces the generator, exhibits the highest SPL, reaching approximately 80 dB.
- The bottom surface also radiates significant noise, with an SPL of approximately 70 dB.
- The rear side, which faces the turbine rotor, has the lowest SPL, around 55 dB.
- The top, left, and right sides of the gearbox exhibit comparable SPL levels, averaging around 60 dB.

The observed SPL distribution aligns with the structural characteristics of the gearbox. The front side contains a greater number of radiating surfaces, leading to higher sound emission compared to the rear side. This suggests that noise mitigation efforts should primarily focus on the front and bottom regions by implementing damping materials or structural reinforcements to minimize radiated noise.

5.2.3 Structural Material Property Sensitivity and Effects of Remeshing-Induced Null Displacements

In the methodology chapter, two key aspects related to the structural properties and remeshing effects of the gearbox casing were discussed. First, when applying displacements obtained from Simpack, the material properties of the gearbox structure do not directly influence the response, as described in Section 4.2.3.1. Second, due to mesh modifications required to clear free edges, certain elements were remeshed, resulting in a change in node numbering. Consequently, Simpack displacements could not be applied to these nodes, and instead, zero displacement boundary conditions were imposed, as

explained in Section 4.2.4. This section presents the validation of these two assumptions through SPL (Sound Pressure Level) results.

It should be noted that due to a bug in Simpack, the displacement values were initially scaled down, leading to incorrect SPL values. When this issue was fixed, time constraints prevented the re-execution of this analysis. However, since the objective of this study is a comparative assessment between different methodologies rather than absolute SPL magnitudes, the scaling issue does not impact the validity of the conclusions.

Effect of Structural Material Properties

To examine whether the material properties of the gearbox casing influence the acoustic response, SPL values were computed at the nodes of infinite elements. There are 1922 nodes on the outer spherical boundary, located at a far-field distance of 2300 mm from the gearbox. The x-axis of the plot represents the node index, while the y-axis represents the SPL in decibels.

Both results in Figure 5.2.10 were obtained using structural ties as the coupling method, with displacements prescribed from Simpack. The difference lies in the assigned material properties:

- Steel (orange line):

DENSITY: 7.8500E-09, 0.0
 Elastic modulus: 210000.0
 Poissions's ratio = 0.3

- Rubber-like material (blue line):

DENSITY: 1.52E-09, 0.0
 Elastic modulus: 3000.0
 Poissions's ratio = 0.3

Observations: As shown in Figure 5.2.10, the SPL results for steel and rubber exhibit nearly identical trends across all node indices. This indicates that the choice of structural material has no significant influence on the acoustic response when nodal displacements are explicitly prescribed. This is expected because, in frequency-domain finite element analysis, imposed displacements serve as fixed boundary conditions. As a result, the material properties of the structure do not influence the acoustic response since the governing equilibrium equations are not solved for displacement of the structure.

Effect of Null Displacements Due to Remeshing

A second validation was conducted to determine the effect of applying zero displacement boundary conditions to remeshed elements. Figure 5.2.11 presents SPL values at infinite element nodes, with the following two cases:

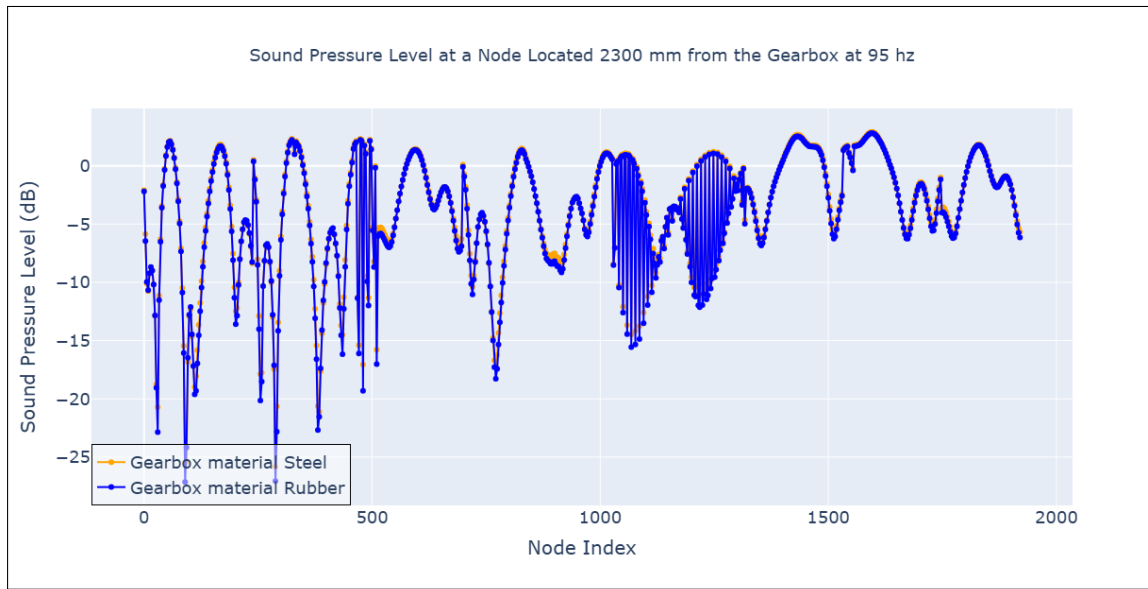


Figure 5.2.10: SPL at 95 Hz at the nodes of infinite elements for different structural materials.

- **Orange line:** Zero displacement applied only to patch elements (used to close gaps in the gearbox mesh).
- **Blue line:** Zero displacement applied to both patch elements and remeshed elements.

Patch elements are introduced solely for meshing purposes to ensure a closed volume for the acoustic cavity. Since these elements do not correspond to physical structures in the actual gearbox, applying zero displacement to them is a logical choice. Remeshed elements, on the other hand, were modified to improve mesh quality by resolving free-edge issues. Since remeshing alters node numbering, Simpack displacements could not be directly applied to these nodes. However, the number of affected nodes is only 3973, which constitutes 1.43% of the total mesh nodes.

Observations: As evident from Figure 5.2.11, the SPL results remain unchanged regardless of whether zero displacement is applied only to patch elements or extended to remeshed elements. This confirms that the presence of null displacement conditions in 1.43% of the mesh does not introduce any significant deviation in the results. Therefore, the decision to exclude Simpack displacements for these remeshed nodes does not compromise the accuracy of the overall acoustic analysis.

Validation Using Equivalent Radiated Power (ERP)

One approach to validate the acoustic analysis results is by comparing the Radiated Power (RADPOW) from the gearbox, calculated in Abaqus, with the Equivalent Radiated Power (ERP). The ERP provides a theoretical upper limit for radiated power, assuming ideal plane wave radiation and 100% radiation efficiency across all radiating

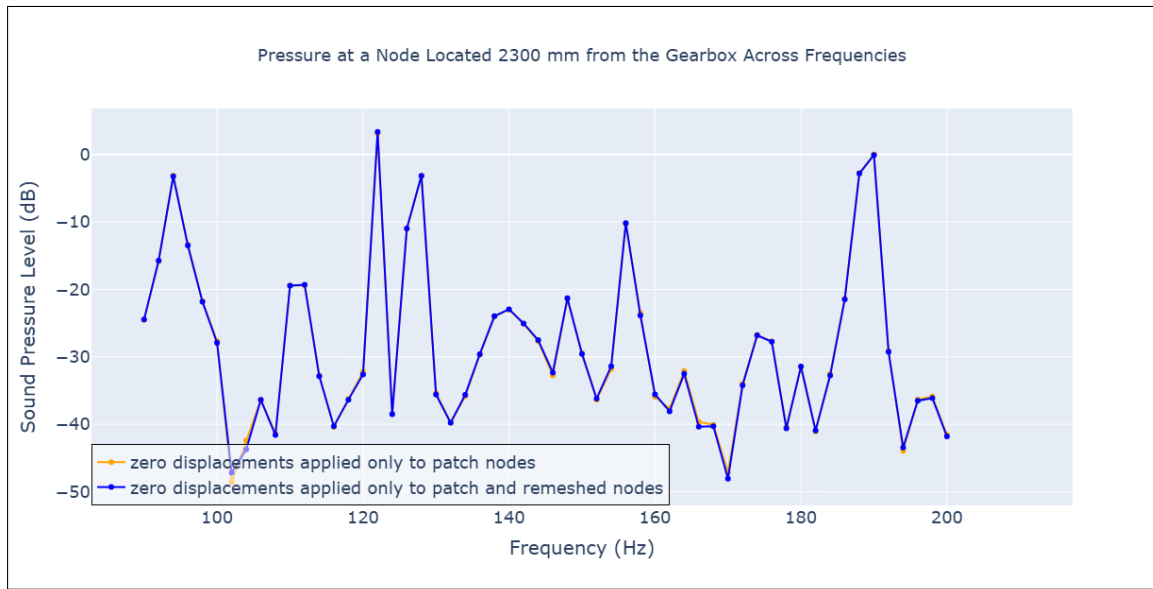


Figure 5.2.11: SPL at 95 Hz at the nodes of infinite elements, comparing the effect of applying zero displacement to remeshed nodes.

surfaces. This comparison helps evaluate the realism and accuracy of the computed acoustic radiation.

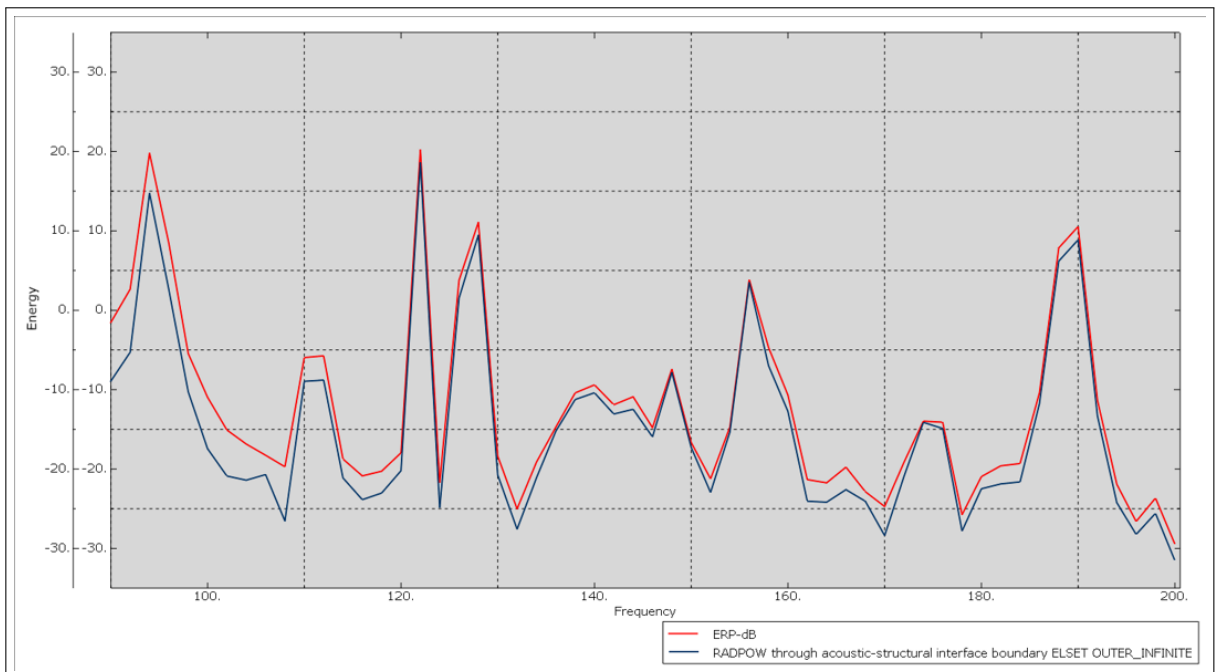


Figure 5.2.12: Comparison of Radiated Power (RADPOW) and Equivalent Radiated Power (ERP) in the ties method. The red curve represents ERP, and the blue curve represents RADPOW.

Observations:

- The ERP values are consistently higher than the RADPOW values across the frequency range, as expected. This is because ERP assumes:
 1. All surfaces of the structure are actively radiating sound.
 2. The radiation efficiency is 100%, which rarely holds true in real-world conditions.
- Unlike the prototype cube model, which is subjected to a point load, the gearbox is loaded under real operating conditions. In the cube model, there was a significant discrepancy between ERP and RADPOW 5.1.4, whereas in the gearbox analysis, the results exhibit a much closer agreement.

Conclusion

This validation study confirms two important findings:

1. The structural material properties do not influence the computed SPL values when displacements are explicitly prescribed from an external source such as Simpack.
2. The application of zero displacement to remeshed elements does not introduce significant errors, as their contribution is negligible relative to the entire structure.

These results reinforce the validity of the adopted methodology and ensure that the comparative analysis remains robust and reliable.

5.3 Comparison of Sound Pressure Level Results between BEMPP and Abaqus

This section examines the agreement of SPL predictions obtained from BEMPP and Abaqus for three experimental configurations involving the same hollow cube (described in Sections 4.3.1 and 4.3.2). In all experiments, a 100 N concentrated harmonic load is applied on the cube face perpendicular to the x -axis, as illustrated in Figure 4.1.2. After the steady-state dynamics (SSD) analysis of the just the cube structure is conducted over a frequency range of 500Hz to 1000Hz, the computed nodal velocities serve as sequential boundary conditions for both BEMPP and Abaqus acoustic analysis. The key difference among the three experiments is how these velocities are assigned to the faces of the cube.

- **Experiment 1 (One Face):** Velocities are assigned only to the single cube face perpendicular to the y -axis, while all other faces are loaded with zero velocity (Figure 5.3.13).
- **Experiment 2 (Two Opposite Faces):** Velocities are assigned to the two opposite faces perpendicular to the y -axis, and all remaining faces are loaded with zero velocity (Figure 5.3.14).

- **Experiment 3 (All Faces):** Velocities are assigned to all six faces of the cube, as shown in Figure 5.3.15.

In all three cases, edge nodes are assigned zero velocity, as their normal direction is ambiguous. Every other modeling detail, loading condition, and output request remains consistent between Abaqus and BEMPP.

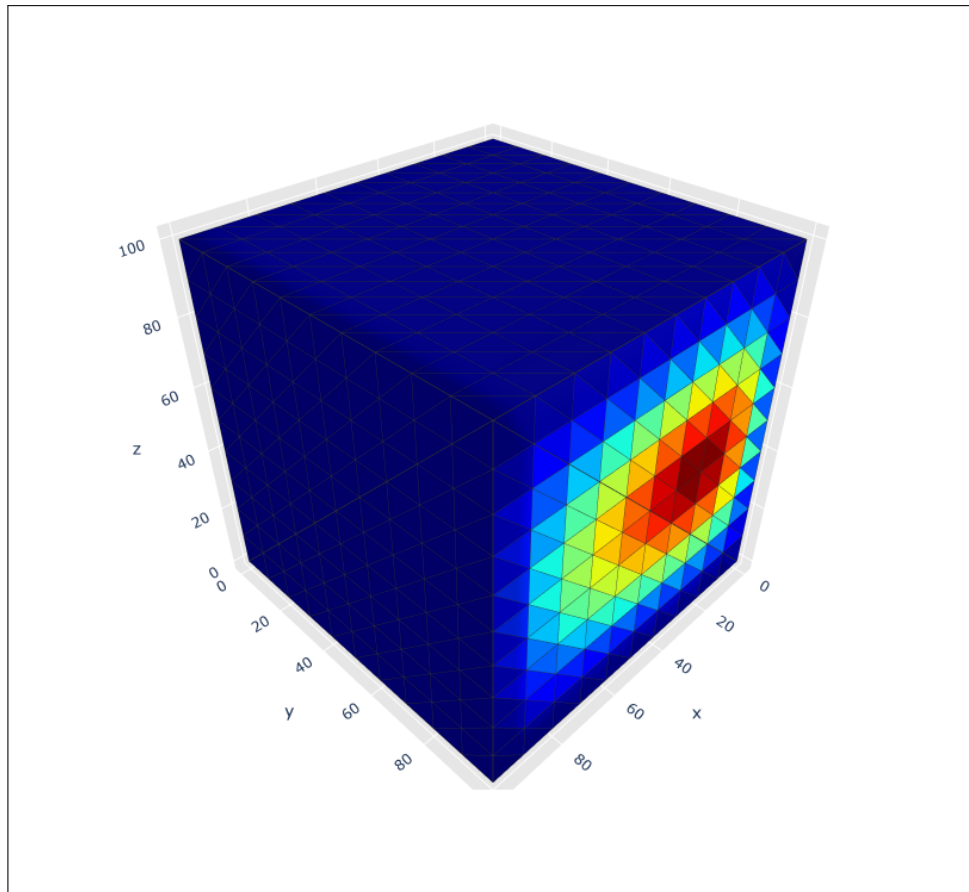


Figure 5.3.13: Experiment 1: Velocity loaded to the single face perpendicular to the y -axis.

5.3.1 Results

Experiment 1: One Face Loaded

Observations:

- As shown in Figure 5.3.16, the two methods agree well overall, with a deviation of about 3 dB at around 790 Hz.
- Both solutions capture resonance peaks near 650 Hz, 810 Hz, and 980 Hz.

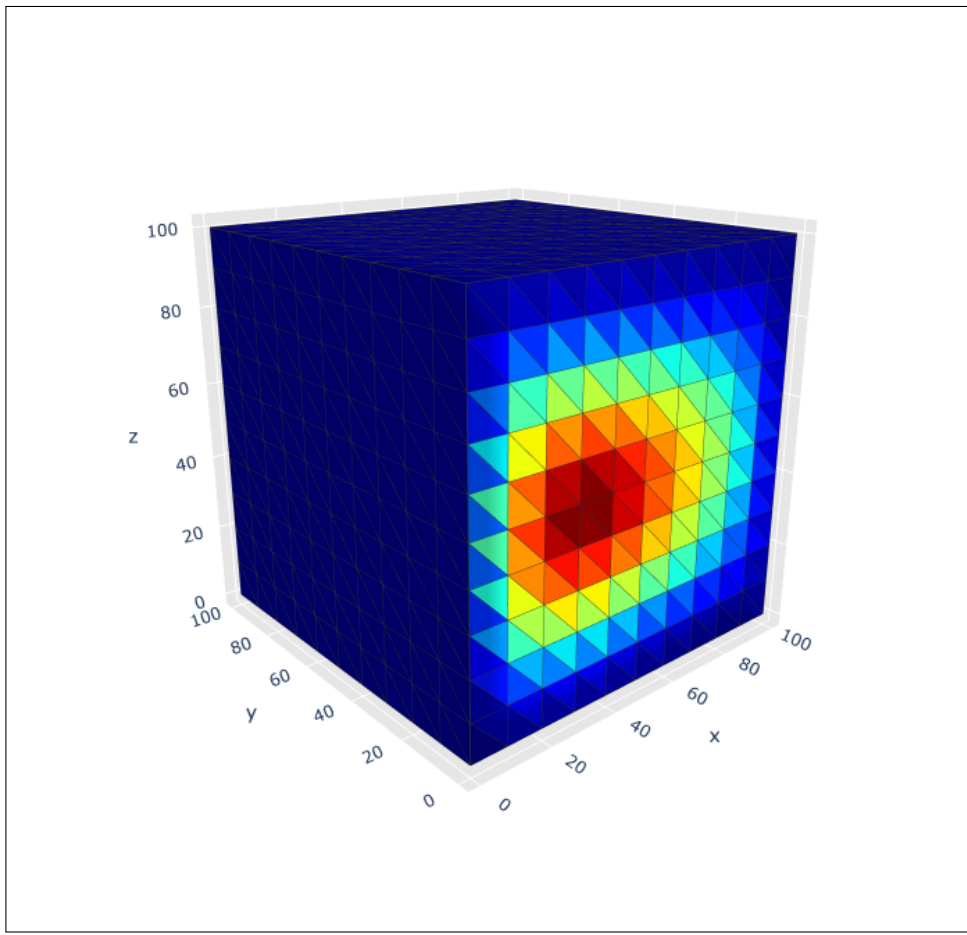


Figure 5.3.14: Experiment 2: Velocity loaded to the two faces perpendicular to the y -axis. The illustrated face is the opposite side of that shown in Figure 5.3.13.

Experiment 2: Two Opposite Faces Loaded

Observations:

- As illustrated in Figure 5.3.17, the results match closely from 500 Hz to 650 Hz, but deviations of up to 10 dB appear above 650 Hz.
- Despite the amplitude mismatch, the resonance peaks at 650 Hz, 810 Hz, and 980 Hz are captured by both approaches.

Experiment 3: All Faces Loaded

Observations:

- Figure 5.3.18 shows significant deviation at almost every frequency, with a difference of about 5 dB from 500 Hz to 600 Hz, increasing up to 18 dB around 800 Hz.
- Despite large amplitude discrepancies, both methods still exhibit resonance peaks near 650 Hz, 810 Hz, and 980 Hz.

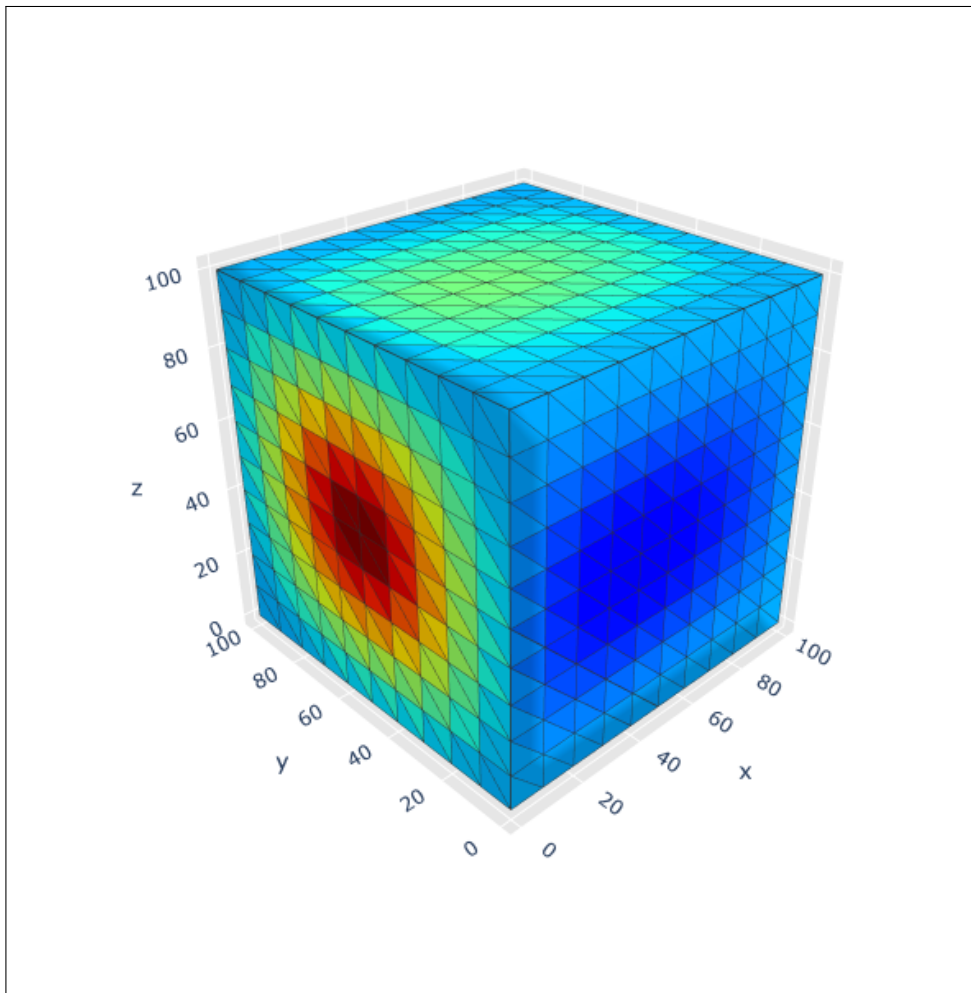


Figure 5.3.15: Experiment 3: Velocity loaded to all faces of the cube.

Discussion and Concluding Remarks

Overall, the three experiments show that the SPL results from BEMPP and Abaqus agree most when only a single face is enforced with velocity boundary conditions, and the discrepancy grows as more faces are included. In principle, larger differences can arise at higher frequencies for reasons linked to mesh resolution and boundary element approximation.

- **Mesh Discretization and Wavenumber Effects:** As noted by the creators of BEMPP [59], “*The use of discretization and the boundary element method to solve Helmholtz problems has been well studied. For sufficiently small wavenumbers k and sufficiently smooth boundaries, the operators involved are coercive, and hence a priori error bounds can be derived. For values of k and domains for which coercivity cannot be shown, error bounds have been shown that involve both the mesh size h and the wavenumber k . If the wavenumber is varied, then the mesh must be refined to keep the value of hk constant in order to maintain a low error.*” Here, h is the mesh size. Since the frequency (and thus k) increases but the mesh remains fixed in the experiments, errors are likely to grow at higher frequencies,

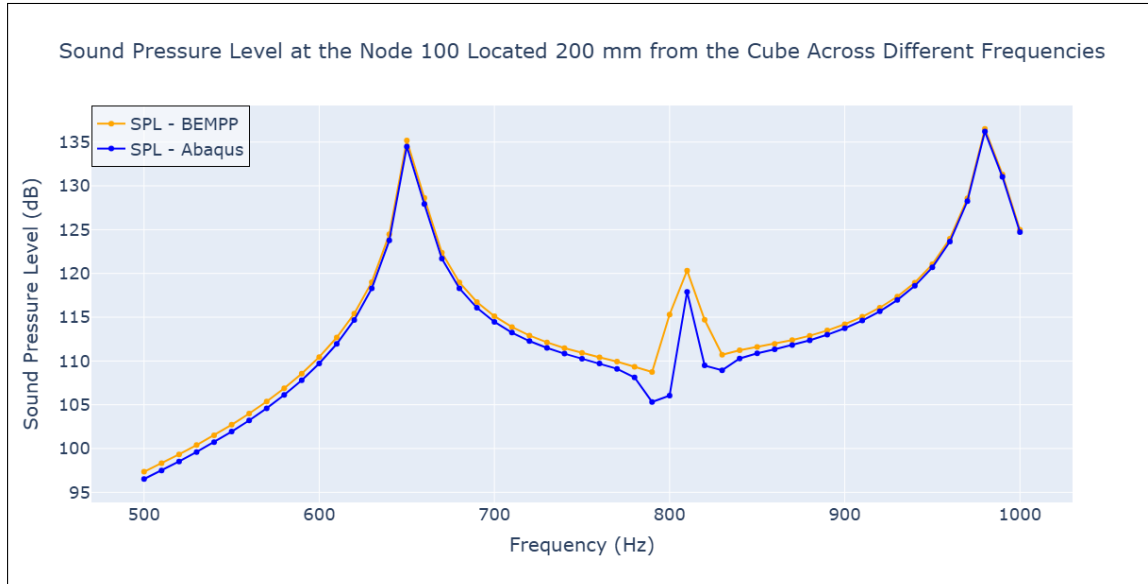


Figure 5.3.16: SPL comparison between BEMPP and Abaqus when only one face (perpendicular to y -axis) is loaded.

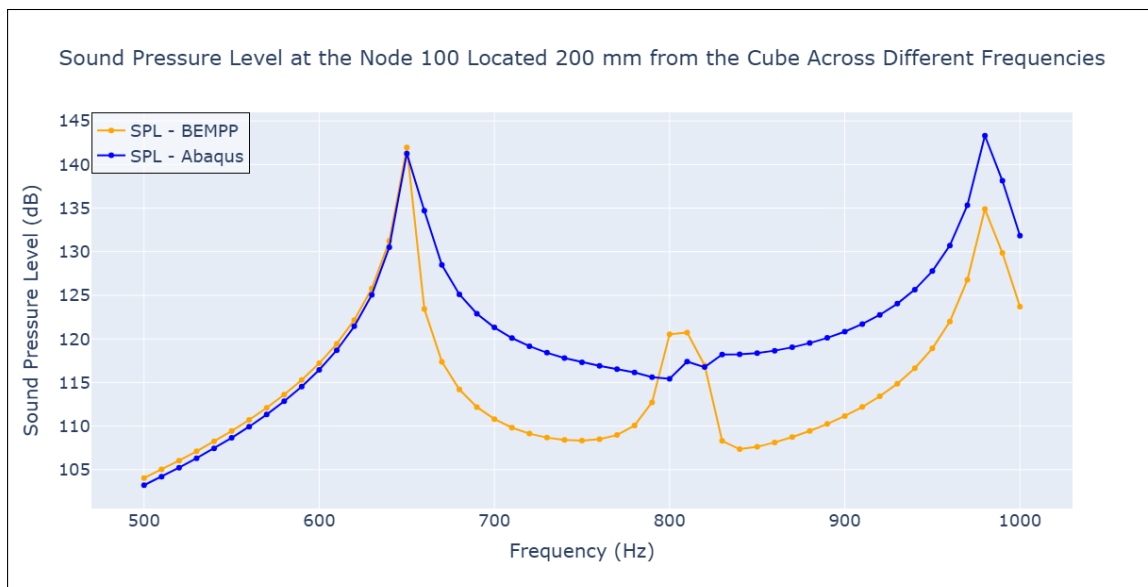


Figure 5.3.17: SPL comparison between BEMPP and Abaqus when two opposite faces (perpendicular to y -axis) are loaded.

potentially explaining the 10 dB to 18 dB deviations in Experiments 2 and 3.

- **Non-Smooth Geometry:** The classical boundary integral formulation (with a -0.5 Id jump term 3.15.1) also assumes smooth boundaries. While a single planar face can be treated as smooth, multiple faces meeting at sharp edges form a non-smooth boundary. Even though edge nodes were given zero velocity, the integral operators might see the full geometry, including corners where the local solid angle causes the jump term to deviate from the ideal -0.5 value. Abaqus's coupling (e.g.,

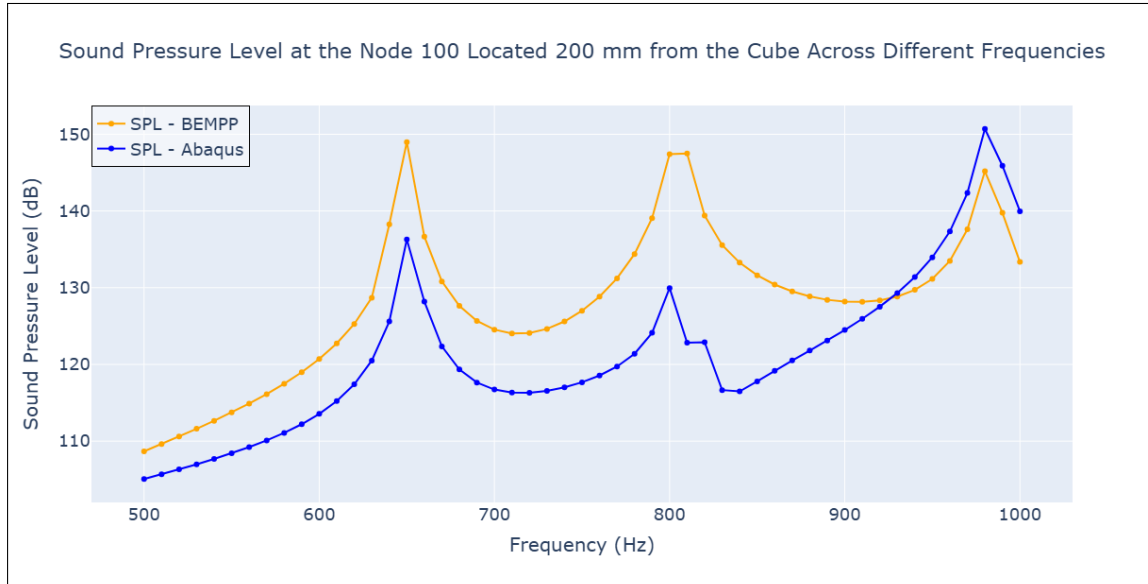


Figure 5.3.18: SPL comparison between BEMPP and Abaqus when all cube faces are loaded with velocities.

via acoustic–structural interface elements) might handle these edge transitions in a more robust manner, explaining why the agreement degrades as more faces are activated.

5.3.2 Validation of the Null-Field Approach

As described in Section 3.15.1, the null-field approach assumes that no acoustic field exists within the interior of a closed boundary. This assumption simplifies the boundary integral formulation for exterior radiation problems by eliminating the need for interior domain discretization.

Figure 5.3.19 illustrates the sound pressure distribution around the cube at a frequency of 500 Hz when two opposite faces are subjected to loading. The contour plot clearly demonstrates that the sound pressure inside the cube is effectively zero, validating the null-field assumption. Additionally, the sound pressure is observed to be at its maximum near the cube’s surface and gradually diminishes with increasing distance due to the geometric spreading of wavefronts.

Summary

- For a single face loaded with velocity, BEMPP and Abaqus results are within ~ 3 dB across most frequencies.
- As more faces receive nonzero boundary velocities, discrepancies become more pronounced—reaching over 10 dB for two faces and up to 18 dB for all faces at certain frequencies.

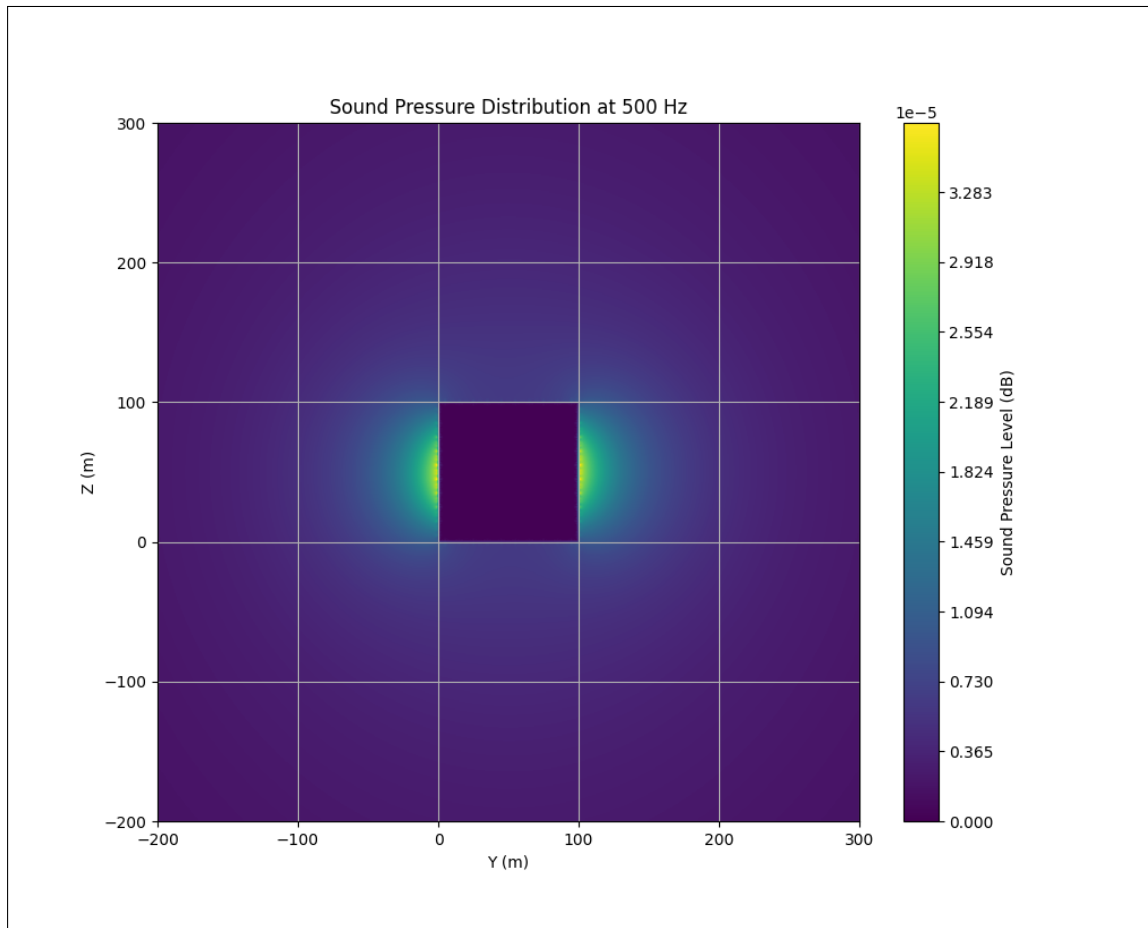


Figure 5.3.19: Contour plot of the sound pressure level around the cube at 500 Hz when two opposite faces are subjected to loading.

- Despite amplitude mismatches, both methods consistently capture the primary resonance peaks, indicating a shared resonance signature.
- A direct wall-clock time comparison between Abaqus and BEMPP is not feasible, as Abaqus solvers leverage GPU parallelization, whereas a modest GMRES solver without a preconditioner was used in BEMPP. However, a meaningful comparison of computational efficiency can be made by examining the number of nodes each method must solve in the acoustic domain. In Abaqus, the solution involves 4700 nodes due to volumetric discretization, whereas BEMPP requires solving only 830 nodes by discretizing only the boundary, demonstrating the efficiency of the boundary element approach in reducing computational complexity.

In future work, a thorough mesh convergence study could elucidate whether refining the discretization reduces the observed divergence at higher frequencies and for multiple faces. Additional strategies for handling non-smooth geometries and edge effects could also improve agreement between BEMPP and Abaqus under normal velocity boundary conditions.

Chapter 6

Conclusion

This thesis set out to advance methodologies in exterior acoustic calculations by leveraging both finite element and boundary element techniques under free-field boundary conditions. The work addressed four major objectives: (1) comparing fully coupled and sequentially coupled analyses in Abaqus, (2) developing a robust procedure for wind turbine gearbox acoustic analysis, (3) validating acoustic calculations with the open-source BEMPP library, and (4) documenting and refining computational best practices to foster progress in structural-acoustic simulations. This chapter summarizes the key findings and implications of the results presented in Chapter 5 and throughout the thesis.

6.1 Summary of Key Findings

This section presents a comprehensive summary of the key results discussed in the 'Results and Discussion' chapter, along with the overall conclusions drawn from the numerical experiments conducted as part of this thesis.

6.1.1 Comparative Analysis of Fully Coupled vs. Sequentially Coupled Approaches

The first objective evaluated whether the *sequentially coupled* method (decoupling the structural and acoustic domains) could reliably reproduce results obtained from a *fully coupled* simulation for a prototype cube:

- **Sound Pressure Level (SPL) Agreement:** The SPL comparisons in Section 5.1 indicate that the sequentially coupled approach closely matches the fully coupled analysis (within 2dB across a range of frequencies), effectively capturing resonance peaks around 620 Hz, 780 Hz, and 900 Hz.
- **Computational Efficiency:** Although the prototype cube model is relatively small (Section 5), sequential coupling required close to 10 % less wall-clock time compared to a fully coupled run. Sparse solver advantages diminish in larger models, so the potential savings from sequential submodels becomes more significant as model size grows.

- **Radiated Energy and ERP Validation:** Using acoustic power outputs (e.g., RADPOW vs. ALLQB) confirmed that the sequentially coupled method provides accurate estimates of radiated acoustic energy. Furthermore, comparing Equivalent Radiated Power (ERP) with RADPOW validated that ERP always exceeds RADPOW, consistent with theoretical expectations of maximum possible radiation.

6.1.2 Methodology Development for Gearbox Acoustic Analysis

The second objective involved integrating displacement results from a time-domain Simpack simulation into an *Abaqus*-based acoustic solver, enabling sequential coupling in an industrially relevant wind turbine gearbox scenario:

- **Displacement-Driven Acoustic Domain:** By prescribing node-level displacements from Simpack in Abaqus, the gearbox casing's harmonic motion was directly translated into far-field pressure predictions, as detailed in Section 5.2.
- **Coupling Strategies (Tie vs. ASI Elements):** Both surface-based ties and Acoustic-Structural Interface (ASI) elements were employed (Section 5.2). SPL comparisons revealed deviations below 2 dB at key far-field positions, validating that either technique can deliver high-fidelity noise predictions, albeit with different mesh requirements and computational costs.
- **Remeshing and Null Displacements:** The study demonstrated that assigning zero displacement to remeshed elements (1.43% of total nodes) introduced negligible SPL error, a practical outcome affirming that partial null displacements do not degrade overall acoustic accuracy.
- **ERP vs. RADPOW in Real Operating Conditions:** Unlike the point-loaded cube, the gearbox receives complex loads from rotating gears. Consequently, ERP and RADPOW more closely aligned here, indicating a higher radiation efficiency across multiple vibratory surfaces.

6.1.3 Acoustic Calculations in BEMPP

A third objective aimed to *validate free-field acoustic simulations* via the open-source Boundary Element Method Python Package (BEMPP) and compare them against Abaqus results for the vibrating cube:

- **Good Agreement for Single-Face Loading:** When only one face of the cube was loaded (Section 5.3), BEMPP and Abaqus agreed within about 3 dB, capturing similar resonance peaks.
- **Increasing Discrepancies with Multiple Faces:** Deviations up to 10 dB and eventually 18 dB emerged when two or more faces were loaded. Mesh resolution, higher wavenumbers, and non-smooth geometry (sharp edges at the cube corners) could have contributed to these disparities.

- **Null-Field Validation:** Figures such as 5.3.19 confirmed that BEMPP’s null-field approach correctly produced near-zero interior pressures, matching theoretical expectations for exterior radiation formulations.
- **Future Directions:** The results highlight the need for refined boundary discretizations and specialized treatments of non-smooth edges or corners to narrow the gap in multi-face loading scenarios.

6.1.4 Advancement of Computational Mechanics Knowledge Base

The final objective focused on methodically documenting *practical* lessons, numerical discrepancies, and theoretical underpinnings:

- **Detailed Documentation:** Key modeling tips, such as edge-node handling, normal velocity boundary conditions, mesh sizing requirements, and submodel constraints in Abaqus, were recorded.
- **Industrial Applicability:** By integrating MBS data (Simpack) with Abaqus, the thesis provides a workflow that can be leveraged in real engineering projects, notably for rotating machinery like wind turbine gearboxes.
- **Comparative Insights:** The side-by-side analysis of fully coupled, sequentially coupled, and boundary-element-based approaches informs future simulation practices, balancing computational resource demands against solution accuracy.

6.2 Recommendations and Future Work

Based on the collective outcomes, the following recommendations and future research directions are proposed:

1. **Mesh Convergence Studies:** Increase mesh refinement in both Abaqus (for high-frequency fluid–structure coupling) and BEMPP (to maintain a low hk ratio). This would help quantify how discretization errors evolve at higher frequencies or when multiple surfaces are actively vibrating.
2. **Handling Sharp Edges in BEM:** Investigate specialized corner or edge treatments in boundary integral equations (e.g., local angle corrections to jump conditions), reducing the discrepancies observed for multi-face loading on polyhedral geometries.
3. **Large-Scale Industrial Applications:** Extend the sequential submodel approach to complex assemblies with multiple substructures, validating the gain in computational efficiency for even larger systems (e.g., entire nacelles of wind turbines).

4. **Advanced Solver Techniques:** Explore fast multipole methods and preconditioning strategies in BEMPP for higher frequencies. For Abaqus, investigate advanced parallelization or GPU-accelerated solvers for fully coupled or sequential runs.
5. **Parametric and Sensitivity Analyses:** Conduct parametric studies on gearbox designs, investigating how changes in structural damping or gear meshing influence far-field noise. Combine these with robust optimization to minimize acoustic emissions under operational loads.

6.3 Concluding Remarks

This work has demonstrated the feasibility of using both Finite Element Methods (in Abaqus) and Boundary Element Methods (in BEMPP) to model free-field acoustic radiation problems. The sequentially coupled approach—integrating Simpack data for complex mechanical assemblies—proved accurate for smaller test structures (the prototype cube) and a wind turbine gearbox. While BEMPP showed strong agreement for simpler loading cases, multi-face loading on the cube revealed non-trivial discrepancies, emphasizing the importance of careful mesh selection and addressing non-smooth boundaries. Overall, these findings confirm that both FEM and BEM can yield reliable, computationally efficient solutions for exterior acoustics, laying the groundwork for future refinements in industrial noise calculation and advanced research in computational acoustics.

Bibliography

- [1] Michele Iodice. Road and soil dynamic characterization from surface measurements, 02 2017.
- [2] ABAQUS, Inc. *Infinite Elements*, 2024. Accessed: January 15, 2025.
- [3] TU Dresden Chair of Machine Elements. Wind turbines (mbs), 2022. Accessed: Jan 25, 2025.
- [4] Bay Audiology. Human audible frequencies range, 2021. Accessed: January 01, 2025.
- [5] Ministry of Environment, Denmark. Regulations on noise from wind turbines. Accessed: January 02, 2025.
- [6] Allan D. Pierce. *Acoustics: An Introduction to Its Physical Principles and Applications*. Springer, 2019.
- [7] R. J. Astley. Infinite elements for wave problems: A review of current formulations and an assessment of accuracy. *International Journal for Numerical Methods in Engineering*, 49(7):951–976, 1999.
- [8] Dassault Systèmes Simulia. Sound radiation analysis of automobile engine covers. Abaqus Technology Brief TB-06-COVER-2, SIMULIA, April 2007.
- [9] Monika Stoyanova. Fem simulation of acoustic radiation from electric drivelines in heavy trucks. Master's thesis, Chalmers University of Technology, Goteborg, Sweden, 2022.
- [10] O. C. Zienkiewicz, R. L. Taylor, and J. Z. Zhu. *The Finite Element Method: Its Basis and Fundamentals*. Elsevier, 2013.
- [11] Friedrich-Karl Benra, Hans Josef Dohmen, Ji Pei, Sebastian Schuster, and Bo Wan. A comparison of one-way and two-way coupling methods for numerical analysis of fluid-structure interactions. *Journal of Applied Mathematics*, 2011:16, 2011. Open access article under the Creative Commons Attribution License.
- [12] Nusser, Katrin and Becker, Stefan. Numerical investigation of the fluid structure acoustics interaction on a simplified car model. *Acta Acust.*, 5:22, 2021.
- [13] Michael Schäfer. Numerical simulation of coupled fluid-solid problems: State of the art and applications. *NAFEMS International Journal of CFD Case Studies*, 5:75–95, 2006.

- [14] Goran Sandberg. *Acoustic and Interface Elements for Structure-Acoustic Analysis in CALFEM*. Number TVSM-7113 in TVSM-7000. Division of Structural Mechanics, LTH, 1996.
- [15] Dhiren Behera, Fan Li, Mine Tasci, Young-Jin Seo, Martin Schulze, Binu Jose Kochucheruvil, Tamer Yanni, Kiran Bhosale, and Phani Aluru. Mbs-fem co-simulation approach to assess strength of automotive chassis components. In *WCX SAE World Congress Experience*. SAE International, April 2025.
- [16] R. D. Ciskowski and C. A. Brebbia. *Boundary Element Methods in Acoustics*. Springer, 1991.
- [17] Peter Moeller Juhl. *The Boundary Element Method for Sound Field Calculations*. Phd thesis, The Acoustics Laboratory, Technical University of Denmark, 1993. Report No. 55, 1993.
- [18] Yun Huang, Mhamed Souli, and Rongfeng Liu. Bem methods for acoustic and vibroacoustic problems in ls-dyna. In *8th European LS-DYNA Users Conference*, Strasbourg, France, 2011.
- [19] David Herrin, Jinghao Liu, F. Martinus, D. Kato, and Sze Kwan Cheah. Prediction of sound pressure in the far field using the inverse boundary element method. *Noise Control Engineering Journal - NOISE CONTR ENG J*, 58, 01 2010.
- [20] Christopher Jelich. *Fast Multipole Boundary Element Techniques for Acoustic and Vibroacoustic Problems*. PhD thesis, Technische Universität München, TUM School of Engineering and Design, 2022. Doctoral Dissertation.
- [21] R. Bolejko and A. Dobrucki. Fem and bem computing costs for acoustical problems. *Archives of Acoustics*, 31(2):193–212, 2006.
- [22] Matthieu Aussal, Francois Alouges, Marc Bakry, and Gilles Serre. Fem-bem applications in vibro-acoustics using gypsilab. In *Proceedings of the 23rd International Congress on Acoustics*, Aachen, Germany, 2019. International Congress on Acoustics.
- [23] Abderrazak Mejdi and Noureddine Atalla. Vibroacoustic analysis of laminated composite panels stiffened by complex laminated composite stiffeners. *International Journal of Mechanical Sciences*, 58:13–26, 05 2012.
- [24] Dassault Systemes. *Coupled Acoustic-Structural Analysis*, 2024. Accessed: January 03, 2025.
- [25] Siemens. Sound fields: Free versus diffuse field, near versus far field, 2020. Accessed: January 15, 2025.
- [26] Akad. ORat PD Dr.-Ing. habil. Sebastian Pfaller. Introduction to the finite element method, lecture notes, 2022. Summer Semester 2022.
- [27] Dassault Systemes. *Choosing between implicit and explicit analysis*, 2024. Accessed: January 04, 2025.

- [28] ABAQUS, Inc. *Format of the Input File*, 2009. Accessed: January 4, 2025.
- [29] NASA. What's the science of sound? Accessed: January 06, 2025.
- [30] Daniel J. Inman. *Engineering Vibrations*. Pearson, 2013.
- [31] ANSYS Innovation Space. Formulation of harmonic analysis, 2019. Accessed: January 7, 2025.
- [32] ABAQUS, Inc. *Material Damping*, 2024. Accessed: January 15, 2025.
- [33] ABAQUS, Inc. *Mode-Based Steady-State Dynamic Analysis*, 2024. Accessed: January 15, 2025.
- [34] ABAQUS, Inc. *Subspace-Based Steady-State Dynamic Analysis*, 2024. Accessed: January 15, 2025.
- [35] ABAQUS, Inc. *Direct-Solution Steady-State Dynamic Analysis*, 2024. Accessed: January 15, 2025.
- [36] Altair HyperWorks. *2D Elements*, 2023. Accessed: January 15, 2025.
- [37] ABAQUS, Inc. *Reduced integration*, 2024. Accessed: January 15, 2025.
- [38] Altair HyperWorks. *3D Elements*, 2023. Accessed: January 15, 2025.
- [39] ABAQUS, Inc. *Acoustic Medium*, 2024. Accessed: January 15, 2025.
- [40] ABAQUS, Inc. *Three-Dimensional Solid Element Library*, 2024. Accessed: January 15, 2025.
- [41] ABAQUS, Inc. *Acoustic Infinite Elements*, 2024. Accessed: January 15, 2025.
- [42] ABAQUS, Inc. *Fully and sequentially coupled acoustic-structural analysis of a muffler*, 2024. Accessed: January 16, 2025.
- [43] R. Srinivasan Puri, Denise Morrey, Andrew J. Bell, John F. Durodola, Evgenii B. Rudnyi, and Jan G Korvink. Reduced order fully coupled structural-acoustic analysis via implicit moment matching. *Applied Mathematical Modelling*, 33(11):4097–4119, 2009.
- [44] Benjamin Cotte and Olivier Doare. Mf207: Acoustics in fluid media - course notes. Lecture notes, 2023. Available online at <https://perso.ensta-paris.fr/~cotte/files/2023-course-notes-MF207.pdf>.
- [45] Frank Fahy. 4 - impedance. In Frank Fahy, editor, *Foundations of Engineering Acoustics*, pages 48–73. Academic Press, London, 2001.
- [46] ABAQUS, Inc. *Using infinite elements to compute and view the results of an acoustic far-field analysis*, 2024. Accessed: January 17, 2025.
- [47] ABAQUS, Inc. *Whole and Partial Model Variables*, 2024. Accessed: January 16, 2025.

- [48] Tara LaForce. Pe281 boundary element method course notes, June 2006. Accessed: 2024-02-01.
- [49] Bempp Handbook. Green's representation theorem, 2024. Accessed: January 20, 2025.
- [50] Christoph Pflaum. Functional analysis for engineers, 2018. Course Script.
- [51] Rick C. Morgans, Anthony C. Zander, Colin H. Hansen, and David J. Murphy. Fast boundary element models for far field pressure prediction. In *Proceedings of the Australian Acoustical Society Conference (AAS 2004)*, Gold Coast, Australia, 2004. Accessed: 2024-02-01.
- [52] Bempp Handbook. Function spaces, 2024. Accessed: January 20, 2025.
- [53] Bempp Handbook. Grid functions, 2024. Accessed: January 20, 2025.
- [54] Bempp Handbook. Boundary operators, 2024. Accessed: January 20, 2025.
- [55] Lloyd N. Trefethen and David Bau, III. *Numerical Linear Algebra*. Society for Industrial and Applied Mathematics, Philadelphia, PA, 1997.
- [56] Altair HyperWorks. *How Element Quality is Calculated*, 2021. Accessed: January 15, 2025.
- [57] ABAQUS, Inc. *Coupled Acoustic-Structural Analysis - Mesh Refinement*, 2024. Accessed: January 16, 2025.
- [58] Occupational Safety and Health Administration, U.S. Department of Labor. Occupational noise exposure. Accessed: January 01, 2025.
- [59] Timo Betcke, Erik Burman, and Matthew W. Scroggs. Boundary element methods for helmholtz problems with weakly imposed boundary conditions. *SIAM Journal on Scientific Computing*, 44(5):A2895–A2917, 2022.

Appendix A

Derivation of Acoustic Power Formula from Energy

Power is defined as the rate at which energy is transferred or dissipated over time. In the context of acoustics, power can be expressed as:

$$P = \frac{E}{T},$$

where P is power, E is energy, and T is the time period over which the energy is transferred.

For a harmonic wave, the time period T is the reciprocal of the frequency f ($T = \frac{1}{f}$). Substituting T into the power equation gives:

$$P = E \cdot f.$$

Thus, multiplying the dissipated energy (ALLQB) by the frequency yields the acoustic power, enabling a direct comparison with RADPOW from fully coupled analyses.

Appendix B

Python Script for Converting Simpack Displacement Data to Abaqus Format

This appendix provides the Python script used for converting displacement data from Simpack into a format suitable for application as boundary conditions in Abaqus. The script reads displacement values, filters nodes based on a predefined list, converts displacement amplitudes from meters to millimeters, and formats the data into an Abaqus input file.

```
1 import numpy as np
2 import os
3 import pandas as pd
4
5 def read_and_process_data(input_directory, nodes_file_path,
6     output_directory):
7     """
8         Reads displacement data from the input directory, filters it based
9         on valid nodes,
10        and formats it for boundary condition input in Abaqus.
11
12        Parameters:
13        - input_directory (str): Path to the directory containing
14            displacement data files.
15        - nodes_file_path (str): Path to the file containing valid node
16            information.
17        - output_directory (str): Path to the directory where the output
18            files will be saved.
19
20        """
21
22        # Read the list of nodes to be processed
23        nodes_data = pd.read_fwf(nodes_file_path)
24
25        # Extract valid nodes into a set for fast lookup
26        valid_nodes = set(nodes_data['ERP_NODE'])
27
28        # Ensure the output directory exists
29        os.makedirs(output_directory, exist_ok=True)
```

```

24
25     for filename in os.listdir(input_directory):
26         if filename.endswith('Hz.inp'):
27             filepath = os.path.join(input_directory, filename)
28
29         # Read displacement data into a DataFrame
30         data = pd.read_csv(filepath)
31
32         # Filter rows to keep only nodes in the valid node list
33         data = data[data['node'].isin(valid_nodes)]
34
35         # Convert amplitude from m/s to mm/s and apply phase
36         data['Displacement X'] = data['Displacement X Amplitude'] *
37             1000 \
38                         * np.exp(1j * data['Displacement X
39                                         Phase'])
40         data['Displacement Y'] = data['Displacement Y Amplitude'] *
41             1000 \
42                         * np.exp(1j * data['Displacement Y
43                                         Phase'])
44         data['Displacement Z'] = data['Displacement Z Amplitude'] *
45             1000 \
46                         * np.exp(1j * data['Displacement Z
47                                         Phase'])
48
49         # Prepare DataFrame for output
50         frames = []
51         for direction, label in zip(['X', 'Y', 'Z'], [1, 2, 3]):
52             temp_df = pd.DataFrame({
53                 'Node': data['node'],
54                 'Direction1': label,
55                 'Direction2': label,
56                 'Real': np.real(data[f'Displacement {direction}']),
57                 'Imaginary': np.imag(data[f'Displacement {direction
58                                         }'])})
59             frames.append(temp_df)
60
61         output = pd.concat(frames, ignore_index=True)
62
63         # Build the output filename
64         output_filename = os.path.join(output_directory, f'
65                                         bc_format_{filename}')
66
67         # Write real and imaginary parts in Abaqus input-file
68         # format
69         with open(output_filename, 'w') as f:
70             f.write('*BOUNDARY, REAL, TYPE= Displacement\n')
71             output.apply(lambda x:
72                         f'{int(x['Node'])}, '
73                         f'{int(x['Direction1'])}, '
74                         f'{int(x['Direction2'])}, '
75                         f'{x['Real']:.12e}\n'),
76                         axis=1)
77
78             f.write('*BOUNDARY, IMAGINARY, TYPE= Displacement\n')

```

```
71         output.apply(lambda x:
72                         f.write(f"{{int(x['Node'])}}, "
73                                 f"{{int(x['Direction1'])}}, "
74                                 f"{{int(x['Direction2'])}}, "
75                                 f"{{x['Imaginary']}:.12e}\n"),
76                         axis=1)
77
78 # File paths
79 input_directory = " "
80 nodes_file_path = " "
81 output_directory = " "
82 read_and_process_data(input_directory, nodes_file_path,
83                         output_directory)
```

Listing B.1: Processing Simpack Displacement Data for Abaqus